FUZZY TECHNOLOGY APPLICATION FOR MOBILE POSITIONING IN CELLULAR COMMUNICATION

Aleksandar Stojcevski
B.E. (Electrical/Electronic)

A thesis submitted in fulfillment of the requirements for the degree of Master of Engineering

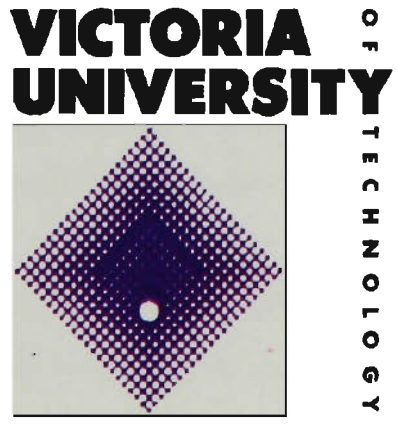

School of Communications & Informatics
Faculty of Engineering and Science
Victoria University of Technology
Melbourne, Australia

September 2000

Declaration

I declare that, to the best of my knowledge, the research described herein is the result of my own work, except where otherwise stated in the text. It is submitted in fulfillment of the candidature for the degree of Masters by Research in Engineering at Victoria University, Australia. No part of this work has already been submitted for any degree nor is being submitted for any other degree.

Aleksandar Stojcevski

September 2000

ABSTRACT

In engineering systems there is generally two classes of knowledge: objective knowledge, which can be quantified using the laws of traditional mathematics, and subjective or intelligent knowledge, that cannot be modeled mathematically but can be expressed in linguistical terms. Fuzzy Logic (FL) is a method that combines these two forms of knowledge, and as such provides a powerful tool for solving real engineering problems.

A fuzzy logic system (FLS) is the methodology of applying FL to engineering systems. In general, a FLS can be considered as a non-linear mapping of crisp (firm) input data to crisp output data. It is the inclusion of subjective knowledge in a FLS that leads to a plethora of mapping possibilities, which may not be possible using traditional mathematical modeling techniques. A fuzzy logic system consists of four main elements: fuzzification, rule based, inference engine and deffuzification.

Fuzzy logic has been successfully adopted in many real-world automatic control systems including automobile transmission, subway systems, industrial robots, washing machines, cameras and air-conditioners. In contrast, the utilization of fuzzy logic in mobile communications systems is recent and limited. Understanding general mobile communications is essential in order to go on and develop a mobile positioning application.

The successful applications of Fuzzy Logic Control (FLC) techniques in many areas draw a huge amount of attention to its industrial applications. However, lack of structured methods and tools for design and analysis is preventing this revolutionary controller from playing a more significant role in mobile communications.

A methodology to construct and analyse a FL controller to be used in mobile positioning would significantly improve the efficiency of FLC design, increase the quality of FLC by allowing the designer to develop and design the controller based on some specifications and requirements, and then validate that design.

I dedicate my work to my father

RADE STOJCEVSKI

His endless support and encouragement has been a great inspiration for the completion of this work.

TABLE OF CONTENTS

ACKNOWLEDGMENTS

I am indebted to many people for advice and assistance. First on my list, my supervisors Dr. Leonid Reznik and Professor Mike Faulkner. Their support and wisdom will never be forgotten. Thanks also to Dr. Jugdutt Singh, Mr. Ranjan Mohapatra, research assistant Melvyn Parrera, and the Mobile Communications & Signal Processing Group at Victoria University for their help.

A special thanks for encorangment goes out to my great friend Mr. Dean Cvetkovic. Thanks also to the Stojcevski family, my father Mr. Rade Stojcevski, Mrs. Vera Stojcevska, Bobby Stojcevski and Filip Stojcevski, for their support, patience and understanding.

Aleksandar Stojcevski

LIST OF ABBRIVIATIONS

FDMA	Frequency Division Multiple Access
TDMA	Time Division Multiple Access
CDMA	Code Division Multiple Access
GSM	Global System Mobile
MPS	Mobile Positioning System
TOA	Time of Arrival
AOA	Angle of Arrival
TDOA	Time Difference of Arrival
RF	Radio Frequency
GPS	Global Positioning System
α	Estimated angle of incidence of the propagation wave
c	Speed of Light
Δt	Difference between the time of arrival signals
λ	Radio signal wavelength
ϕ	Arriving electrical phase angle
μsec	Micro seconds
m	Meters
FCC	Federal Communication Commission
E911	Emergency nine one one
FM	Frequency Modulation
AM	Amplitude Modulation
km	Kilometres
FL	Fuzzy Logic
FLC	Fuzzy Logic Control
DSP	Digital Signal Processing
SNR	Signal to Noise Ratio
s(t)	Received Signal Power
m(t)	Local Mean of the Received Signal

r(t)	Fast Fading Component
A(n)	Discrete Time Signal
σ	Standard Deviation
v	Velocity of Mobile
T	Sampling Interval
$R_A(k)$	Autocorrelation
t	Path Delay
L	Distance between Base Station and Mobile Station
BS	Base Station
MS	Mobile Station
X_m	X coordinate of Mobile
Y_m	Y coordinate of Mobile
X_{BS}	X coordinate of Base Station
Y_{BS}	Y coordinate of Base Station
AVL	Automatic Vehicle Location
D	Distance between Base Stations
$\Re$	Rhomboid
COG	Centre of Gravity
FM	Fuzzy Mean
WFM	Weighted Fuzzy Mean
FAAH	Fuzzy Adaptive-interval and Hysterisis threshold handover
AVG	Averaging Interval
HYS	Hysterisis Level
K_2	Propagation Constant
d_o	Correlation Distance
K_1	Transmitter Power
apdp	Average Power Delay Profile
CPS	Cambridge Positioning Systems
RMS	Root Mean Square
P(x,y)	Circular Distribution
BCCH	Broadcast Control Channel

P_t	Transmitted Power
G_a	Antenna Gain
G_f	Lognormal Fading
C/I	Carrier to Interference Ratio
MATLAB	Computing environment for high performance numerical computing and Visualisation
C/N	Carrier to Noise Ratio
rmse	Root Mean Square Error
τ	Delay Spread
T_{bi}	Excess Time Delay
α_i	Mean Angle of Arrival at Mobile
LOS	Line of Sight
τ_m	Mean Delay
θ_i	Angle of Arrival
Hz	Hertz
μs	Micro Seconds
NLOS	Non Line of Sight
E-OTD	Enhanced-Observed Time Difference
MLC	Mobile Location Centre
DTCD	Digital Channel Designation
N	snapshots
α_n	Amplitude of Incoming Waves
T_n	Delay of Incoming Waves
m	Nakagami Parameters
CIR	Channel Impulse Response
CPP	Channel Power Profile
ICI	Incoherent Integration
E_b/N_o	Bit Energy to Noise Power Spectral Density
RTD	Real Time Difference
BTS	Base Transceiver Station
OTD	Observed Time Difference

CDF	Cumulative Distribution Function
bsv	Array containing Base Station coordinates
t	Time of Arrival (seconds)
Γ	Bit Energy to Noise Power Ratio
W_i	Weighted Average
W_{Si}	Belief Degree based on Signal Strength
$W_{\Gamma i}$	Belief Degree based on Bit Energy to Noise Power

LIST OF FIGURES

LIST OF TABLES

CHAPTER 1

INTRODUCTION THEORY

1.1 Introduction

Reliable communications is a virtual component for improvement in performance and increased functionality in mobile location. It provides a very valuable opportunity to present relevant information to the mobile and its occupants. Many quality services can be provided to mobiles using communications technologies.

Communications technologies are poised for major expansion in two key areas: wireless data communications and high-speed wireless (wire-based) communications supported by the Internet and ancillary networks. Ultimately it will be the marriage of these two key technologies that will bring about a revolution resulting in a new information society. Wireless data applications play a critical role in making the vision of mobile computing a reality. Today's competitive and fast-placed business climate demands tools that allow people to communicate at their own convenience and discretion.

1.2 Existing communications technologies

Mobile communications networks need to support many different applications within a wide set of user services including traffic management, emergency management, electronic payment and last but not least mobile location. Each application has specific needs that may best be satisfied by a particular communications technology. Because no single communications technology can satisfy all of these requirements, a hybrid implementation of technologies is likely to be required for a regional or statewide communications network.

Both analog and digital systems are available for mobile radios (the digital systems are essentially related to voice digitisation and to digital transmissions). The major advantages of the digital systems over the analog systems are increased spectrum

efficiency, more consistent audio quality throughout more of the coverage area, inherent privacy from analog scanners, and greater data rate capability.

Some of the transmission and switching methods used for transmission of information is briefly considered next. Three major channel access methods exist: FDMA (frequency-division multiple access), TDMA (time-division multiple access), and CDMA (code-division multiple access) [1]. FDMA and TDMA can be implemented on either narrowband channels (e.g., 12.5 kHz) or wideband channels (e.g., 200 kHz), whereas CDMA is restricted to the wideband architecture. Two principal switching techniques are available: circuit stitching and packet switching. Circuit switching requires the complete end-to-end connection over both the wireless and wired segments before any voice or data can be sent. Packet switching divides the information into packets and transfers packets of data between network nodes over different connections until the packets reach their final destination and are reconstructed for the user. The main difference between these two methods is that circuit switching reserves the required bandwidth in advance, whereas packet switching acquires and releases it on an as-needed bias.

In general, mobile services can be classified into conventional (nontrunked) mobile systems and trunked mobile systems. Each conventional mobile system has one channel available for each specific group of users. In other words, users are grouped so that each group of users is assigned to a different channel. This system is less efficient than trunking because users can only communicate if their channel is free. Since each group of users shares a common radio frequency, the users end up competing for airtime. The trunked mobile system allows all available channels to be shared among a large group of users, so that no one is waiting as long as free channels are available. For instance, a typical trunked land mobile radio system can have up to 28 channels, one of which is a dedicated control channel that automatically assigns the open channels to users. When a user wants to transmit, both the transmitting radio and the receiving radios are automatically assigned to one of the 28 available radio channels. This system is better at conserving spectrum, since no individual radio user will have to wait to transmit if a

trunked radio channel is available. Depending on how the available spectrum is used, these systems can also be classified as narrowband or wideband. In the narrow architecture, the total frequency band is split into several narrowband channels. In the wideband architecture, most of the spectrum is available to each and every user.

1.3 Mobile Location Systems

Mobile positioning has received a lot of attention recently. Applications are both of commercial and public interest. Most papers published today illustrate the performance of a mobile positioning technique applicable to the Global System Mobile (GSM) network. The ability of a GSM network to locate a mobile station is reduced, for the time being, to the facility required by the mobility management function, i.e. the cell identity. There are some ways of improving a rough position of a mobile unit.
One of them for example is by using the timing advance information and the management reports. The accuracy could be in the order of a few hundred meters. This figure is still not accurate enough for the effective development of a number of new added value services and emergency services.

Some of the general questions that arise among us today about mobile positioning are questions such as: What does GSM based positioning do? What is the Mobile Positioning System (MPS)? What are its applications? and what are the standards today? GSM based positioning is used to geographically locate mobile phones and to distribute the positioning information to different applications. All existing mobile phones can potentially be positioned since no changes are needed in the phone itself. Mobile positioning system (MPS) is the system used to find out and provide the geographical position of a mobile phone to an application. A cellular positioning system is only using the infrastructure and characteristics of the mobile telephony network to find out the geographical location of a mobile unit. Positioning could be used in whole range of applications. Examples of positioning applications are:

- Fleet management
- Tracking asset or goods

- Stolen vehicle recovery
- Emergency call positioning
- Local traffic and weather information
- Directions to different closest gas stations, etc.

Mobile location systems can be broadly categorised onto two classes: autonomous and centralised. Whenever location functions are performed at the mobile end with no remote host or centralised computing facilities involved, the system will be referred to as autonomous system. Otherwise, the system will be referred to as a cenralised system.

Good systems architecture is very important for successful location. Users' requests and developers' improvements generally lead to system expansion. A good architecture must provide a stable base for the future evolution of the system. In other words, the systems must be stable and predictable, but still flexible enough to meet changing demands and operational environments over a reasonable fraction of the expected system lifetime. On the other hand, unrestricted enhancement of a finished system (even when supported by a well-defined architecture to begin with) may affect system stability.

The methods discussed in this section of the chapter can be used either at the mobile end or the host end located on a fixed infrastructure. Based on the classification described at the beginning of this section, if these methods determine the mobile location at the mobile end, the corresponding system is called autonomous system. If they determine the mobile location by a host computer on the infrastructure end, it is called a centralised system. Three commonly used measurement techniques for terrestrial positioning are time of arrival (TOA), angle of arrival (AOA), and time difference of arrival (TDOA). All of these approaches use the concept that the radio frequency (RF) signal propagates at a constant velocity and that the signal path is predictable. The first technique, TOA, measures the propagation time of signals broadcast from multiple transmitters at known locations to determine the location of the mobile device. This is the same technique used

in global positioning systems (GPS) positioning. The difference is that for terrestrial positioning the emitters are not in space, but on the Earth's surface, typically taking the form of base stations or towers. A detailed discussion of the TOA principle is given in chapter 6.

The AOA technique uses RF triangulation to calculate the mobile position. In infrastructure-based implementations, the signal is transmitted from a vehicle equipped with a RF transmitter. In this approach, a phased array of two or more antennas is used at a single cell site to receive the propagation wave. The following equation is often used for the two-antenna array located at a single site, as shown in Figure 1.1.

$$\hat{\alpha} = \arcsin\frac{c\Delta t}{d}$$

where α is the estimated angle of incidence of the propagation wave (assumed planar) at the antenna array, c is the speed of light (assuming that the radio-wave velocity is approximately equal to the speed of light), Δt is the difference between the times of arrival signal at each antenna, and d is the distance between the antennas used to receive that signal. Note the assumption that the radio-wave velocity is approximately equal to the speed of light, which may not be valid in certain applications.

A special case solution can be made by the observation that a single phase wave striking two closely spaced antennas at any one site will show a difference in electrical phase of two received signals. Given that $d = 0.5\lambda$ (where λ is a radio signal wavelength), the estimated incidence angle (arriving azimuth angle) becomes

$$\hat{\alpha} = \arcsin\left(\frac{\Delta\phi}{\pi}\right) = \arcsin\left(\frac{\phi_1 - \phi_2}{\pi}\right)$$

where ϕ_1 and ϕ_2 are arriving electrical phase angles for antennas 1 and 2, respectively.

The phased arrays of the antennas are used at two or more cell sites capable of receiving the propagated signals from the mobile. The location of the mobile is determined by the intersection of the two angles of incidence α_1 and α_2 as shown in Figure 1.1.

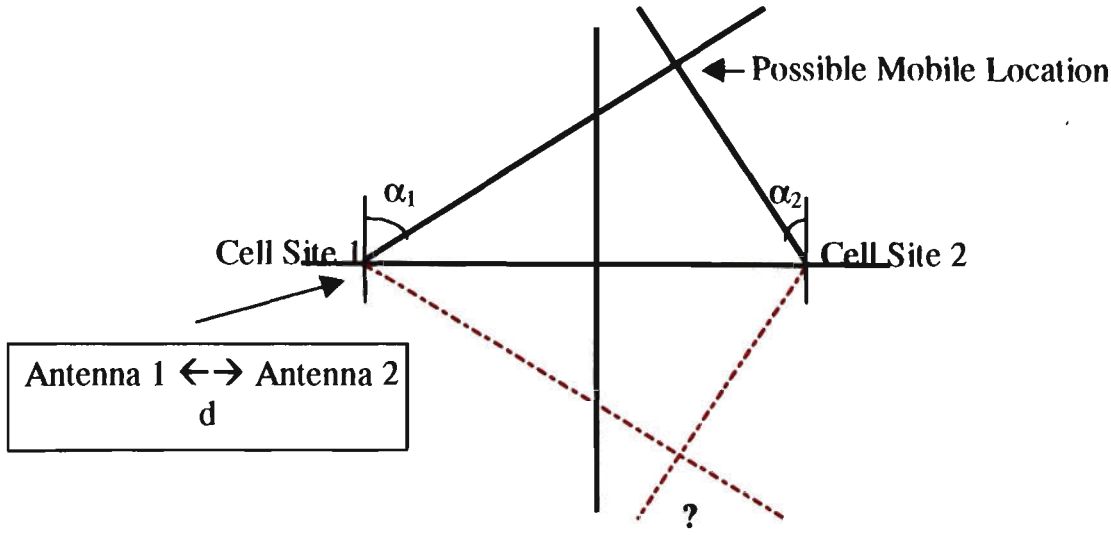

Figure 1.1: *Location determination by angle of arrival (AOA).*

A two antenna infrastructure-based approach has been shown above. A three-antenna array is actually better because a two-antenna array will have difficulty calculating the angle of incidence when it is close to a right angle. Theoretically, these antennas could be on the mobile side to receive the propagation radio waves from transmitters at the base station. For economic reasons, antenna arrays are seldom used on the mobile side.

There are both advantages and disadvantages to using the AOA for the determination of mobile position. On the positive side, there is no need to maintain time synchronization between cell sites (or base stations) to perform mobile positioning. Only two sites are required to determine the location of a mobile. Because it does not use multisite time-synchronised system (as TDOA does), the overall performance of AOA as a location technology should be less affected by RF channel bandwidth. This is an important feature to keep in mind when dealing with various RF technologies (such as 30 kHz AMPS and 10 kHz NAMPS at the low end to 1.25 MHz CDMA at the upper end) in a single system.

The major drawback to AOA is its susceptibility to signal blockage and multipath reflection. This results in fairly high error margins for the estimated mobile positions. This is especially true in urban areas, where errors in the order of hundreds of metres can

occur. Due to signal scattering, it is conceivable that position calculations based on angle of arrival could result in a position estimate that places the mobile in the opposite direction from its actual direction relative to the receiving base sites. These ambiguous solutions can be eliminated using additional technologies such as the RF profile method. Another problem with AOA is that each site or mobile device (depending on the infrastructure-based or mobile based solution) needs to have at least two antennas, which adds additional cost to the system. However, this may not be a problem for some established sites that have a phased array of antennas already.

The third type of terrestrial-radio-based location technique is TDOA. The TDOA technique utilises RF trilateration to calculate the mobile position. RF trilateration differs from triangulation in a way that it calculates the distance between the mobile and a fixed set of reference sites that are time synchronised. The calculated distance from the mobile can be determined by either of the two methods, measuring the transit time for a radio signal (group of pulses) between the mobile and reference sites. The method using pulse modulation for the radio signal is less affected by multipath propagation than the method using phase modulation, which means that pulse modulation method is more accurate. On the other hand, pulse modulation requires a higher bandwidth than phase modulation. The radio signal could also be transmitted first from the site to the mobile with the mobile then responding back to the site. In this case, the calculated distance must be divided by two. Figure 1.2 illustrates the basic principle of this location technique.

How TDOA technology determines a location is discussed below. If a time-synchronised signal is known (either generated by the moving mobile or by time-synchronised fixed RF transmitters) at sites 1, 2 and 3 as shown in Figure 1.2, the signal transmission path lengths d_1, d_2, d_3 can be determined. The difference between these path lengths can be measured by the time (or phase) differences of the signals between the transmitters and the mobile. The estimated location derived from the time or phase difference pairs will be at the intersection of two hyperbolas as shown in Figure 1.2. Assuming that the time difference is used to derive the distance, and a receiver in the mobile is used to receive the signals transmitted from three sites, these hyperbolic curves may be calculated as

follows (using the curve h1 as an example): The mobile receiver detects the pair of transmissions from sites 1 and 2, and determines the difference in arrival times Δt_{12}. This time difference can be translated into a path length difference as follows:

$$d_1 - d_2 = c\Delta t_{12}$$

As in the direction of AOA, it has been assumed that the radio-wave velocity is approximately equal to the speed of light (which may not be true in certain applications). Substituting the unknown coordinates of the mobile and the known coordinates of sites 1 and 2 (as shown in Figure 1.2) into the previous equation, the following could be obtained.

$$\frac{x^2}{a^2} - \frac{y^2}{b^2} = 1$$

where $a = 0.5c\Delta t_{12}$ and $b = 0.5(4D^2 - c^2\Delta t^2_{12})^{1/2}$. This is a hyperbolic function with the two sites as foci of the hyperbola. It should be recalled that a hyperbola is a collection of points with a constant difference between the distances to each focus. Similarly, another hyperbola h_2 can be derived. The intersection of these two hyperbolas is the mobile location.

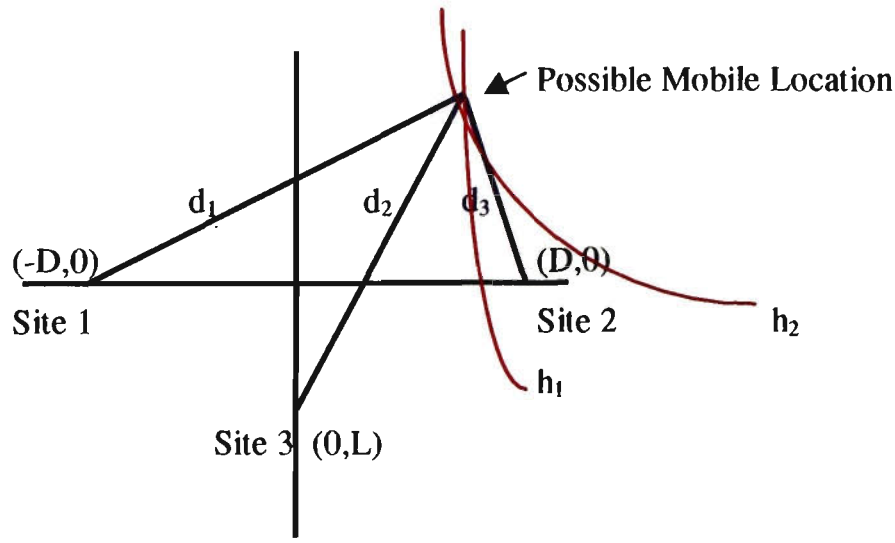

Figure 1.2: *Location determination by time distance of arrival (TDOA).*

Use of the TDOA technique for real-time location calculations requires fewer antennas and is less susceptible to signal blockage, or multipath reflection than using AOA. The main disadvantage of TDOA is the requirement for maintenance of a synchronised time

source between all base sites. It may be difficult to implement and maintain the multisite synchronised time keeping accuracy required to measure the propagation of a RF signal. It should be noted that this may not present a problem to the CDMA-based network at all since its sites have already been synchronised. Radio waves have a speed of approximately 300 m/μsec, so that 1 μsec (one millionth of a second) time error in a single site could place a mobile 300m away from its actual position. Most location systems require a position accuracy of less than 300m. In fact, the Federal Communications Commission (FCC) and the Emergency 911 (E911) Reports and Orders [2] requires the United States cellular network to be able to locate at least 67 % of the E911 calls within 125 metres accuracy by October 1, 2001.

Another problem with TDOA is that channel bandwidth may impact the performance of this technology. The time difference measurement in TDOA may be affected by the narrow channel bandwidth since high-resolution time measurements require a narrow pulse (or equivalent), and the narrower the pulse the greater the bandwidth required. By contrast, narrow channel bandwidth is not a problem for the AOA technology. This makes TDOA less accurate in narrowband analog systems than in wideband systems. To improve overall accuracy of location, some implementations have attempted to use a hybrid of the two techniques (TOA/AOA, AOA/TDOA, etc.).

Another form of terrestrial-radio-based location technology has been developed by Pinterra [3], [4]. This system uses signals from commercial FM radio stations in conjunction with a reference station to calculate the location. This technique uses the pilot tones of FM stations (which are generally in the range of 19 kHz) to calculate the location. The location is determined via triangulation: The mobile receiver converts the phase measurements to the range measurements based on the signals received from at least three radio stations. This technology requires installation of a reference station (observer) at a known location in each metropolitan area. The reference station calculates phase and frequency drift corrections for each FM radio station. These corrections are transmitted to the mobile receiver over a FM subcarrier or other broadcast medium to synchronise the transmissions and stabilise the frequencies. This technology has the

advantage of wide coverage due to the high concentration of FM stations in many countries. FM stations can often cover up to 20,711 km^2. Additionally, since FM broadcasts utilise frequencies (87 – 108 MHz) that are lower than GPS or cellular networks, the signal is less affected by obstacles such as buildings or hills. Because the FM signals can penetrate into buildings, this technology can be embedded with many portable devices often used indoors. The system has a claimed accuracy of 10 to 20 metres.

1.4 Project Formulation

1.4.1 Objectives of the work

General Aim

The research objective of the project is to develop intelligent methodologies for improving the accuracy of mobile positioning in the cellular communications system. The research is targeted at a real-time implementation using existing communications technologies.

Specific Aims

In order to achieve the overall aim of the project the following activities need to be fulfilled:

1. Develop a simulation model for mobile positioning using the Matlab environment. This model could be used to evaluate a rough mobile location. The performance of the model needs to be verified and compared with the conventional models for mobile positioning.
2. Design and simulate an intelligent control system for the positioning model. Different structures will be investigated in order to obtain the best possible accuracy.
3. Investigate the theoretical aspects of the performance and the accuracy of the proposed logic controller compared with other existing techniques.
4. Prove that a proposed method allows for significant improvement in accuracy and realibility.

1.4.2 Methodologies & Techniques

1. The primary disciplines, which one needs to research in this project in order to develop a successful and an accurate mobile location are Mobile Communications and Fuzzy Logic and Control. Knowledge of these disciplines is needed to analyse and develop algorithms capable of extracting information about the strength of the signals. An intelligent controller to make the necessary adjustments for improving the accuracy in locating the mobile unit may then use this information.

2. The structure of the controller will take a form of an adaptive learning algorithm for tracking the mobiles movement. Such a controller will be developed using either or a combination of fuzzy logic and neural networks.

3. Development, testing and refinement of all theoretical work will be accomplished by using a software simulation package. This also provides an environment for testing ideas and concepts before committing to an in depth analysis. Computer simulations will be used to evaluate performance criteria and to collect results for an algorithm comparison and development.

1.4.3 Thesis breakdown

Chapter 1

This chapter gives an introduction to general cellular communications and introduces the idea of mobile positioning. The chapter concludes with the project formulation including the aims of the project, its techniques and methodologies.

Chapter 2

This chapter is a literature review chapter of past work and published papers on cellular communications and mobile positioning.

Chapter 3

Chapter 3 introduces some existing positioning models. Some of the models summarised in the chapter are the Ericsson model and the Cambridge Positioning Systems Limited model.

Chapter 4

This chapter looks at a brief breakdown of the Ericsson model, proposed and developed by Ericsson, Sweden.

Chapter 5

This chapter concentrates on summarising the Ericsson model proposed by P. Lundqvist, H. Asplund, S. Fisher and E. Larsson, in greater detail.

Chapter 6

Chapter 6 introduces two positioning methods. The Up-Link TOA method, and the Enhanced-Observed Time Difference (E-OTD) method.

Chapter 7

This chapter looks at the calculation and statistical evaluation of two positioning methods. The first method named "Average Algorithm" positioning method is the work of Ericsson. Method 2 in this chapter named "More Preferable Solution" positioning method is my own method, developed to improve the accuracy in mobile positioning over method 1.

Chapter 8

This chapter firstly gives a brief background in fuzzy logic, before using this fuzzy theory to produce another positioning method named "Enhanced Fuzzy" positioning method. The method once again is my own work, with an aim to improve method 2.

Chapter 9

This chapter compares the techniques and results of all three methods concluding with the most successful method. It also gives the reader some direction for future work in this area.

CHAPTER 2

THEORETICAL INTRODUCTION & LITERATURE REVIEW

2.1 Introduction

Fuzzy logic has been successfully adopted in many real-world automatic control systems including automobile transmission, subway systems, industrial robots, washing machines, cameras and air-conditioners. In contrast, the utilization of fuzzy logic in mobile communications systems is recent and limited. Understanding general mobile communications, in particular the meaning of handover and its operations is essential to a researcher in order to go on and develop a mobile positioning application. It can be explained by the fact that the two problems are interrelated and may have similar solutions. Due to this reason, a fair research in handover was first performed, before any of the research in mobile positioning. This literature review analyses some handover and positioning algorithms applied in mobile communications and then studies a feasibility of fuzzy logic application to improve handover and positioning quality.

2.2 Analysis of Handover Algorithms

Handover is the mechanism that transfers an ongoing call from one cell to another as a user travels through the coverage area of a cellular system. As smaller cells are developed to meet the demands for an increased capacity, the number of cell boundary crossings increases. Each handover requires network resources to reroute the call to a new base station. Minimising an expected number of handovers decreases the switching load. The design of reliable handover algorithms is crucial to the operation of a cellular communications system and especially important in micro-cellular systems where the mobile may traverse several cells during a call.

Handover decisions can be based on various measurements such as the signal strength, bit error rate and estimated distances from base stations. The most widely discussed handover algorithms are those based on the average signal strength [5,6,7], although other "link quality measurements" based on the bit error rate, Signal to Noise Ratio(SNR) and distance have been proposed or utilised. In this review I focus exclusively on a

handover algorithm that is based on the received signal strengths from a number of serving base stations. The mobile measures the signal strength from the base stations. From these measured data a decision is made whether a handover should be made or not. If a handover needs to be made, a new base station is selected. If a mobile measures the signal strength from M different base stations, the handover decision can in the most general way be described as: $b(n) = F(B_0(n), B_1(n),.....B_{M-1}(n))$

where $b(n) \in (_{0,1,.....,M-1})$

$B_i(n)$ is the sequence of samples from base station number i up to sample number n. The function F is evaluated at each sample and the result b(n) is the handover decision. If $b(n) = b(n-1)$ no handover is made, on the other hand if $b(n) \neq b(n-1)$ a handover is made to the base station number b(n). Whether the mobile itself makes the decision or whether it transmits the measured data back to a fixed network and lets the network judge is not considered in this review. However, the call might be lost if the channel response to the base station is so inferior that the measured data cannot be sent reliably. The only results of the performance of handover algorithms that have been presented are results from simulations [8], [9], [10], [11].

There are previous studies that show that recording the received signal strength at the base station may not be reliable for handover decisions, especially in systems employing power control [12]. Kelly and Veeravalli [13] focus exclusively on handover decisions derived from signal strengths taken at the mobile rather than at the base station. Previous, more detailed research has shown that recording measurements at the base station is more cost efficient and is also conscientious for experiments due to the stability and location of a base station. Maturely to these reasons, my focus in the research is on recording measurements of signal strength at the base stations rather than at the mobile.

2.3 Signal Strength Model

This signal model was proposed by Mikael Gudmundson [14]. The model of the received signal power at the base station, s(t), can be written as:

$s(t) = m(t)*r(t)$, where:

m(t) is the local mean of the received signal and assumed to be lognormally distributed [4]. r(t) is a fast fading component that is assumed to be removed by a low pass filter at the receiver. Since m(t) is lognormally distributed, it is preferably to study the sampled signal in dB, therefore the discrete time signal A(n) is defined as:

$$A(n) = 20 \log[\, m(nT) \,].$$

The distribution of A(n) is Gaussian with average α and standard deviation σ. σ is typically in the range between 5 and 12 dB. The average α is dependent on the distance d between the base station and the mobile as:

$$\alpha = (K_1 - K_2) * \log(d),$$

where K_1 depends on the transmitted power in the base station and K_2 typically is a constant in the range of 20 (corresponding to the direct line-of sight propagation[1]) to 60. When the mobile is moving the average α is not constant therefore A(n) in general will not be a stationary process. Consequently, if the average $\alpha(n)$ is subtracted from A(n), the difference A'(n) will be stationary process with zero mean and the same standard deviation as A(n).

$$A(n) = A'(n) + \alpha(n).$$

The signal $A(n) = 20 \log[\, m(nT) \,]$ in two points separated by the distance of D is assumed to have the correlation ε_D. Further it is assumed that the correlation is decaying exponentially with distance. If the mobile is moving with a velocity v and the sampling interval is T the autocorrelation of A'(n) will be:

$$R_A(k) = E\{ A'(n) A'(n+k) \} = \sigma^2 a^{|k|}$$

where

$$a = \varepsilon_D^{vT/D}$$

[1] Subscribers moving in urban microcells will encounter two types of handovers, the line if sight (LOS) handover from one LOS base station to another, and the non-line of sight (NLOS) handover from a LOS base station to a NLOS base station [15].
Reliable handovers are difficult in the LOS case due to the propagation phenomenon known as the "corner effect" [5]. In the corner effect, the mobile encounters a sudden large reduction in the signal strength with the serving base station as it rounds the corner and loses the LOS component. Consequently, the call will be dropped if the mobile is moving quickly and/or the handover is not performed fast enough. To avoid this problem fast moving mobiles can be connected to "umbrella cells" (overlaid macrocells) so that the NLOS handovers are avoided altogether.

2.4 Analysis of Positioning Algorithm

As shown above there have been a number of handover problems and tasks appearing in the cellular communications system and a lot of solutions have been proposed for each problem. However, another very enticing topic, which is reasonably new to the cellular communications system, is locating or positioning of a mobile unit. Just like with handover, positioning of a mobile unit utilizes the signals transmitted from base stations in cellular communications system.

An interesting application of a mobile positioning is by using the CDMA (Code Division Multiple Access) network [16]. A CDMA network was first proposed by QUALCOMM [17,18] and performance tests have been successful. Here, the mobile measures the arrival time differences of at least three pilot tones[2] transmitted by three different cells. By intersecting hyperbolas the mobile position can be estimated. The accuracy of the positioning depends on the sampling rate and the multi-path environment. The mobile detects the pilot tones that are transmitted from at least three cell sites and measures the time differences between them as shown below in fig1.

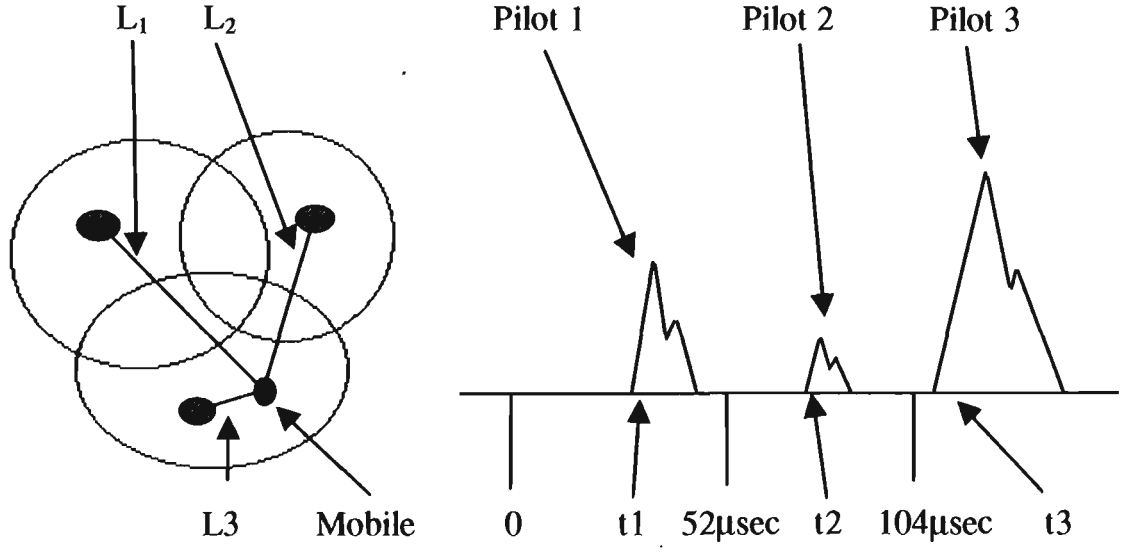

Figure 2.1: *Arrival times of pilot tones to the Mobiles.*

The differences between the pilot tone's arrival times are:

$$L_1 - L_2 = (t_2 - t_1 - T_1) * c$$

[2] The pilot tone is the reference channel used, which is a main down-link channel. The pilot tone transmitted by each cell is used as a coherent carrier frequency for synchronisation by every mobile in that coverage area. The pilot tone is transmitted at higher TX level than the other channels thus allowing extremely accurate tracking.

$$L_3 - L_2 = (t_3 - t_2 - T_2) * c$$

$$L_3 - L_1 = (t_3 - t_1 - T_3) * c$$

where T_1, T_2 and T_3 are fixed code phase differences between the pilot tones, t_1, t_2 and t_3 are path delays of three different pilot tones, c is the speed of light and L_1, L_2 and L_3 are the distances between the base stations and the mobile.

The calculation can be performed at the mobile or the information sent to the Base Station (BS) to reduce the processing time in the mobile. The position of the mobile is calculated by solving the following hyperbolic functions (refer to figure 2):

$$\sqrt{(X_2-X_m)^2 + (Y_2-Y_m)^2} - \sqrt{(X_1-X_m)^2 + (Y_1-Y_m)^2} = L_2 - L_1$$

$$\sqrt{(X_3-X_m)^2 + (Y_3-Y_m)^2} - \sqrt{(X_2-X_m)^2 + (Y_2-Y_m)^2} = L_3 - L_2$$

$$\sqrt{(X_3-X_m)^2 + (Y_3-Y_m)^2} - \sqrt{(X_1-X_m)^2 + (Y_1-Y_m)^2} = L_3 - L_1$$

X_1, X_2, X_3, Y_1, Y_2, Y_3 are known as Base Station locations. X_m and Y_m are the mobile coordinates.

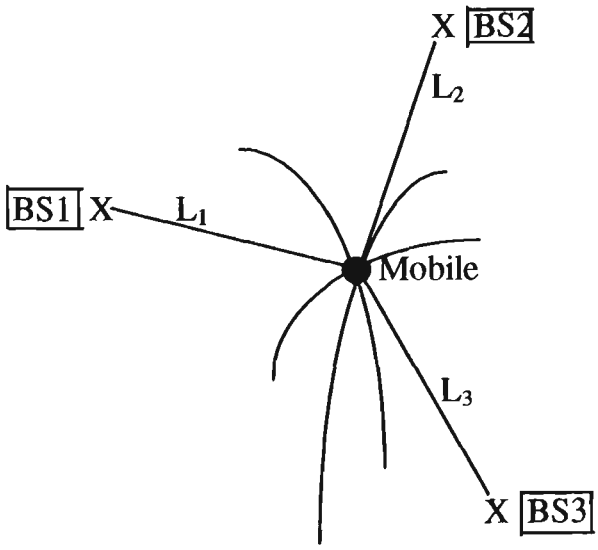

Figure 2.2: *Position finding by use of hyperbolas.*

A further pleasing application of mobile positioning is the method of Automatic Vehicle Location (AVL) presented by Song [19]. Here, a special device is embedded into a cellular mobile phone installed in a vehicle. When this vehicle is travelling through a

cellular territory, the device receives signals from serving base stations and calculates the attenuation of the signals to locate the current vehicle position.

Based on the above contention concerning handover and mobile positioning, I would like to propose a simple mobile distribution, which could be a right commencement of research in determining a mobile unit location.

2.5 Mobile Position Distribution

Clusters of hexagonal cells that are repeated all over the service area can represent the cellular system. The base stations are positioned in the centre of each cell. In the sequel we consider only those two base stations that are closest to the mobile, and at the distance of say D from each other. In this case it will be sufficient to study the rhomboid $\Re$ between the two given base stations as shown in fig3.

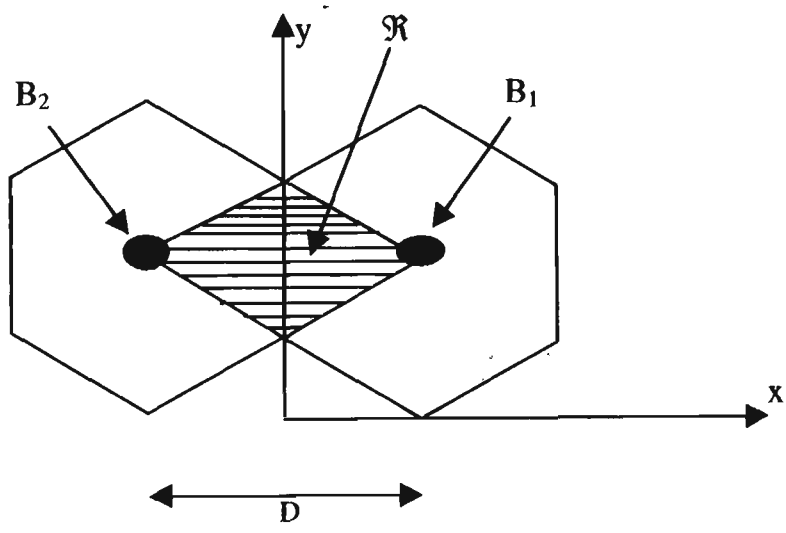

Figure 2.3: *Area of possible mobile positions.*

Here the mobile is assumed to be anywhere in the rhomboid $\Re$ with an equal probability, and outside $\Re$ with zero probability.

2.6 Fuzzy Logic

The field of fuzzy control systems is one of the most active and fruitful areas of research, in which the fuzzy set theory is applied. Fuzzy set theory was first introduced by Zadeh [20] in 1965, when he formulised qualitative concepts that had no precise boundaries.

Zadeh realised that people could base their decision on imprecise, non-numerical information. In his early work (1965), he indicated that humans could control and operate under complex, uncertain and new situations better than machines.

A very general definition, which encompasses the majority of Fuzzy Logic Control (FLC) systems, may be formulated as follows:

> *A FLC is a system which enhances the performance, reliability, and robustness of control by incorporating knowledge, which cannot be accommodated in the analytical model upon which the design of a control algorithm is based, and that is usually taken care of by manual modes of operation, or by other safety and ancillary logic mechanisms* [21].

The general architecture of FLC usually consists of three main parts, which make the following operations:

1) Fuzzification 2) Fuzzy Processing 3) Defuzzification.

1) Fuzzification;

In this phase the crisp input to the controller is converted into a fuzzy value or symbolic representation. Generally, inputs to the FL Controller are non-fuzzy in nature, but the data manipulation in a FL Controller is based on the fuzzy set theory. Hence, fuzzification of the input is necessary. To transform non-fuzzy inputs (crisp) into fuzzy inputs, membership functions must first be determined. Once membership functions are assigned, fuzzification takes a real input value and compares it with the stored membership function information to produce a fuzzy input value.

2) Fuzzy Processing

In this phase, fuzzy inputs are processed according to the rule base, which is the set of rules representing the available knowledge in some domain. The inference process takes the fuzzy value produced in the fuzzification process and produces a fuzzy output through *symbolic reasoning* based on the former knowledge stored as a set of rules. To

express knowledge by means of fuzzy rules one needs logical connectives. The most used logical connectives in standard fuzzy controllers are: AND and THEN [22]. For implementation of the operators the so called T-norm method is applied [20].

Although many inference methods and approaches are reported in the literature [23], the most frequently used inference methods are:

1) Mamdani (*symbolic*) type of rules that was implemented in the first applications of fuzzy control [24,25]. The consequence of this type of rules is a symbolic one, which means that the controller output is large. The Mamdani type of rules produces a fuzzy controller output as a result of the fuzzy inference process, which has to be defuzzified to obtain a numerical controller output.

2) The other type of fuzzy rules is a Sugeno type rules [26], where the consequent of a fuzzy rule is a linear function of the controller input.

3) Defuzzification

This last step is the reverse of the fuzzification operation. The fuzzy output from the rule base is transformed into a crisp value realisable by the plant or system under control. Dividing the output universe of disclosure into several intersecting areas (membership functions) performs this operation. A closer look at an influence of this specific part of a fuzzy controller is worthwhile. The best known defuzzification methods are: centre of area or centre of gravity (COG), fuzzy mean (FM) or centroid, weighted fuzzy mean (WFM) and mean of maxima defuzzification methods [27].

Choosing a wrong defuzzification method can adversely affect the results achieved by the inference of fuzzy rules. It appears that an application of a specific defuzzification method can also affect the characteristics of a fuzzy controller. For example, using the weighted fuzzy mean (WFM) method transforms a Mamdani type controller to a Sugeno type. Speed and accuracy are the most important criteria for validating any defuzzification techniques used.

The block diagram below represent the general architecture of a FLC.

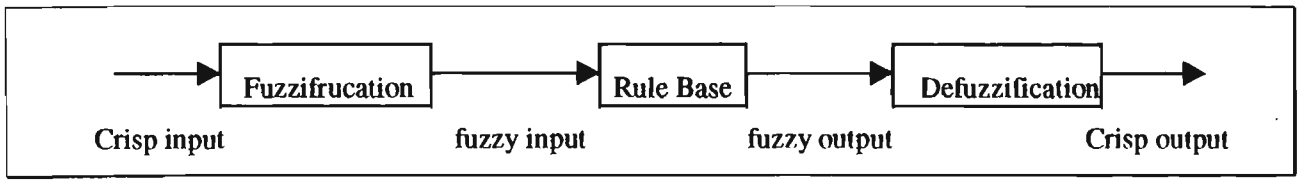

Example rule:

if temp is very hot
then fan-speed is high

As presented previously, some handover algorithms attempt to dynamically adjust either the signal averaging or the hysterisis level. Adaptive signal averaging algorithms have recently been performed based on the estimation of the maximum Doppler frequency and the velocity estimation. These algorithms were shown to outperform their constant counterparts. Consequently, the authors of some previous papers were motivated to use fuzzy logic with an aim to improve handover decisions, in order to decrease number of handovers.

A handover algorithm referred to as the *Fuzzy Adaptive Averaging-interval and Hysteresis threshold handover* (FAAH) is introduced in [28]. The design of the algorithm is intended to be used under a lognormal fading environment. The algorithm employs two fuzzy logic controllers. The first controller takes into account a signal variation and a change in averaging interval (AVG) accordingly. The second controller dynamically adapts the hysteresis level (HYS) with signal differences between two base stations. Conventional algorithms with fixed signal averaging interval and/or fixed hysteresis level have a lack of flexibility under changing mobile environment. The FAAH is designed to strike a balance among handover frequency, averaging delay and the chance of a lost call. The experimental procedure consists of a so-called 'testbed' model constructed used to test handover algorithms. The handover problem is formulated as a one-dimensional problem. The 'testbed' uses two base stations, BS1 and BS2. The mobile unit moves with constant speed from BS1 to BS2 along the straight-line path. This is similar to users travelling in a vehicle at a constant speed on highway.

The received signal r(d) from either BS1 and BS2 is the sum of path loss and lognormal fading l(d) as:

$$r(d) = K_1 + K_2 \log(d) + l(d)$$

where d is the distance from either BS1 or BS2. The parameter K_1 is determined by the transmitter power, and K_2 is the propagation constant. The lognormal fading process is generated with zero-mean white Gaussian processes passed through a single-pole autoregressive filter. The autocorrelation of the filter's impulse response is set to be:

$$Rs(d) = \sigma_s^2 \exp(-d/d_o)$$

where σ_s is the standard deviation of the white Gaussian process, d is the distance from either BS1 or BS2, and d_o is the correlation distance. Multipath fading is not considered as the fading is averaged out in the time averaging process.

The table below summarises the numerical values used for simulation.

Number of base stations	2
Frequency	900 MHz
Mobile unit trajectory	Straight Path
Sampling distance	1 metre
Mobile unit step size	1 metre
Fading Process	Lognormal Fading
Standard Deviation (σ_s)	6 dB
Transmitter Power (K_1)	0
Path Loss (K_2)	30
Decay Factor of Exponential Correlation Function (d_o)	20

Table 2.1: *Simulation Parameters*

The handover process is illustrated in Fig 4. At each sampling time, the signal strengths are measured and directed to the handover controller. The signal measured from each base station is averaged with a rectangular window of fixed size of 10 sampling time. A constant hysteresis of 6dB is added to the averaged signal of the previous connected station in order to discourage handover to a weaker station. The handover controller with fixed averaging interval (AVG) and hysteresis threshold (HYS) is shown in figure 4a.

The values of the AVG and HYS are chosen to optimise the result on the number of handovers and averaging delay. The FAAH controller is shown in figure 4b. The values of AVG and HYS are constantly changed in order to optimise the handover performance.

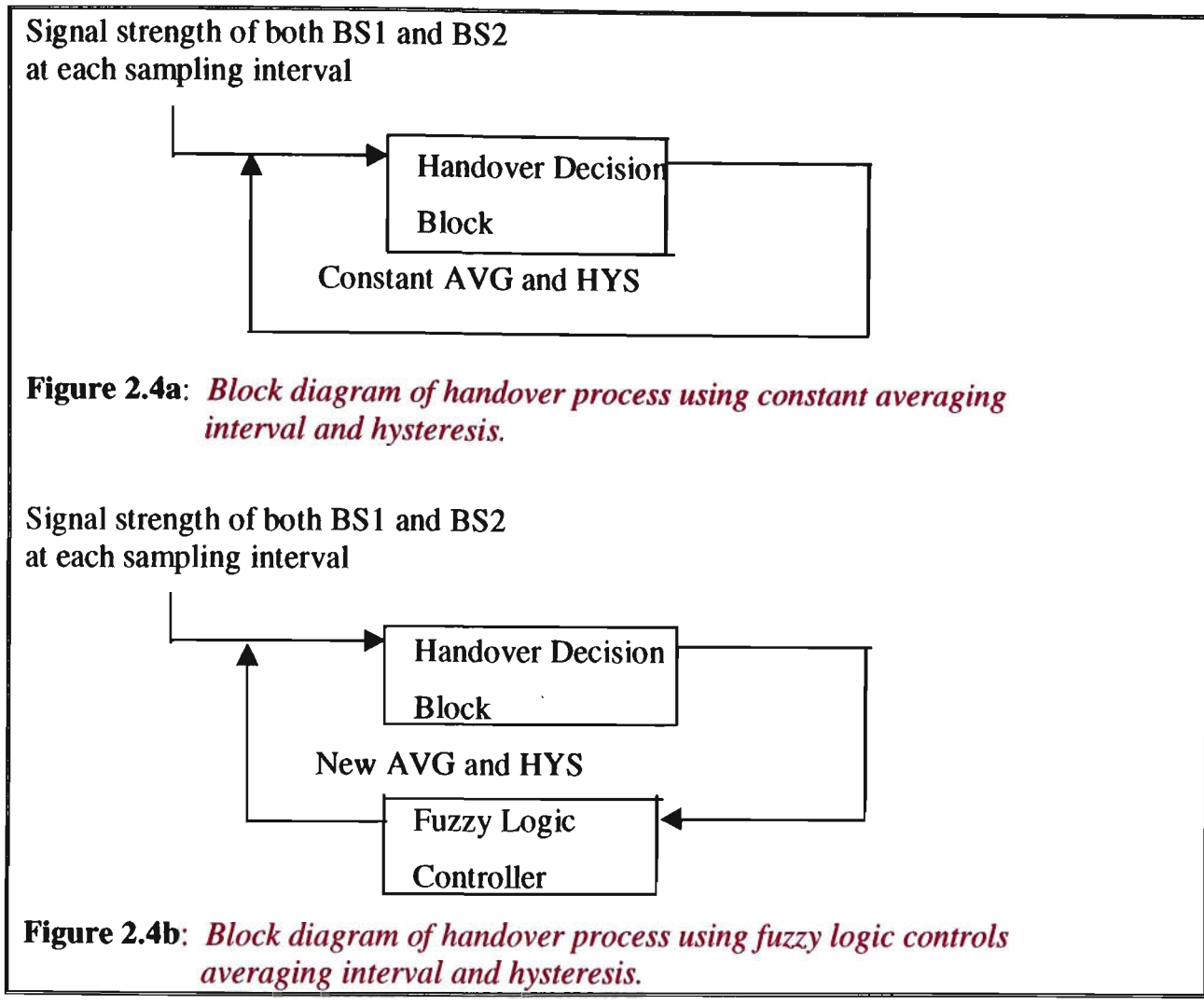

Figure 2.4a: *Block diagram of handover process using constant averaging interval and hysteresis.*

Figure 2.4b: *Block diagram of handover process using fuzzy logic controls averaging interval and hysteresis.*

Figure 2.4: *Handover Process*

The control rules and the corresponding membership functions are formulated to take into account a delay due to averaging interval, chance of losing the call, and the number of handovers.

The experimental results demonstrated that FAAH enhances the system handover performance over conventional algorithms by about 50%.

An application of fuzzy logic to improve the handover characteristics of cellular wireless communications systems is introduced in [29]. The effect of different membership functions and decision rules on the performance of a fuzzy logic aided handover procedure is investigated in a typical mobile radio environment. Sugeno inference method is used and the results are compared with the conventional approach.

In conventional handover strategy, the handover decision is based on the difference between d_i of the received signal strengths from two competing base stations. In the scenario depicted in Figure5, the mobile unit is moving from base station A to base station B at a constant speed V. A and B are D meters apart and the mobile is currently d meters away from the base station A.

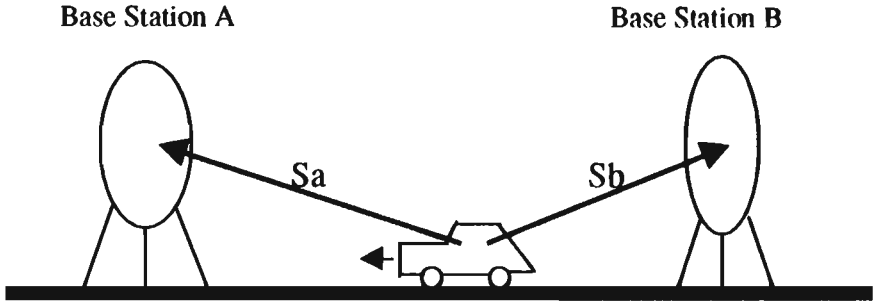

Figure 2.5: *Mobile communications with two base stations A and B[19].*

In an ideal environment without shadow fading, the received signal strengths Sa(d) and Sb(s) from the base stations A and B are given by

$$Sa(d) = K_1 - K_2 \log(d) \qquad (1)$$

$$Sb(d) = K_1 - K_2 \log(D - d) \qquad (2)$$

The constant K_1 relates to the transmit power from the base station, K_2 characterises the ratio path loss (with $K_2 \cong 30$ being typical in urban environment).

Unfortunately, shadowing in the real-world environment makes the received signal strength unpredictable. In this environment, the mobiles received signal strengths (in dB) from the base stations A and B are respectively:

$$Sa(d) = K_1 - K_2 \log(d) + u(d)$$

and

$$Sb(d) = K_1 - K_2 \log(D - d) + v(d)$$

The random variables u(d) and v(d) account for the random signal fluctuations due to shadowing effect of the surrounding terrain. The result from many propagation measurements shows them to follow the well-known lognormal distribution. On that account mathematically, both u(d) and v(d) are modeled as independent identically distributed zero-mean Gaussian random variables with standard deviation σ_s.

CHAPTER 3

EXISTING POSITIONING MODELS

3.1 Introduction

When presenting a mobile positioning application, a researcher must first derive a model to be utilized for locating a mobile. This chapter describes some existing models that have been utilised for positioning in the cellular communications system.

3.2 Ericsson Model

Lundqvist [30] describes a channel model, which has been developed for use in a Wireless Positioning Project. The model was subsequently submitted [31] to T1P1, the body responsible for the Global System Mobile (GSM) standardisation in the U.S. The model is quite general and can also be used for other purposes than to evaluate position.

The channel model has the following features:

- Based on physical, measurable parameters, such as: power delay shape, delay spread, angle of arrival distributions and fading statistics.
- Wide-band model.
- Short-term behavior of the channel is modeled.
- Represents the general channel behavior in a range of typical environments, corresponding to geographically diverse conditions.
- Antenna diversity.

Generation of the modeled radio channel for a specific MS-BS configuration is a six-step process. The six steps are:

1. Generate the delay spread
2. Generate an average power delay profile (apdp)
3. Adjust the power delay profile so that it produces the desired delay spread.
4. Generate short-term fading of the impulse response by the physical process of summation of partial waves.

5. Generate multiple, partially correlated channels for multiple BS antennas (space diversity).
6. If desired, filter to any lower bandwidth.

Even though the model is quite good there are some limitations to it. The following limitations of the model should be kept in mind, so as not to apply the model outside its area of validity.

- Wide-Sense Stationarity is assumed, so dynamic changes in the propagation environment are not modeled. All movements of the mobile are assumed to be on a local scale, with no movements around street corners or into houses etc.
- The model, especially the delay spread model, is intended to give the average behavior rather than to be able to reproduce the specifics of any given real-world location.

The above mentioned channel model is described at a greater level in chapter 6, where the mathematical aspects of the model are considered.

3.3 Cambridge Positioning Systems Limited

The model described below was used by Cambridge Positioning Systems Limited [32].

In order to model position fixes, one reasonable distribution available is an elliptical gaussian, characterised by its central coordinates, major and minor axes and an angle of rotation. It is shown, with reference to result [33], that in some cases this is indeed an accurate model. In fact, the RMS of those results gives a good estimate for the 67 percent confidence region.

The key factor in this discussion is that, except in the special cases mentioned above, a set of position fixes cannot be modeled as having been drawn from a single, simple distribution. The shape of any realistic distribution has to depend on the geometrical disposition of the handset with respect to the Base Stations (BSs) that were used in the position calculation. The single distribution model can therefore only be used on position measurements taken from a fixed location (and sometimes not even then, if the BS list is unstable).

Each position measurement is then treated as having been drawn from its own unique elliptical distribution. The shape of this distribution can be predicted from the covariance matrix in x and y which falls naturally out of any least square position calculation. Cross [5] gives a derivation of the least square solution and discusses covariance matrices in detail.

Simplistic "circular" Model

Consider a set of N position fixes, $\{r_n\}$ with n = 1..N, where

$$r_n = \begin{pmatrix} x_n \\ y_n \end{pmatrix}$$

is the two-dimensional vector position of the nth fix, all being taken from a single known location:

$$R = \begin{pmatrix} X \\ Y \end{pmatrix}$$

For simplicity X and Y are set to equal zero. If the effects of geometry and multipath described above did not exist, a Gaussian distribution of position fixes, centered on the actual position could be expected. This distribution is given by

$$P(x, y) = \frac{1}{2\pi\sigma^2} e^{\frac{-(x^2+y^2)}{2\sigma^2}}$$

This "circular" distribution $P(x,y)$ is shown in figure 3.1.
It can easily be shown by changing to polar coordinates (r,θ) and by integrating over θ that the expected distribution of radial errors is given by:

$$P(r) = \frac{r}{\sigma^2} e \frac{-r^2}{2\sigma^2}$$

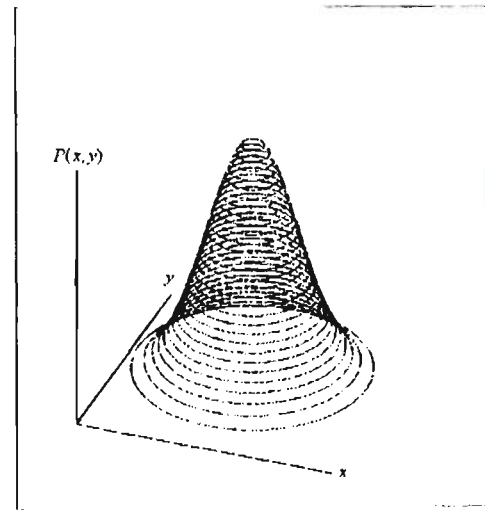

Figure 3.1: *Circular Distribution*

As expected, the distribution of radial errors is not Gaussian. The following figure shows a plot of *P(r)*.

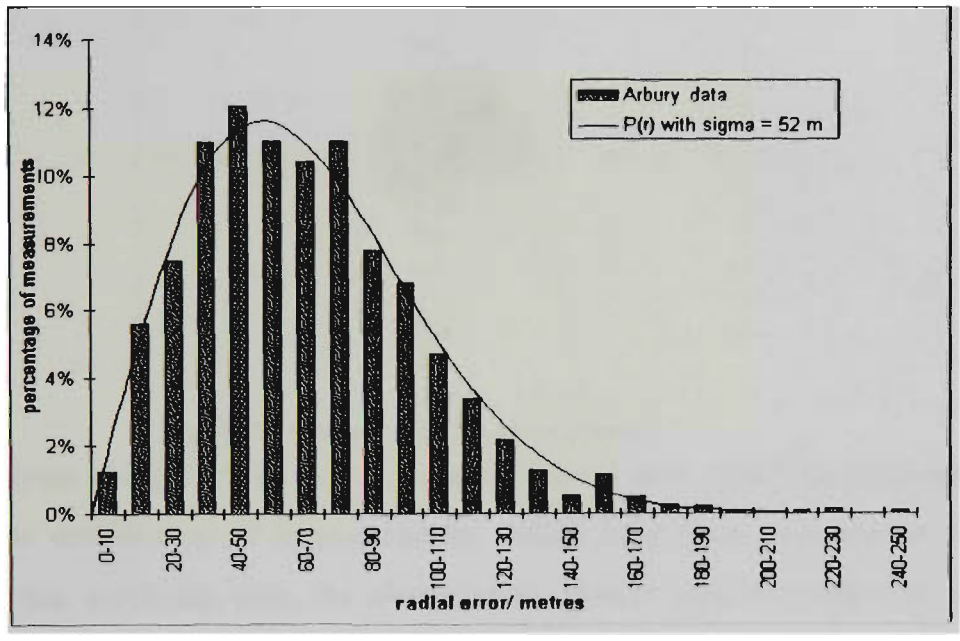

Figure 3.2: *The observed and predicted, spread of measurements.*

Therefore the RMS error is found to be:

$$\sqrt{\int_0^{inf} r^2 P(r)dr} = \sqrt{2\sigma}$$

Even though the above is a simple model, the confidence level given by the RMS is only

$$Confidence\_level = \int_0^{\sqrt{2\sigma}} P(r)dr = 1 - e^{-1} = 63.2\%$$

63 %, as it's shown below:

A circle of radius:

$$\sqrt{2\ln 3}.\sigma = \sqrt{\ln 3}.RMS$$

bounds the 67 % region, predicting that when analysing data taken from a single location, to meet the E911 requirements, a RMS value of 119 metres is required.

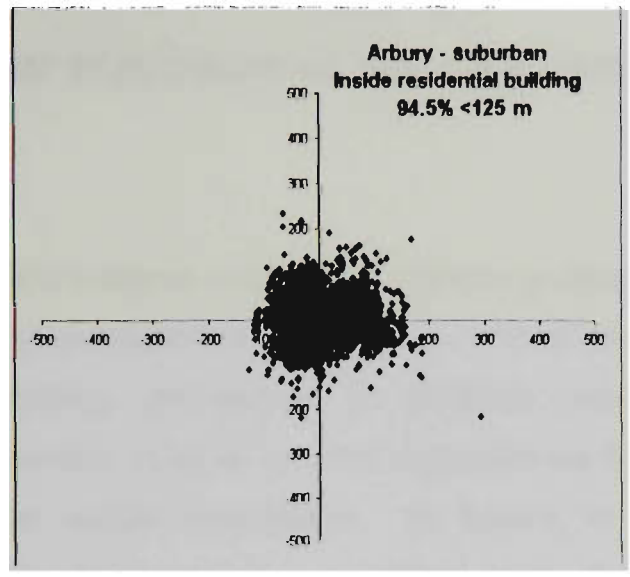

Figure 3.3: *Results from residential area.*

The result shown in figure 4.3, taken from a residential area, suburban environment [33] has a circular distribution of measurements, which have been centered on the actual position. In this particular case, the above model should very well apply to this plight [34].

CHAPTER 4

ERICSSONS' POSITIONING MEASUREMENTS SYSTEM

4.1 Introduction

In order to evaluate and compare results from different positioning methods, it is highly desirable to define a common positioning simulator. One of the most important effects in evaluation of positioning performance is multipath propagation. Results and performance of positioning systems are very dependent on how severe the multipath propagation is in the certain environment. As known, in mobile communications multipath is of a high order in more dense populated areas. Due to this case a simulator is more efficient than field trails when evaluating performance with respect to multipath, since it can model a vast number of radio channels. Again due to the importance of multipath, it is essential to define a common channel model when comparing positioning performance.

This chapter looks at Ericssons proposed positioning simulator, focusing on the system simulator, radio link simulator and the channel model. The proposed channel model has a multipath statistic that corresponds to a large number of field measurements. Additional explanation of the channel model is described in chapter 5.

4.2 Positioning Simulator

Simulating the measurement performance over a radio link is not sufficient enough in order to evaluate the positioning performance. Therefore an integrated positioning simulator is required.

The positioning simulator constructed by Ericsson can be divided into the following parts (see figure 4.1):

- A System Simulator (refer to section 4.2.1)
- A Radio Link Simulator (refer to section 4.2.2)

- A Channel Model (refer to section 4.2.3)

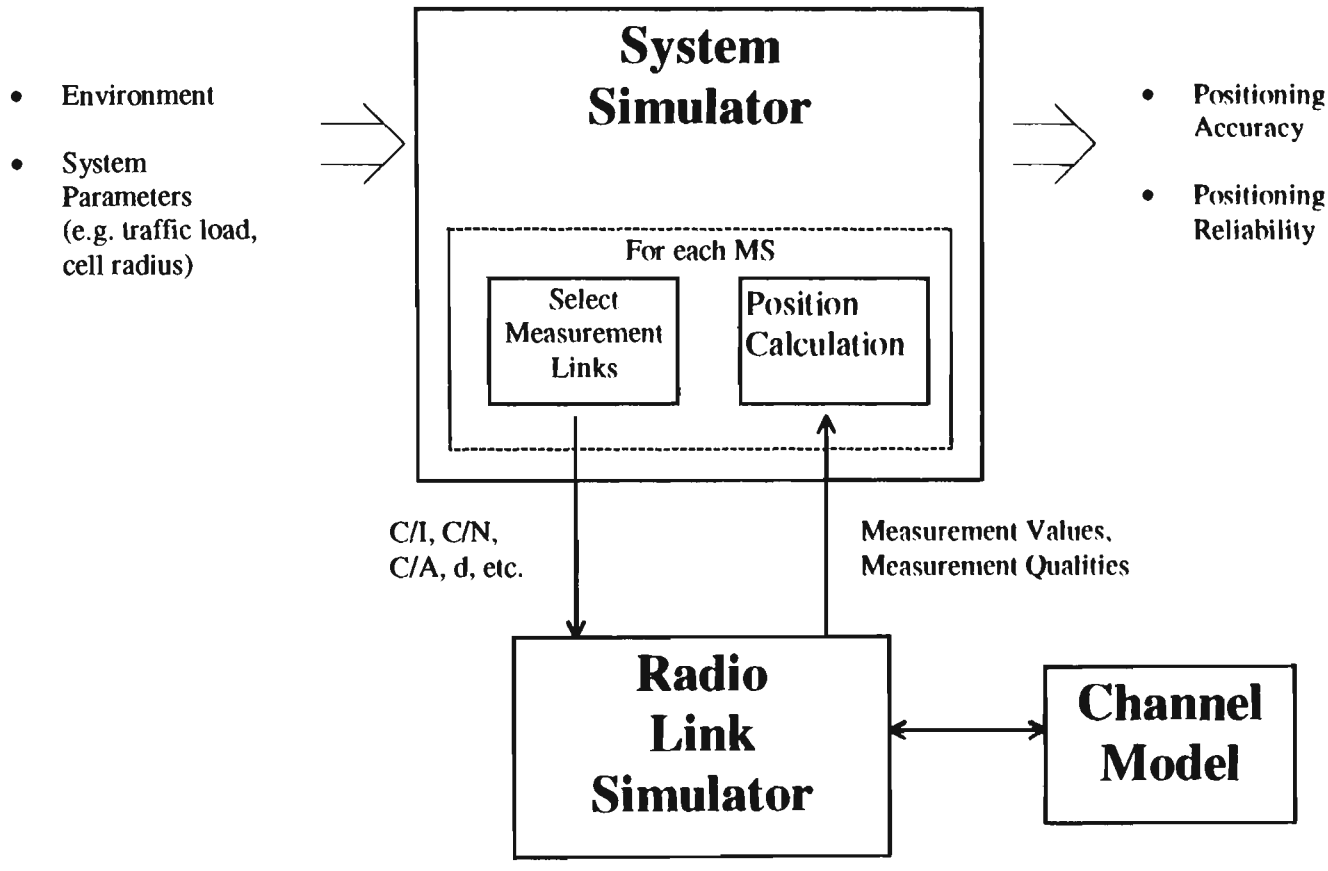

Figure 4.1: *Positioning Simulator*

4.2.1 System Simulator

4.2.1.1 Structure of the System Simulator

Initiation

The System Simulator is the basis of the Positioning Simulator. Base stations are placed over an area in a uniform hexagonal pattern, and frequency plan is defined (see figure 2).

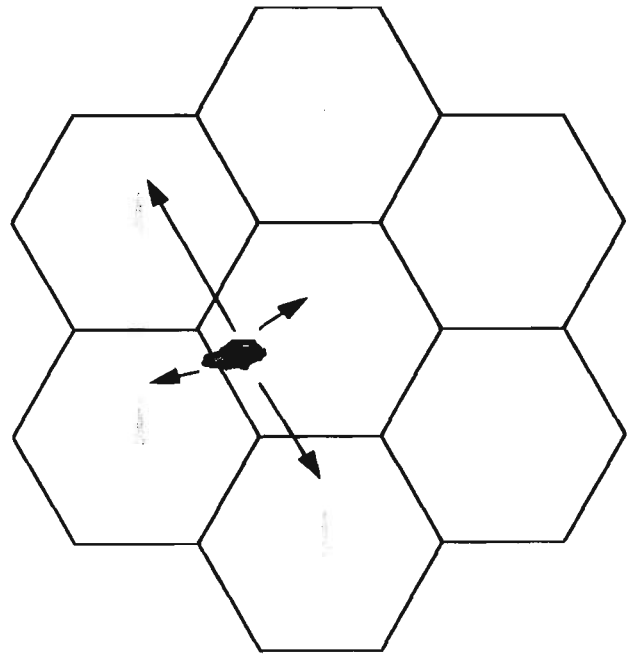

Figure 4.2: *System Simulator*

The frequency plan assigns each Base Station (BS) one Broadcast Control Channel (BCCH), and a number of traffic channels. Once the frequency plan is defined, mobile stations are randomly distributed. The number of mobile stations is chosen according to the desired offered traffic. MSs close to the borders of the cell area have a more advantageous interference. Therefore, in order to avoid this situation, a wrap around technique is used. This means that for example, if a MS is located on the northwest border, it can be distributed by BS on the southwest side.

A "lognormal fading map" is calculated, which determines the correlation of the lognormal fading between different points on the cell plan. Therefore parameters such as correlation distance for the lognormal fading and inter-BS lognormal fading correlation are taken into account. Fast Rayleigh fading is not modeled. The system simulator does

not deliver the mean Carrier/Interference (C/I) values. The mean C/I values are passed to the radio link simulator, which then simulated fast fading and multipath propagation.

Path Loss Calculations

The received signal power in the system is calculated as shown below:

$$P_r = P_t + G_a + L_p - a\log(d) + G_f$$

where P_t is the transmitted power, G_a is the antenna gain in the direction to the MS, L_p and a are environmental dependent constants, and G_f is the lognormal fading. The attenuation due to the transmitter-receiver distance is modeled according to the Okumura Hata formula:

$$g_{path-loss} = L_p + \gamma 10\log(d)[dB]$$

where d is the distance in km. Lp and γ can be found in [35]. Different antenna diagrams are used to define the antenna gain. The shadow fading due to for example houses or trees are modeled as lognormal distributed variables.

Channel Allocation

A system simulator can either be static or dynamic. Since the time duration of a positioning measurement is rather short, a static simulator is sufficient. Another reason for this choice is that snapshots of the system are taken. To model the dynamic behaviour of the system, handover margins are used. A certain mobile randomly tries to connect to a BS with a signal strength that is within the handover margin from the closest base station.

The traffic (call set-up and completion) can easily be defined by the Erlang concept of offered traffic. The offered traffic is translated into the number of MS in the static simulator, which means that the number of available channels in the system is fixed and finite. Therefore, only a certain number of the mobile stations are able to be connected. The ratio of connected MSs to the total number of MSs is calculated and is called channel utilization. The total number of placed MSs is chosen to give desired channel utilization [36].

C & I Calculations

Calculations are carried out on the total received signal powers and interference powers for all possible radio links, based on the channel allocations. Therefore, cochannel and adjacent channel interference is taken into account. For communications purposes, only C/I on the allocated channel for a particular MS is required, whereas for positioning purposes, C and I for all BS-MS radio links are required since measurements must be performed to more than one BS. At a later stage in the system, the radio link simulator receives the C and I values that were obtained in the system simulator. The radio link simulator is described in section 4.2.2.

Dropping calls with too low C/I

The Carrier/Interference ratio on the traffic channel is checked for low C/I values. If the C/I ratio is below 9 dB on the uplink or downlink channels, the MS is considered not to be able to maintain the call. If this situation is present, the mobile station is omitted from the calculation.

4.2.1.2 System Simulator Parameters

General Parameters

All parameters required for the system simulator are listed in the following table:

Parameters	Suggested values
Number of traffic channels per BS	6
Adjacent Channel Attenuation	18 dB
BS Antenna height	30 m
Lognormal correlation distance	110 m
Inter-BS Lognormal fading correlation	0
Handover margin	3 dB

Table 4.1: *General parameters to the system simulator.*

Power & Noise levels

In practice, the noise-limited environments will only be effected by the output power and by the receiver noise settings. In a real mobile system uplink and downlink are normally balanced, therefore the relationship between received power and receiver noise is equal. To compensate for a higher noise level recorded in the mobile station, and for uplink diversity gain, the BS output power is slightly higher than the output power of the MS.

Uplink (Access bursts on TCH)

For the uplink, the MS peak output power used is 0.8 W (29 dBm), and the receiver noise in the BS is –118 dBm. Two types of simulations have been performed. The first featuring the power control feature and the other without power control. The difference in the two types is follows:

1) Power Control.

   Power control is used in a real system. That is, MS output powers on the TCH channels are adjusted to reach a better interference situation. However, a MS to be positioned transmits access bursts with peak power. Therefore, using the power control feature enhances the C/I ratio for the positioning links by a large factor.

2) Without Power Control

   In this situation, all mobile stations transmit at peak power 100 % of the time.

Downlink (BCCH)

With the downlink signals, the BS transmits continuously with full power on the BCCH channel. The base station in this situation is not subject to any power control. Simulations are run for balanced links, which means that the relationship between transmission power and receiver noise is the same as for the uplink channel. It should be noted that absolute values of transmit power and noise power does not affect the result in any way, which indicates that their specification is not required.

Despite the above comments, the link budget is sometimes argued to be better for downlink than for uplink. The base station transmits with higher power (typically up to

40 W contrary to the MS's power, which corresponds to 0.8 W). However, the noise level in the mobile station is higher than that in the base station.

Environment Dependent Parameters

The table below shows four important parameters which all depend on the environment in which the mobile station is operating in.

Environment	Cell radius (m)	Standard deviation of lognormal fading	Lp@1km [dB] 900 MHz	Mean Channel Utilization (%)
Urban (indoor)	500	8.5 dB	126 + 13.5	80
Suburban (indoor)	1500	8.5 dB	116 + 13.5	80
Urban (outdoor)	500	6 dB	126	80
Suburban (outdoor)	1500	6 dB	116	80
Rural (outdoor)	10000	6 dB	98	40

Table 4.2: *Parameters dependent on environment*

Cell Planning

In modern mobile systems like today, 3/9[1] is a common reuse factor for traffic channels. For BCCH, 4/12 is commonly recommended. Both frequency planning 3/9 and 4/12 is investigated.

4.2.1.3 Output from the System Simulator

The following data is the output from the system simulator:

- Mobile Station and Base Station coordinates
- Carrier, Interference and Noise (thermal noise) levels

- Information on the channel allocation

The system simulator has been implemented in a number of MATLAB functions. Full code of these functions could be found in Appendix A.
For all environments listed in table 4.2, simulation results of mobile positioning have been summarised in chapter 7.

4.2.2 Radio Link Simulator

The radio link simulator requires development according to the whole measurement method. An essential part of this simulator is the channel model. The proposed channel model is presented in its wide-band version in Section 4.2.3, and with a GSM adaptation in Section 4.2.4.

It is very crucial that the same channel model is used when evaluating different positioning measurement system. The reason being is obvious and simple. Multi-path propagation and fading, which are inherent in mobile communications, have a great influence on the positioning performance.

With an assumption of a certain channel model environment, a measurement value and quality can be determined for each link realization based on distance, angle, C/I, C/A, and C/N. Results such as these are definitely interesting, i.e. to find the root mean square error (rmse) under certain assumptions, but real positioning results are achieved when this simulator is combined with the system simulator.

Figure 3 shows the radio link simulator with the necessary inputs and outputs from the channel model.

[1] The frequency reuse strategies are often referred to as frequency planning and are expressed as m/n, where m denotes the number of sites per cluster and n denotes the number of cells per cluster.

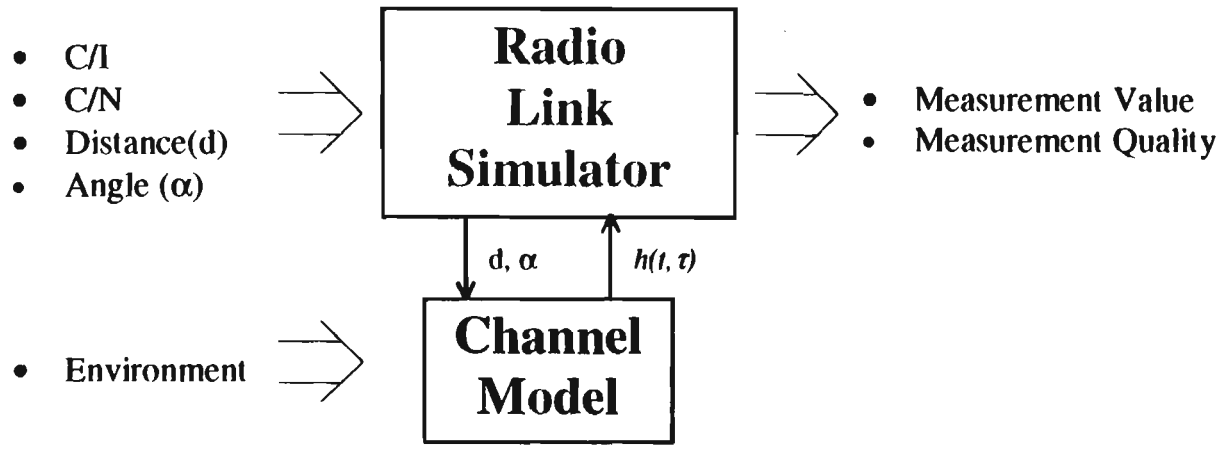

Figure 4.3: *Radio Link Simulator*

4.2.3 Channel Model

The channel model described by Lundqvist [37], uses the same basic structure as the CODIT model [38], [39], but with some fundamental differences. The differences are due to the following:

- The modeling of the delay spread as a distance dependent parameter.
- Field measurements presented by Motorola [40] – [42], and by Ericsson [43], [44].
- Modeling of base station antenna diversity.

For a full detailed description on the channel model, refer to chapter 5.

CHAPTER 5

PROPOSED CHANNEL MODEL

5.1 Introduction

In order to compare different positioning proposals, a common channel model is required. This chapter describes such a model, based on requirements specific to evaluation of positioning techniques. The general requirements of the channel model have been introduced in chapter 4, Section 4.2.3, therefore this chapter will describe the channel in detail.

5.2 Modeling Parameters

5.2.1 Delay Spread

Delay spread measurements are very common in mobile communications, and have been performed in many different environments under all kinds of conditions. An extensive summary of delay spread measurements can be found in the literature by Greenstein [45]. Usually, there is large difference between different measurements, and it has been found difficult to categorise the delay spread. An attempt to categorise the delay spread has been made by Greenstein [45], and is summarised below.

The Greenstein delay spread model is based on two conjectures:

1) At any given distance from the base station, the delay spread is lognormally distributed.
2) The median delay spread increases with an increasing distance.

The above conjectures have been supported by measurements to a certain degree. The proposed model is:

$$\tau_{rms} = T_1 d^{\varepsilon} y \qquad (5.1)$$

Where τ_{rms} is the rms delay spread, T_1 is the median value of the delay spread at d = 1 km, ε is an exponent with values between 0.5 and 1, and y is a lognormal variable, meaning that Y = 10 log y is a Gaussian random variable with standard deviation σ_Y.

The following table lists the parameter values for different environments.

Environment	T_1 (μsec)	ε	σ_Y (dB)
Urban microcell	0.4	0.5	2 – 6
Urban macrocell	0.4 – 1.0	0.5	2 – 6
Suburban	0.3	0.5	2 – 6
Rural	0.1	0.5	2 – 6
Mountains	> 0.5	1.0	2 – 6

Table 5.1: *Suggested parameter values for the Greenstein delay spread model*

The model summarises a lot of previously reported delay spread measurements in a compact way. That is the reason why this model has been chosen to be used in the positioning channel model. One should also distinguish at this stage the difference between the urban environment, and the bad urban environment, where the latter is usually characterised by high-rise buildings or large open areas such as fields or lakes. Bad urban environments have been reported to have very high delay spreads, which are not observed in all urban environments [46].

The distinction could be made by setting T_1 to 0.4 μsec for the urban environment and 1.0 μsec for the bad urban environment. In this case, the urban and the urban microcell will be exactly the same.

For the mountainous environment, Greenstein suggests that the value for T_1 is greater than 0.5 μsec. As there is no evidence for any preferred value to be used, for simplicity $T_1 = 1.0$ μsec is used here.

It should be noted that there is a large spread between different measurements, which can make it difficult to decide on typical parameters. This is further complicated by the fact that some delay spread measurements may have been obtained in extreme environments, where the researchers have been looking for extreme rather than typical environments.

5.2.2 Correlation of delay spread measured at different base stations

For a mobile position to be positioned correctly, it is required to have some kind of knowledge about the correlation between the delay spread measured at two or more base stations. To the authors' knowledge, there hasn't been any direct addressing on the above mentioned question, but Greenstein indirectly provides a solution to the question by stating that delay spread seems to increase with shadow fading. The solution is based on only one result, obtained in [47]. Using these results, Greenstein proposes a correlation coefficient of –0.75 for the correlation between delay spread and shadow fading.

An investigation performed by Ericsson on correlation of shadow fading for different base stations shows that the key parameter for the correlation is the angular difference between the two base stations. For large angular differences the correlation is low, while for small angular differences (less than 20 degrees) the correlation is high. The correlation at different base stations can be neglected by making an assumption that small angular differences will be rare. Due to the high correlation between delay spread and shadow fading, low correlation between delay spreads measured from different base stations can be expected. To prove the above expectation, a direct investigation is required. Even though there has been only one result supporting the correlation between delay spread and shadow fading, it should be noted that deep shadowing is very likely to "even out" the power delay profile.

5.2.3 Power delay profile shapes

As important as the delay spread for wide-band channels is not a great deal of measurements of the delay profile have been included in the literature. Reason being is because the delay spread is a single value, which makes it easier to study its characteristics. Some proof [48], [49] suggests that the power delay profile is typically exponential. However, from geometric scattering arguments, it is not an easy task to generate an exponential shape [50]. The CODIT model [38], [39], which is based typically on real measurements, does not contain any exponential shapes.

5.2.4 Fading and angles of arrival

The basic idea in mobile communications is that urban channels are Rayleigh fading and rural channels are Rice fading. In order of wide-band channels, only the CODIT measurements provide sufficient information. Angles of arrival at the mobile are usually generated according to a uniform distribution, proven with the local scattering model [51]. Measurements published not so long ago [52], [53] concentrate directly on the angles of arrival at the base station. For macro-cells, the angles of arrival are in a narrow angular interval around the direction to the mobile, which means that its measurements are in favour of the scattering model.

5.3 Channel model based on the CODIT model

Taking the delay spread into account, a typical radio channel can be generated according to some model assumptions. As mentioned in chapter 3, several channel models already exist. One of them is the CODIT model [38], [39]. The CODIT model is a wide-band model, which is based on measurements taken in different environments. Most widely used environments are urban, rural, suburban, mountainous and rural hilly. In each environment a number of scatterers are generated (Figure 5.1). Each scatterer is characterized by an average power Ω_i, an excess time delay T_{bi}, a mean angle of arrival at the mobile α_i, and Nakagami-m fading with a specified m_i value. The figure shows a typical suburban channel consisting of six scatterers, as shown in the power delay profile (Figure 5.1, upper left). Excess delay is defined as the delay relative to the direct (LOS) path.

The fading of each scatterer is generated by letting the scatterer consist of a large number of partial waves, all arriving at the same delay but at different angles. The angles are chosen from a truncated Gaussian distribution, centered around the mean scatterer angle of arrival α_i (Figure 5.1, lower left, and example for scatterer #5). The CODIT model uses an angular standard deviation of 0.15 radians and the phases of the partial waves are considered to be random.

The power distribution of the partial waves is chosen in order to generate Nakagami-m fading of the scatterer (Figure 5.1, lower right, example for scatterer #5). This will cause each scatterer to fade independently as the mobile moves.

This model is valid for the local behavior of the radio channel where the assumption of WSSUS (Wide-Sense Stationary Uncorrelated Scattering) holds. The range over which this assumption is valid is estimated to be a few tens of wavelengths. In the CODIT model, a scatterer corresponds to a set of partial waves originating from a single object (building). The partial waves of one scatterer all have the same excess delay, but have different angles of arrival at the mobile and different amplitudes.

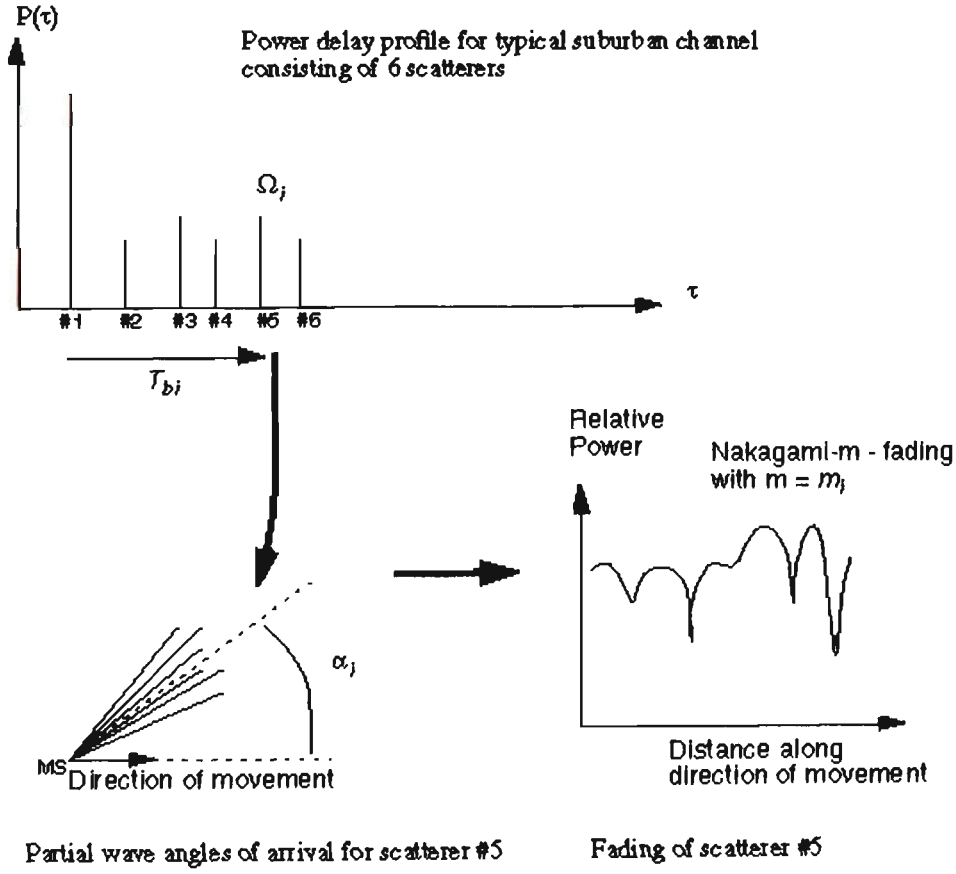

Figure 5.1: *The basics of the CODIT channel model.*

The parameters for the CODIT model are listed in Table 5.2. Ω_i is the relative average power, and m_i is the Nakagami-m parameter, with $m_i = 1$ for Rayleigh and $m_i > 2$ for Rician fading. α_i is the mean angle of arrival at the mobile and T_{bi} is the excess delay.

Environment	Scatterer #	Relative Power Ω_i	Fading parameter m_i	Mean angle of arrival α_i	Excess delay T_{bi} (μs)
Urban	1,..,20	[0.5, 1.5]	1	[0,2π]	[0, 2.4]
Suburban	1	1	15	[0,2π]	0
	2,..,6	[0.1, 0.4]	[1, 5]	[0,2π]	[0.1,15.8]
Suburban Hilly	7,..,20	[0, 0.1]	1	[0,2π]	[15,80] + [0,10]
Rural	1	1	25	[0,2π]	0
Rural Hilly	2,..,20	[0, 0.1]	1	[0,2π]	[15,80] + [0,10]

Table 5.2: *Parameters for the CODIT channel model*

As it can be seen in Table 5.2 and in Figure 5.3, the hilly environments are obtained by adding a second set of scatterers (corresponding to diffuse scattering from a hillside or mountain) arriving in a 10 μs window at 15-80 μs excess delay. It should be noted that the diffuse scatterers all have the same mean angle of arrival at the mobile.

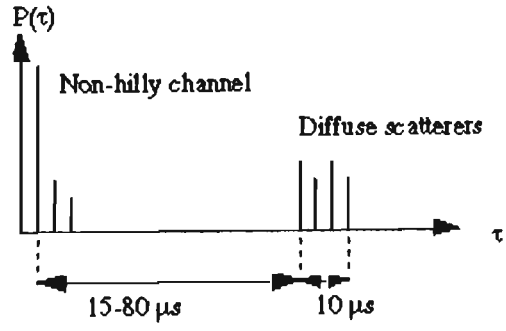

Figure 5.2: *Generating the diffuse scatterers for the Hilly channel models of the CODIT model.*

5.4 Matching the delay spread of the channel model to the delay spread model

Up to the latest stage of the CODIT model, it can be said that this model does no provide delay spread values, which confirm with result measurements provided in [45]. Taking the urban channel, the delay spread is of the right magnitude, but with very little spread. The suburban channel gives delay spreads which are much greater than those measured, and the rural channel will not have any delay spread at all. If the CODIT model is to be used in the mobile positioning task, the above problems need to be corrected, considering the importance of delay spread to positioning.

One solution is to generate delay spread values according to the Greenstein model (section 5.1.1), and use these values as an input to the CODIT model. Through this procedure, a channel is generated which will have the required delay spread. For the urban and the suburban channels, this can be achieved by changing the maximum time delay in a way of re-scaling the time axis. This is unable to be done in the rural channel, therefore the suburban channel will have to be used in the rural environment. Due to this change, it should be noted that the difference between the suburban and rural environment would obviously be the delay spread values. The average shape of the channel will remain the same.

For the hilly environment, several strategies are available for modifying the channel to give the wanted delay spread. The excess delay of the second set of scatterers may be changed, or the power of those scatterers may be increased or decreased. A further requirement would be that the first part of the channel (excluding the late scatterers) should be identical to the normal suburban/rural channel. Therefore, due to the fact that the excess delay of the diffuse scatterers is often constant or slowly varying within the cell, this parameter cannot be allowed to vary freely for different base station-mobile station configurations. Due to this, it is necessary to specify the excess delay of the diffuse scatterers, and increase or decrease their relative power to get the desired delay spread. To simplify further, all of the diffuse scatterers will need to be equally amplified or attenuated.

An expression for the delay spread of the channel as a function of the relative powers can be obtained by approximating the power delay profile with two peaks. One at excess delay of 0 with average power equal to the sum of the powers of the basic suburban power delay profile, and a second peak at excess delay corresponding to the center of the window containing the diffuse scatterers. For a two-path power delay profile, the delay spread:

$$\tau_{\text{rms}} = \sqrt{\frac{\sum_i (\tau_i - \tau_m)^2 P_i}{\sum_i P_i}}$$

where τ_m is the mean delay, which can be reduced to:

$$\tau_{\text{rms}} = \frac{\sqrt{P_1 P_2} \cdot (\tau_1 - \tau_2)}{P_1 + P_2}$$

The above equation is now solved to produce:

$$\frac{P_2}{P_1 + P_2} = \frac{1}{2}\left(1 \pm \sqrt{1 - 4k^2}\right)$$

or at the same time to give:

$$\frac{P_2}{P_1} = \frac{1 - 2k^2 \pm \sqrt{1 - 4k^2}}{2k^2}$$

where the k parameter takes values between 0 and 0.5.

$$k = \frac{\tau_{\text{rms}}}{(\tau_2 - \tau_1)}$$

5.5 Unresolved issues

As mentioned previously, one of the problems with using the CODIT suburban instead of the CODIT rural is the difference in fading for the two channels. The suburban channel consists of a number of scatterers with one line-of-sight (LOS) component, having an m value of 15. The rural channel on the other hand is composed of a single LOS scatterer, having an m value of 25. When using the suburban channel at bandwidths where the scatterers will not be resolvable, only a single peak will be visible, and this will fade deeper than a m=25 Nakagami due to the superposition of several Rayleigh-fading scatterers to the m=15 LOS scatterer. When using a narrow angular distribution of the

partial waves (CODIT uses an angular standard deviation of 0.15 rad), the distance between fading minima will become larger than the usually observed $\lambda/2$. At lower bandwidths, *e.g.*, GSM, this effect will not be noticeable as several scatterers with different mean angles of arrival will be superimposed due to the limited time resolution. However, at higher bandwidths, when individual scatterers become resolvable, this will cause slower fading of the scatterers than what we have observed from measurements. The measurements indicate that even at bandwidths of 5 MHz the distance between fading minima will still be close to $\lambda/2$.

These unresolved issues with the CODIT model lead to some unanswered questions. Some of the questions are as below:

1. Are the impulse response shapes described in Table 5.2 typical?
2. Is the fading statistical representative, both at wide and narrow bandwidths?
3. Is the superposition of a set of waves arriving within a narrow angular distribution a correct way of generating the fading of each peak?

5.6 Definition of the environments

Through out the text so far terms like urban, suburban, mountainous, rural, etc. have been used without any definition on each of them. Table 5.3 below defines each environment used though out the literature.

Terrain	**Definition**
Urban	Densely populated areas, multi-story buildings, offices, city centers.
Suburban terrain	Populated areas, residential houses. Villages.
Rural	Sparsely inhabited areas, fields, and forests.
Bad Urban	Skyscrapers in (or close to) line of sight of base station and mobile. Distant buildings visible over large open areas (such as fields, rivers, lakes), in (or close to) line of sight of both base station and mobile.
Hilly	Locations with large hills or mountains within <15 km, visible from both base station and mobile.

Table 5.3: *Terrain Definitions*

5.7 Base station antenna diversity

One of the demands on the model is that it should be able to take into account spatial diversity at the base stations. Spatial diversity is produced by radio waves impinging on the base antenna, coming from all different directions. Most often the angular distribution of arriving waves is very narrow, resulting in higher spatial correlation than at the mobile. At the mobile station, angles of arrival are also coming from all different directions. Several literatures have investigated correlation and diversity [51], [54], and [55]. F. Adachi in [55] proposes a simple model for angular spread seen at the base station. The angles here are Gaussian distributed with a standard deviation of σ_θ, where:

$$\sigma_\theta \approx \frac{r_H}{d}$$

The scatterers in the model are assumed to be distributed in a circle with radius r_H around the mobile. The mobile station is at a distance d from the base station (Figure 5.4).

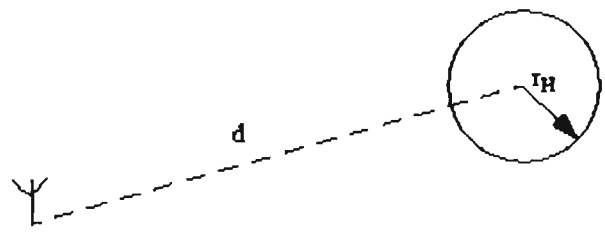

Figure 5.3: *Model of the local scattering.*

Cross-correlation results obtained using this model agree well with measurements. As information on the time delays of the scatterers is known through the channel model, a further refinement could be made on the angle of arrival model. By making the standard deviation (in radians) σ_θ a function of the excess delay T_{bi} the following is achieved:

$$\sigma_\theta(T_{bi}) = \frac{c \cdot T_{bi}}{d}$$

c is the speed of light, equal to $3 * 10^8$ *m/s*.

Each scatterer has a base station angle of arrival generated from a Gaussian distribution with standard deviation being a function of excess delay. A direct wave with an excess delay of 0, would always arrive at an angle to the mobile, whereas other waves have an angular probability distribution which widens with increasing delay. From a physical

point of view this is justifiable, as increase in delay means greater probability of large deviations from the direct path.

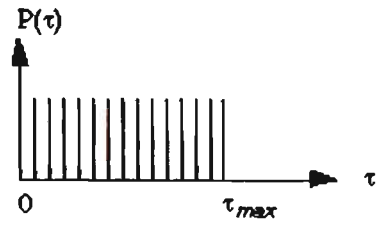

Figure 5.4: *Sample channel for evaluation of the base station angle of arrival model.*

The power azimuth spectrum shown in Figure 5.6 is obtained from the simple channel model depicted from Figure 5.5. It is assumed that all scatterers have equal power and the excess delay is uniformly distributed in an interval of $(0,\tau_{max})$, which is similar to the CODIT urban channel described earlier in this chapter. For each scatterer, the angle of arrival is generated from a Gaussian distribution with standard deviation given in radians, and the total power azimuth spectrum is calculated. For comparison purposes, a Laplacian distribution is also shown in Figure 5.6. Laplacian distribution has been suggested in [52], as a better fit to measured power azimuth spectra than the Gaussian distribution.

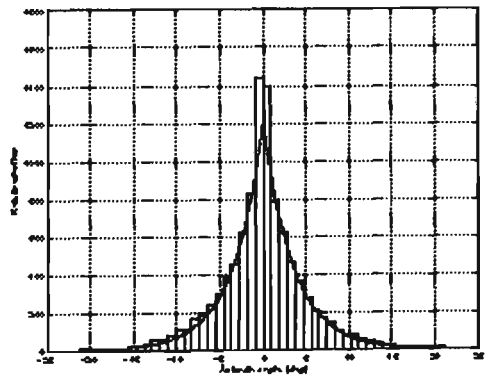

Figure 5.5: *Power azimuth spectrum using the model with uniform excess delay distribution and equal scatterer power (bars), and for a Laplacian distribution (continuous line). The x-axis is the azimuth angle [deg] and on the y-axis the relative power.*

Antenna diversity plays a role in the channel model in the following way:

- For each scatterer, an angle of arrival θ_i is generated at the base station by a Gaussian distribution.
- The complex phase of each scatterer is shifted relative to a reference point according to:

$$\Delta\varphi = \frac{2\pi}{\lambda} r_j \cos(\Theta_j - \theta_i)$$

where (r_j, Θ_j) are the polar coordinates of the base antenna relative to the reference position. Figure 5.7 shows that the phases of the waves arriving at angle θ_i at antenna 1 will be shifted by:

$$\Delta\varphi_1 = \frac{2\pi}{\lambda} r_1 \cos(\Theta_1 - \theta_i)$$

relative to the phases at the origin.

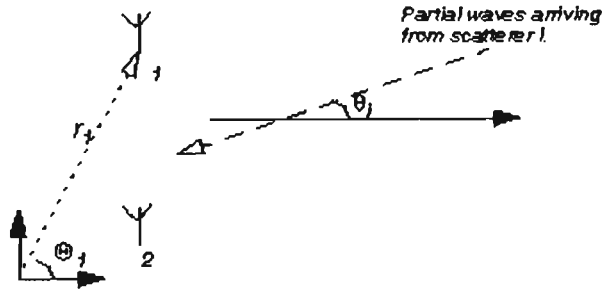

Figure 5.6: *Phase shifts of waves due to their angle of arrival at the different base station antennas.*

The purpose of this type of modeling is to get the relative phase shifts of the radio waves at different base antenna positions.

5.8 GSM Adaptation

This section describes a FIR Filter Implementation of the channel model for GSM Simulations.

5.8.1 FIR Filter Implementation

The proposed implementation of the CODIT based channel model in GSM simulations is by means of a FIR filter. The channel model delivers the complex amplitude $a_i(t)$ and

delay $\tau_i(t)$ of each path i from which the time-variant infinite bandwidth channel impulse response $h(t, \tau)$ is formed and is the basis of the FIR filter implementation:

$$h(t,\tau) = \sum_{i=1}^{N} a_i(t)\delta(\tau - \tau_i(t)) \rightarrow (5.1)$$

The discrete time implementation of the channel model consists of a tapped-delay-line with a tap spacing defined by the system sampling period T and tap weight coefficients $g_n(t)$, where $n=0,...,L$ is the tap index. The product of the maximum excess delay of the environment and the system-sampling rate determines the number of required taps L, i.e., the length of the FIR filter.

The tap weights $g_n(t)$ can be calculated by taking the signal bandwidth into account. W denotes the bandwidth occupied by the real band-pass signal. The band occupancy of the equivalent low-pass signal is $|f| \leq \frac{1}{2}W$, which allows to define the system sampling rate $1/T=W$. The channel can be considered band-limited with null spectral components out of the system bandwidth, sampling it with the same rate. Therefore, the multiplicative tap weights $g_n(t)$ are obtained by filtering $h(t, \tau)$ with an ideal low-pass filter with cut-off frequency $1/2T=W/2$ and sampled at rate $1/T=W$ [8]:

$$g_n(t) = \int_{-\infty}^{\infty} \frac{\sin\left(\pi W\left(\tau - \frac{n}{W}\right)\right)}{\pi W\left(\tau - \frac{n}{W}\right)} h(t,\tau)\,d\tau \rightarrow (5.2)$$

Substituting $h(t, \tau)$ (equation 5.1) into the equation above yields the tap weights of the FIR filter implementation of the channel model:

$$g_n(t) = \sum_{i=1}^{N} a_i(t) \frac{\sin\left(\pi W\left(\tau_i(t) - \frac{n}{W}\right)\right)}{\pi W\left(\tau_i(t) - \frac{n}{W}\right)} \rightarrow (5.3)$$

Therefore, each complex amplitude $a_i(t)$ delivered by the CODIT model is multiplied by a sinc function shifted by the amount of the corresponding time delay $\tau_i(t)$ and summed up for all scatterers N.

The sampling frequency used for the proposed "Positioning Simulator" has been chosen to 16 times the bit rate in GSM, *i.e.*, $1/T = W = 16 \cdot (13e6/48)$ Hz $\approx 16 \cdot 270833$ Hz $\approx$ 4333333 Hz. This relative high sampling frequency has been chosen to allow the simulations over-sampling at the receiver which may improve the performance of time delay estimation algorithms in a TOA or TDOA based positioning system. In order to implement equation 5.3, the sinc function has to be truncated. In the proposed "Positioning Simulator" , the impulse responses are truncated to 30 microseconds which allows also to handle the delay spread of the "Mountains" environment.

The channel output signal is obtained by convolution of this sampled impulse response with the simulated GMSK signal (sampled at the same rate). Since the channel is power normalized, the signal mean power is kept after this convolution. This allows to simulate interference signals and thermal noise, which can be added to the channel output signal.

5.8.2 Sampling in Time Domain

With time-variance being relatively slow for all bands (900,1800 and 1900 MHz), the channel can be assumed quasi time-invariant, i.e. time-invariant over the duration of one burst. Therefore, no change of the delay profile during a burst has to be modeled and hence, only one sample of the delay profile is required for each burst. Since the channel model is only a function of position, moving vehicles can be easily simulated. For each burst a new channel impulse response is computed based on a given desired position. This also allows to simulate accelerating moving mobiles.

5.8.3 Frequency Hopping

The radio interface of GSM uses slow frequency hopping. Because the channel impulse response delivered by the proposed modified CODIT model has infinite bandwidth, frequency hopping can be easily implemented by filtering out the frequency bands of interest. The complex impulse response of equation (6.1) for one burst is multiplied by $\exp(j2\pi f_H \tau_i(t))$, which results in a frequency translation with magnitude f_H , *i.e.*, with spectrum $H(f-f_H)$. Defining for each burst a different frequency f_H the channel to use for each burst is centered on frequency 0 in base-band. This translated impulse responses are then filtered and sampled as described in section 6.7.1.

5.9 Additional explanation on the channel model

5.9.1 Antenna space diversity

For a single plane wave impinging on two spatially (locally) separated base station antennas, the only difference between the received signals will be a phase rotation due to the projected distance difference (Δs in Figure 5.8). However, if we superimpose two or more plane waves arriving from different directions, the signals in the two antennas will tend to become decorrelated. The amount of decorrelation is dependent on the spatial separation of the antennas and the angles of incidence of the waves. If the spatial separation is small, the phase differences will also be small and therefore the resultant signal vectors will be very similar. Also, if the angles of incidence are within a narrow angular interval, every plane wave will have a similar phase shift between the two antennas giving a resultant signal vector at the second antenna which is only a complex rotation of the first.

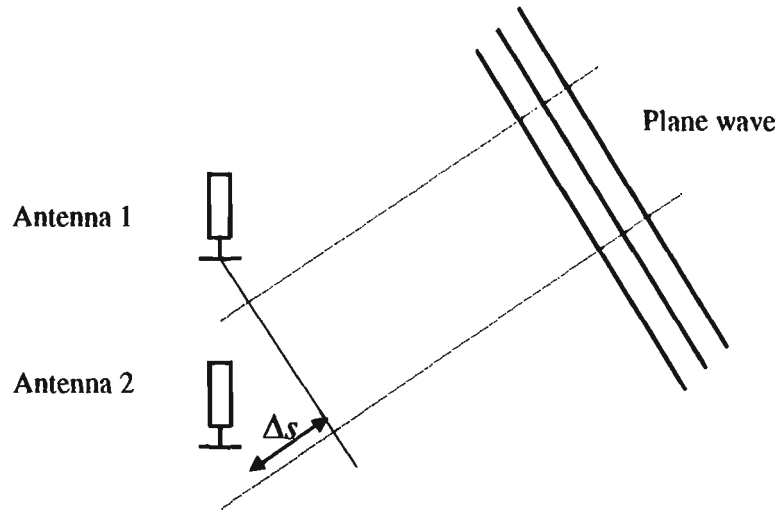

Figure 5.7: *Plane wave impinging on two spatially separated antennas.*

Antenna diversity is a method where the signals in the two antennas are combined in order to reduce the probability of deep fades. The probability reduction will increase with decreasing correlation between the signals at the two antennas.

In the channel model, the aspect of antenna diversity can be considered in a simplified manner. Generating angles of arrival of the (plane) waves corresponding to each scatterer does this. By specifying the relative positions of the base antennas, the phase shift of each wave compared to a reference point can be calculated, from the projected distance from the reference point. Superposition of the waves arriving at each antenna will give the total received signal vector, which will be more or less correlated with the signals received at other antennas.

The key problem in the channel model is to generate the angles of arrival correctly. The relative positions and number of base station antennas, while important for diversity, are not specified in the channel model but may be freely set by the user.

The assumption of local scattering [51], [55] is a good starting point. The assumption is that the major part of the scattering of multipath waves takes place in the vicinity of the mobile (Figure 1.2). This means that the spread of angles of arrival at the base station will be small. Adachi et al. [55] calculates the cross correlation under the assumption that the angular distribution is a Gaussian, and shows this to agree reasonably well with measurements performed at a MS-BS separation of 1.3 km.

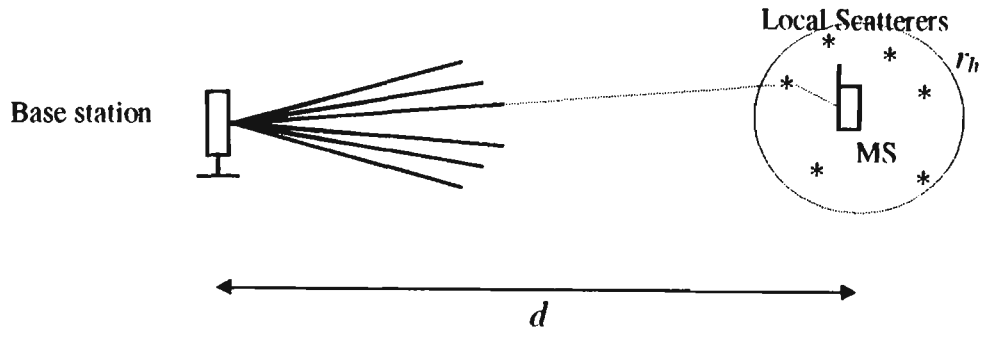

Figure 5.8: *Local scattering*

Some empirical evidence for the angle of arrival distribution is given by [52] claiming the distribution to be Laplacian. Also, an increase of angular spread with decreasing base station antenna height is indicated.

We have based our model on the simple assumption by Adachi, where the angles of arrival are Gaussian distributed with standard deviation $\sigma = r_h / d$. Here r_h is the radius of the area containing the local scatterers. The parameter r_h is very likely environment dependent and probably distance dependent, and assigning a value to it may be difficult. Our modification of this model consists of relating the radius r_h to the excess delay τ for each scatterer according to $r_h = c\ \tau$ where c is the speed of light.

This means that every scatterer will have a different angle of arrival, taken from a Gaussian distribution around the true angle to the mobile. The standard deviation of the distribution is directly proportional to the excess delay.

A physical justification for this modification is that the LOS path does, of course, always arrive at the angle to the mobile, and that the more a path is delayed relative to the LOS path, the larger the angular deviations of it.

Using the proposed model for the standard deviation, the LOS path, having an excess delay of 0, will also have an angular standard deviation of 0. However, for increasing excess delays, the angular standard deviation will also increase, in conformity with the physical argument given above.

So, how is this implemented in the channel model?

1. After generating the relative powers and delays of the scatterers for a given channel, the angles of arrival at the base station are generated. The angle of arrival for each scatterer is taken from a Gaussian distribution, where the standard deviation of the distribution is proportional to the excess delay of the scatterer according to $\sigma = c\tau/d$.

2. The base antenna positions are given by the user (Channel.m, parameter b). These positions are given in meters (x,y) relative to an (arbitrary) reference point. Also, the angle to the mobile (in the same co-ordinate system) may be specified. This angle is added to all angles of arrival generated during step 1.

3. When the instantaneous channel is calculated (for different locally varying mobile positions), each partial wave is also additionally phase shifted given by the projected distance of that particular wave to the reference point. For each base antenna, the resulting channel is calculated. Due to the spatial displacement of the base antennas, these channels will be more or less decorrelated.

5.9.2 Number of scatterers

Is the number of scatterers sufficient?
The channel model uses relatively few scatterers, 6 in the Suburban/Rural and 20 in the Urban/Bad Urban environments. The question is if these numbers are sufficient for accurate modelling of the channel.

The thing that could happen if too few scatterers are used is that the channel becomes resolvable at GSM bandwidths. This in itself is no problem as each scatterer will still fade individually, but the performance of time–based positioning methods could become too optimistic. With all scatterers resolvable, the process of measuring the arrival time of the first one is very much simplified.

So, the question is: How often will the channel become resolvable? The GSM time resolution is approximately 5 μs. This means that in order to resolve the scatterers, they

should be spaced at least 5 μs, which roughly calculated corresponds to a maximum excess delay for the urban/bad urban channel of 95 μs (20 scatterers spaced 5 μs) and a maximum excess delay of 25 μs for the suburban/rural channel.

The delay spreads corresponding to the maximum excess delays above are roughly 15.8 μs for the exponential Bad Urban/Urban and 8.0 μs for the Suburban/Rural. From the Greenstein expression for the median delay spread, we see that these delay spreads correspond to median values in cells sized larger than 200 km. So it is clear that much less than 50% of the channels will be resolvable. To investigate just how much less we first note that for a lognormal distribution generated from a Gaussian with standard deviation 4 (dB), the 2%-quantile corresponds to 6.7 times the median. In other words, for a lognormal distribution with median a, 2% of the values in the distribution will be larger than $6.7 \cdot a$, if the generating Gaussian distribution has a standard deviation of 4 dB.

We estimated the limit for resolving the channels at 15.8 μs and 8.0 μs delay spread above. To find out at what distance 2% of the channels are resolvable, we just divide the above values with 6.7 to get the median delay spread values, and then calculate the distances using the relation [45]:

$$median(\tau_{rms}) = T_1 d^{\varepsilon}$$

The results are:

Bad Urban (Exp): 5.6 km
Urban (Exp): 14 km
Suburban: 4.8 km
Rural: 14.3 km

So, to summarise, at the distances given above, approximately 2% of the channels will become resolvable. Considering the uncertainties associated with selection of parameter values etc. the significance of resolving the channel in less than 2% of the cases will be small.

5.9.3 Scaling of the time axis

As long as the channel is unresolvable or only partially resolvable (see above) the scaling of the excess delay axis should be an acceptable way of achieving the desired mean excess delays and delay spreads. For partially resolvable channels each time bin will still contain the contributions from several scatterers.

5.9.4 Range of validity

The reported delay spread measurements, which led to the Greenstein delay spread model, were performed in cells of the following sizes:

Urban:	0.6, 1.0, 3.5, 5.0 and 7.0 km
Suburban:	2.0 and 2.2 km
Rural:	2.2 and 5.0 km
Mountains:	6.0 and 12.9 km

A conclusion from this would be that the model is valid at least for distance up to the respective maximum value above, that is:

Urban:	< 7 km
Suburban:	< 2.2 km
Rural:	< 5 km
Mountains:	< 12.9 km

Furthermore, the use of generic environment types is an idealisation of reality. Many real-world areas do not fit into these environments or belong to more than one. The model is only able to predict general channel behaviour in the defined environments, not to reproduce results from specific areas.

5.9.5 Delay spread vs. distance –some physical reasons

The measurements reviewed by Greenstein et al. [45] support the conclusion that delay spread increases with distance. A physical explanation for this might be that the larger the distance, the greater the possibility that the strong LOS path is obstructed. Also, for a given excess delay the relative path length will decrease with increasing distance, giving

less excess path loss. This will shift the weight of the power delay profile to larger excess delays, giving higher delay spreads.

As an example, consider a wave arriving at excess delay 3 μs. This wave will have travelled an extra 1 km. For a BS–MS separation of 1 km, the wave will have travelled double the distance of the LOS path, which will give a much higher path loss in addition to the reflection loss. However, if the BS–MS distance is 5 km, the extra 1 km will not matter as much to the path loss. Thus, at the greater distance there will be more power at higher excess delays, giving a larger delay spread.

Why not only one channel model?

The question have been raised if the different channel models (Bad Urban, Urban, Suburban, Rural and Mountains) could be replaced by one common channel model. The argument is that for the Urban, Suburban and Rural channels, the delay spread vs. normalised distance (distance divided by cell radius) is quite similar for all three, so it would be possible to use just one channel model, replacing distance with normalised distance.

A few arguments why this should not be done:

The normalised distance is an unnatural parameter, related to the distance via the defined cell radii. Once we base our channel model on the normalised distance, we cannot change the cell radii. Other parameters than the delay spread are also dependent on distance, such as antenna diversity and path loss. It would be difficult to base these on normalised distance instead. A single channel model could probably not include the Bad Urban and Mountains channels. Other Parameters than the delay spread are also of importance for TOA estimation. For example some environments have a line–of–sight (LOS) component, others have no LOS. This can not be handled by a single channel model.

5.10 Matlab Software Package

The channel model has been implemented in three Matlab 5.1 functions:

- chanmod.m
- subscatt.m
- channel.m

The first function, chanmod.m generates the scatterers for a given environment. Next, subscatt.m generates the partial waves according to the CODIT implementation for generation of fading of scatterers. Finally, channel.m calculates the infinite-bandwidth impulse response for different mobile positions and base station antennas.

The GSM adaptation is done in one Matlab 5.1 function:

- getchan.m

Below follows a brief description of each function.

For full syntax on the Matlab files refer to Appendix B.

chanmod.m

```
[sc,atrms] = chanmod(d,env,[DiffDelay],NRe,[trms])
d          = The base station - mobile separation in kilometers
env        = The environment type, one of the following:
             'Urban'
             'BadUrban'
             'UrbanExp'
             'BadUrbanExp'
             'Suburban'
             'Rural'
             'Mountains'
```

'OnePeak' A single, non-fading peak at excess delay 0, useful for testing simulators.

DiffDelay = The excess delay in seconds at which the diffuse reflections of the Mountains type channel start arriving. Only necessary for the Mountains terrain.

NRe = The number of channel realizations

trms = Delay spread of the channel. Optional. If specified, the generated channels will all have this delay spread value, otherwise delay spread values will be generated according to the Greenstein model.

sc = An array containing the parameters of the scatterers for each realization of the channel. In general, a 3D array, where the third dimension corresponds to the different realizations.

atrms = The delay spread of each generated channel.

subscatt.m

```
subsct = subscatt(sct)
```

sct = The parameters for the scatterers of one channel (2D-matrix). Typically, sct will be a submatrix of sc, corresponding to a single realization.

subsct = 2D-matrix with the amplitude, phase, delay, AoA at mobile and AoA at the base station for each partial wave.

channel.m

```
Ac = channel(subsct,x,lambda,[b],[aoa])
```

subsct = The parameters for the partial waves of one channel (2D-matrix).

x = A vector with positions along the mobile path in meters.

lambda = The radio wavelength.

b = A matrix of base station antenna positions, useful for antenna diversity calculations etc. Default [0 0].

aoa = The angle to the mobile as viewed from the base station in the same coordinate system as b. Default value 0.

Ac = A 4D array, with complex amplitude and delay of each peak along the first two dimensions, results for the positions in x along the third and results for the positions in b along the fourth.

getchan.m

```
function [h] = getchan(sc,lambda,x,t,b,aoa,Fs,hopp_freqs,HoppingMode)
Calculates GSM channel impulse response from wideband channel
h           =  GSM channel impulse responses
sc          =  see function chanmod.m
lambda      =  RF wavelength in meters
x           =  vector of mobile positions in meters
t           =  realization number
b           =  coordinates of BTS antennas
aoa         =  angle from BTS to the MS
Fs          =  internal sampling frequency [Hz]
hopp_freqs  =  hopping frequencies (center frequencies in base band)
HoppingMode = 'random' : creates frequency hopping vector with
                         random order of specified frequencies
              'cyclic' : creates frequency hopping vector ordered
```

cyclic

CHAPTER 6

POSITIONING METHODS

6.1 Introduction

This chapter presents work on cellular position location techniques. The aim is to describe the latest approaches of current trends in mobile positioning research. What types of approaches are taken? How do the system assumptions differ? The Time of Arrival (TOA) method and the Enhanced-Observed Time Difference (E-OTD) method are closely considered in the chapter. All calculations in this thesis, particularly calculations shown in chapter 7 correspond to the TOA method.

Any cellular positioning method could be divided into two methods, terminal based or a network-based method. If the method does not require any change to the mobile station, then that method is taken to be a networked-based method. If the mobile station needs changes, then the positioning method used would be terminal based [56].

6.2 The up-link TOA method

The up-link TOA positioning method is based on measuring the Time of Arrival (TOA) of known signal sent from the mobile and received at three or more measuring units. The known signal is the training sequence of preferably a random access burs but possibly also a normal burst transmitted by the mobile. This method will work with existing mobiles, i.e. there is no modification to the handset required, which makes this method to be recognised as a network based method. In network based methods, the network controls some special receivers. These receivers perform measurements on all signals coming from the mobile stations. These special receivers are within range base stations or just normal stand-alone receivers. In terminal based methods, the mobiles themselves perform measurements on signals coming from the base stations. It is such an importance to the E911 that the TOA method is a network based positioning method due to the fact that it allows positioning of all mobile station on the market. TIP1, which is the standards committee in the US, has decided to standardise the up-link TOA

positioning method for GSM so that it meets the North American regulatory requirements [2].

This up-link TOA method works as described below.

Once a positioning request arrives at the Mobile Location Center (MLC), the mobile that needs to be located is vigor by the network to transmit a certain sequence. In GSM, the mobile is forced to perform a handover, where the mobile starts to send access bursts on a TCH. The handover is not completed if the mobile receives no response from the network. In this situation, the mobile station transmits access bursts until a set timer expires. In GSM, this timer is usually set to 320 ms, which means that the mobile unit transmits approximately 70 access bursts.

In the IS-136 (TDMA) system, the mobile unit is vigor to transmit shortened bursts. The transmission of shortened bursts can be forced by the network by setting a bit in the Digital Channel Designation (DTCD) message that is sent to the mobile station to assign a traffic channel. Until a control message from the network is sent to the mobile, the mobile unit continues to transmit shortened bursts. If the mobile does not receive a control message a timer expires.

The MLC sends information about used frequency and measurement starting time to the TOA measurement receivers, which in this case are assumed to be located at base stations. The job of the TOA measurement receivers now is to capture the bursts from the mobile stations and to estimate a TOA value relative to the receiver internal time base. The TOA measurement is in itself a technical problem. The limiting factor for TOA measurement accuracy is multipath propagation. In an urban environment where multipath propagation could be dramatic and delay spread values in the order of microseconds are obtained. A TOA estimation algorithm suited for cellular multipath channels is proposed in [57]. [58] uses this TOA algorithm to produce results in the GSM system and in the IS-136 (TDMA) system. The results are summarised below.

GSM System

The result in [58] shows that utilizing more than the minimum number of base stations can reduce the measurement error. With 5 base stations the positioning error is less than 120 m in 67 % of the cases. The above mentioned result is for an urban environment. In suburban environment, the positioning accuracy with only 3 base stations is only 80 m in 67 % of the cases. In this particular environment, it can clearly be summarised that, increasing the number of measuring base stations, improves the positioning accuracy.

IS-136 (TDMA)

The results in the urban and suburban environments show that the limiting factor in a cellular positioning system is multipath propagation and non line-of-sight (in the urban environment all measurement links have non line-of-sight). In the IS-136 system only 30 kHz bandwidth is available, compared to a 200 kHz bandwidth in the GSM system, which sets the limit for TOA estimation accuracy [3]. However from the results in [4], even in the urban environment with dramatic multipath propagation the FCC requirement can be fulfilled with 6 serving base stations.

6.2.1 TOA Estimation

6.2.1.1 The Estimation Problem

The TOA estimation problem could be stated as follows. Consider N snapshots (bursts) of the T-spaced sampled received signal.

$$r_i[n] = r(nT, x_i) =$$

$$\sum_k a[k]h((n-k)T, x_i) + n_i[n] =$$

$$\sum_k a[k]h[n-k, x_i] + n_i[n]$$

where $i = 1 \ldots N$

Here, the discrete (T-spaced sampled) channel $h[n,x]$ is introduced. The desired estimate of the TOA is $\tau' = T_1$, which is the time of arrival of the first incoming wave, or in other

words the Line of Sight (LOS) component. It should be noted that in a real propagation environment, a LOS component might not be present.

6.2.1.2 Channel Estimation Algorithm

Before the channel estimation algorithm is obtained, realisations of the channel model for different MS positions must first be derived. This data model is based on the delay spread model derived in chapter 5.

Data Model and Propagation

Let x denote the position of the MS, α_n and T_n the amplitude and delay of the incoming waves respectively. The channel impulse response at a certain x position can be written as:

$$c(t,x) = \sum_n \alpha_n(x)\delta(t - T_n(x))$$

Where $T_N \geq \ldots \geq T_2 \geq T_1$. Over a short measurement interval, the delays T_n are assumed to be constant, which mean that $T_n(x) = T_n$. The statistics of the amplitude α_n are typically Nakagami-m distributed. The phase $arg(\alpha_n(x))$ is almost uncorrelated at different points x.

Assume a sequence of binary symbol a[k] containing a known training sequence is transmitted. Let $g_T(t)$ denote the transmitter filter impulse response, and $g_R(t)$ the receiver filter impulse response. Therefore, the received signal at a certain location x can be written as:

$$r(t,x) =$$
$$c(t,x) \otimes g_T(t) \otimes g_R(t) \otimes \sum_k a[k]\delta(t - kT) + n(t) =$$
$$h(t,x) \otimes \sum_k a[k]\delta(t - kT) + n(t)$$

In the above equation, the $h(t,x)$ denotes the composite Channel Impulse Response (CIR), T is the symbol time, and n is the additive noise. The additive noise n consists of interference and filtered noise.

Now that the data model is defined, the estimation algorithm could be obtained. The first step in this estimation algorithm is to obtain estimates for the N discrete channel impulse responses (CIR). Using the data model defined earlier and assuming white noise, the following minimisation is required:

$$\hat{h}_i = \{\hat{h}_i[k]\}_{k=1}^{K} =$$

$$\arg \min \left\{ \sum_n \left| r_i[n] - \sum_k a[n-k]\hat{h}_i[k] \right|^2 \right\}$$

The problem is turning out to be a least square problem, but if the autocorrelation function of the training sequence is good, then a solution could also be found by simple correlation.

Next, the Channel Power Profiles (CPP) are defined.

$$CPP_i[n] = \left|\hat{h}_i[n]\right|^2$$

These CPPs are combined incoherently to obtain the weighted sum:

$$c[n] = \sum_i \gamma_i \left|\hat{h}_i[n]\right|^2$$

It should be noted that, since $arg(\alpha_n(x))$ is uncorrelated between different channel realisations, the integration could not be performed coherently. γ_i are weights based on estimated quality of each h_i. The n_{max} maximising $c[n]$ is found to determine the location of the area of interest, which is the region containing the training sequence.

Around the n_{max} position, a few taps of the channel estimates $g_i[n] = h_i[n-n_{max}]$ for each of the N received CIRs are extracted. The band limitation of $h(t)$ is exploited to obtain the DFT interpolation $g_i(p)$, which approximates $h(pT-n_{max}T)$ at point pT, where p is the rotational number.

6.2.1.3 Multipath Rejection (ICI-MPR)

A simple TOA estimate could be to perform only an incoherent integration (ICI), which is as shown below:

$$g(p) = \sum_i \gamma_i \left|\hat{g}_i(p)\right|^2$$

From this the TOA shown below could be estimated.

$$\hat{\tau}_{ICI} = T \cdot \arg\max\{g(p)\}$$

However, this solution will be biased due to the limited resolution of multipaths. To encounter multipath propagation, subsets of randomly chosen CPPs are formed and incoherent integration is performed within each subset. Therefore, the aim is to exploit the fading statistics since it is likely that some subsets will consists mainly of CPPs having relatively strong LOS component. The use of different types of diversity, frequency hopping and a moving mobile will help to provide independent channel realisations.

Based on quality estimates of each h_i, weights are calculated and partial sums of these CPPs are formed, as shown below:

$$S_m(p) = \sum_{i \in \Omega_m} \gamma_i \left| \hat{g}_i(p) \right|^2$$

where S_m corresponds to the m^{th} subset Ω_m consists of g_i incoherently summed, and disturbance due to noise in the g_i estimates. For each value of S_m, a quality measure is calculated. The subsets Ω_m are chosen randomly, but each of them contains enough elements to ensure that estimated quality of each partial sum is higher than a certain threshold. An advantage of this procedure is that is that the subsets will sometimes comprise bursts that contain mostly bursts received on the shortest path, which is the LOS path.

TOA estimates for each partial wave are obtained as shown below:

$$\hat{\tau}_m = T \cdot \arg\max\{S_m(p)\}$$

If LOS component is present in the measurement process, then a final TOA estimate could be obtained by taking the mean value of all subsets TOAs:

$$\hat{\tau}_{ICI-MPR}\,|_{LOS} = mean\{\hat{\tau}_m\}$$

To decide whether a LOS component is present or not, the standard deviation of all subset TOAs is compared with the standard deviation of an estimate of the noise. If there is a LOS component present during large parts of the measurement, the standard

deviation of all subset TOAs will be equal to the standard deviation of the measurement noise. The estimated standard deviations are used to decide whether the estimated TOA is performed on a radio link with a strong LOS component present or not. If the hypothesis of a LOS measurement is not rejected, the final TOA estimate is calculated according to the mean value of all subset TOAs equation.

If the standard deviation of the subset TOAs is greater than the estimated standard deviation of the noise, then the measurements are assumed to have been performed under dramatic multipath conditions. In a case such as this, the estimates according to the mean value of all subset TOAs will contain a strong bias error. In a noise free environment, the lowest TOA value of the set will be close to the TOA value of the shortest propagation path. However, due to the interference/noise and limited resolution of the channel estimate, a lower percentage level of the subset TOAs is a more accurate estimate. The standard deviation of all subset TOAs is calculated and subtracted from the mean value to obtain the final TOA estimate [61].

$$\hat{\tau}_{ICI-MPR}\,|_{NoLOS} = mean\{\hat{\tau}_m\} - std\{\hat{\tau}_m\}$$

6.2.2 TOA Simulation chain

Figure 1 shows the simulation chain of the time of arrival estimation procedure. Random information bits *d(k)* are assembled into bursts together with one of the specified training sequence codes (TSC). Each burst is differentially encoded and GMSK modulated with BT=0.3. The modulated signal is then transmitted over a model of the air interface. At the receiver white Gaussian noise (AWGN) or co-channel interference is added. The received signal is filtered by a receiver filter and sampled at bit rate T.

The de-rotated burst is then fed into the TOA estimation algorithm, which determines an estimate of the time-of-arrival, as described in section 6.2.1 of this chapter.

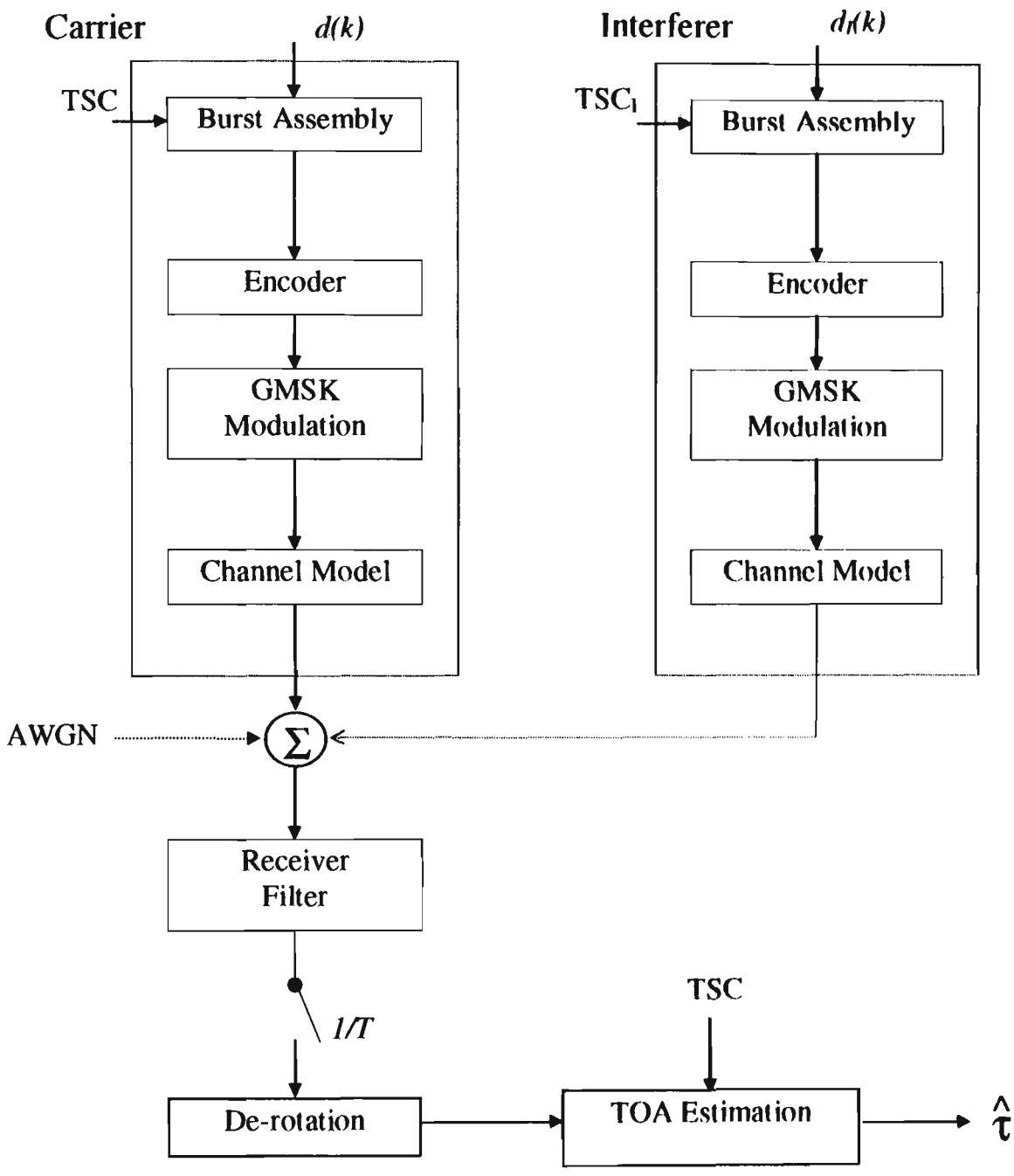

Figure 6.1: *GSM transmission chain with time of arrival estimation.*

6.3 The Enhanced-Observed Time Difference (E-OTD) Method

Enhanced Observed Time Difference (E-OTD) location method is based on measurements done by the mobile station (MS). It is possible to implement an E-OTD system where also location calculation using these measurements is done in the mobile station both in idle and dedicated modes. This way, several benefits are obtained both in idle and active states. In this chapter MS based E-OTD location calculation in idle state is discussed.

6.3.1 MS Based Location System

Mobile based E-OTD location method can be implemented so, that the network sends to the MS Base Transceiver Station (BTS) coordinates, Real Time Difference (RTD) values, and possibly other necessary information which is required in E-OTD method regardless where real location is calculated. If the BTSs are not synchronized, the Mobile Location Center (MLC) generates RTD values for each BTSs relative to its neighbors. Then each BTS sends these RTD values and its own and neighbor BTSs coordinates to the MSs using e.g. SMS Cell Broadcast. The MS is able to calculate its position in idle state based on OTD measurements and the extra information from the network. Figure 2 shows a generic E-OTD signaling flow in the case where the MS calculates its own location. In this figure the application is assumed to be network based, but quite often the application will be in the mobile itself and possible network originated location procedure can be avoided.

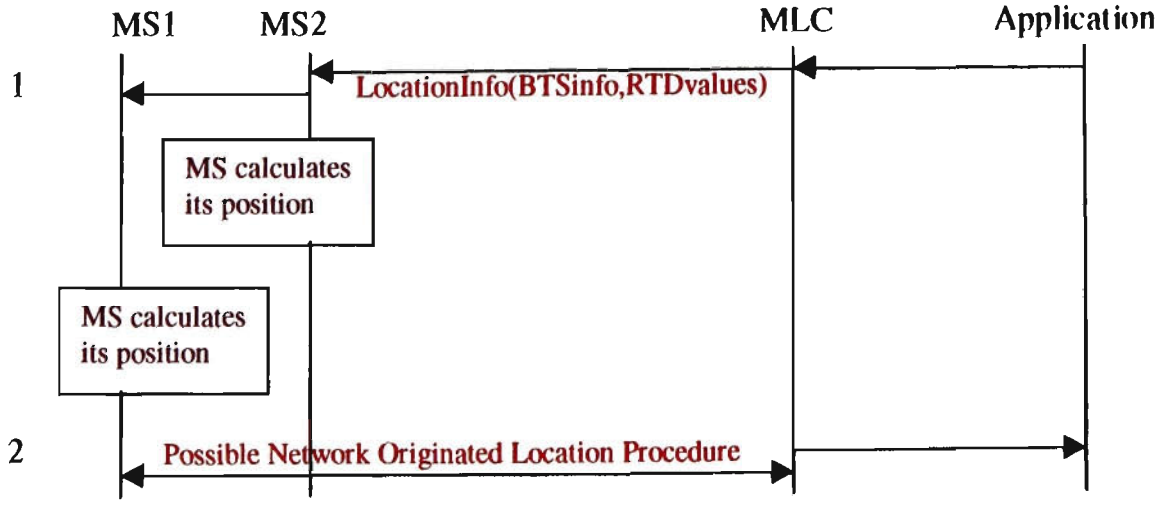

Figure 6.2: *Generic E-OTD signaling flow in MS based location calculation.*

In figure 6.2 it has been assumed that:

1. The MLC calculates the RTD values for all BTSs and each BTS transmits these RTD values and its neighbor's coordinates. If the BTSs are not synchronized, the RTD values must be sent periodically to the MS. The RTD sending frequency depends on the quality of the network synchronization (the updating frequency could be for example in the order of 1-2 minutes). The extra information from the network can be encrypted so that only those MS subscribers, that have subscribed for MS based E-OTD location calculation service, can decode the information. This enables operators to charge for location service.

2. Some network based application may request the location of the MS either directly or through MLC.

6.3.2 Benefits and Applications

The above described system enables the MS to calculate continuously and real time its own position using OTD measurements. There would be no need to have active two-way communication with network at all, i.e., additional network signaling capacity would not be needed, all required measurements and data could be obtained in idle mode. The continuous OTD location calculation in MS makes possible to improve the location accuracy, e.g. by having continuously running filtering. The MS can also obtain information about its movements.

The location is therefore available for the MS at all times, continuously in idle mode and when in call mode. Possible applications for this continuos location will be chart applications, tariff applications (e.g. home zone) and location information could be also one tool for Mobile Execution Environment (MexE).

Location calculation in MS offers several benefits for tariff applications:

- Tariff zones are easier to provision (e.g. subscribers home's coordinates can be used, there is no need to do any activation measurements).

- Tariff zones are easier to maintain, there in no need to worry about new BTS coverage areas, i.e. the zones can be separated from GSM network topology.
- Smaller and more reliable zones are possible.
- User indication is possible, i.e. he or she can be notified continuously, also in idle state, whether he or she is inside special tariff zone.

The operator will benefit from the increased traffic generated by these new applications which are using MS based location. Also the operator's tariff applications will work better: e.g. in home zone service the cheap home zone tariff can be given to much smaller area than using only CI, and simultaneously the reliability will be high and thus the end users will be more satisfied to this service. Additionally, the operator controls the coordinates of the base station and RTD values, so the use of MS based location calculation service can be charged.

6.3.3 E-OTD Computations

When time of arrival measurements are made in an uplink or a downlink based method, assuming some knowledge about the synchonisation state of the network, the differences of time of arrival called also E-OTD are made. The aim of this section in the thesis is to explain the E-OTD positioning method and to show that some cautions must be taken while computing the E-OTD. The location procedure can be divided into 2 processes P1 and P2:

$$\text{TOA\_1, TOA\_2, ..., TOA\_n} \xrightarrow{\text{P1}} \text{E-OTD\_1, E-OTD\_2, ..., E-OTD\_(n-1)} \xrightarrow{\text{P2}} \text{x,y)}$$

P1: E-OTD computations from the TOA measurements in the mobile or the base station. For n TOA measurements correspond (n-1) E-OTD, n>2 in case of 2 dimensions.

P2: Estimation of the x and y coordinates by an algorithm of triangulation.

If some confidence values of the TOA parameters are computed, then for each E-OTD the confidence value will be, for example, the sum of the 2 confidence values of the

corresponding TOA. If such confidence values are available and well-computed, the precision of the final location can be enhanced.

6.3.3.1 Cramér-Rao bound

This bound shows the best performance that the estimator can reach. As 2 parameters need to be estimated, x and y, the bound is given by a matrix with 2 dimensions. The bound on each parameter to be estimated is given by the diagonal elements of this matrix. When performing a location trial with n base stations, this bound depends on the coordinates, x and y, of the mobile :

$$CRB_n(x,y) = \begin{pmatrix} \sigma_x^2(x,y) & a^*(x,y) \\ a(x,y) & \sigma_y^2(x,y) \end{pmatrix}$$

The resulting variance is simply the sum of the diagonal elements of this matrix. The expectation of the precision over the whole network is chosen to be computed. The mean value of the error over all the pixels in the network is computed assuming that the E-OTD are all gaussian zero mean and decorrelated. Borders effect are not considered. It can be shown that:

$$RMS_n = \frac{\iint \sqrt{\sigma_x^2 + \sigma_y^2}\, dxdy}{\iint dxdy} \cdot \frac{\sqrt{\pi}}{2} = \frac{\iint \sqrt{Tr\left[CRB_n(x,y)\right]}\, dxdy}{\iint dxdy} \cdot \frac{\sqrt{\pi}}{2}$$

The simplest way to compute the E-OTD is the following:

$$\begin{bmatrix} E-OTD\_1 \\ E-OTD\_2 \\ \dots \\ E-OTD\_(n-1) \end{bmatrix} = \begin{bmatrix} -1 & 1 & 0 & 0 & 0 \\ -1 & 0 & 1 & 0 & 0 \\ \dots & \dots & \dots & \dots & \dots \\ -1 & 0 & 0 & 0 & 1 \end{bmatrix} \begin{bmatrix} TOA\_1 \\ TOA\_2 \\ \dots \\ TOA\_n \end{bmatrix}$$

The E-OTDs are computed according to the base station to which the mobile is connected. The idea behind that is the fact that the link between this base station and the mobile is the best one in term of signal strength.

Another scheme of computing the E-OTD is the following:

$$\begin{bmatrix} E-OTD\_1 \\ E-OTD\_2 \\ \cdots \\ E-OTD\_(n-1) \end{bmatrix} = \begin{bmatrix} -1 & 1 & 0 & 0 & 0 \\ 0 & -1 & 1 & 0 & 0 \\ \cdots & \cdots & \cdots & \cdots & \cdots \\ 0 & 0 & 0 & -1 & 1 \end{bmatrix} \begin{bmatrix} TOA\_1 \\ TOA\_2 \\ \cdots \\ TOA\_n \end{bmatrix}$$

In this case each E-OTD depends on the last 2 TOA measurements. The consequence of this definition is that the E-OTDs have better correlation properties.

CHAPTER 7

POSITION CALCULATIONS AND STATISTICAL EVALUATION

7.1 Introduction

The position calculation function utilises the available measurements, e.g., TOA measurements from three or more BS-MS links, to produce a position estimate. The statistical evaluation is based on computing the difference between the estimated position, given as:

$$EstimatedPostion = (\hat{x}, \hat{y})$$

and the true position of the mobile station, given as:

$$\text{True position} = (x, y).$$

Statistics on the circular error could be presented by plotting the cumulative distribution function (CDF) of absolute location error. Another possibility is to compute the root mean square error (rmse), which is given by the following equation:

$$rmse = \sqrt{\frac{1}{N}\sum_{i=1}^{N}\left((x_i - \hat{x}_i)^2 + (y_i - \hat{y}_i)^2\right)}$$

Where N is the total number of positioned mobile stations. The *rmse* calculation is very sensitive to occasional poor estimates (caused for example by poor measurements or lack of measurements). A measure which is less sensitive to these rare so-called outliers is obtained by omitting a fraction of MS's (e.g., 10%) which are the worst cases in the *rmse* calculation.

Due to the modular structure of the simulator, it is possible to study the different aspects of system simulation, link level simulation (e.g., TOA estimation) and position calculation not only integrated but also separately. Analysis of the output of the radio network simulator allows investigations of the expected Carrier / (Interference+Noise) values at serving and neighboring BS's for different parameters, e.g., cell radius or

channel utilization. This gives valuable information about the required sensitivity for example of TOA estimation algorithms. For positioning, measurements need to be made on links other than the one with the serving base station. In cellular systems, the signal strength at neighboring BS's is typically low, resulting in a very poor C / (I+N) situation.

Radio link simulations allow to study the performance of e.g., TOA estimation algorithms as function of C/I or Eb/No for different channel types [61]. This gives valuable information about the required C / (I+N) to get a certain TOA estimation accuracy.

7.2 "Average Algorithm" Positioning Method

The following calculations show a position calculation using method 1 named "average algorithm with 2 solutions to each base station pair". It uses a Urban_outdoor_3/9.mat statistics file, which contains data about the coordinates of each base station used, and coordinates of the original mobile station in an urban outdoor environment. By simulating Example2.m, which complete code is shown in Appendix C, the following data on each base station-mobile station connection is obtained:

BS1:

C/I = 16.9001 dB

Eb/No = 41.3556 dB

Distance from BS1 to MS = 333.644 m

BS2:

C/I = -7.9653 dB

Eb/No = 14.0221 dB

Distance from BS1 to MS = 1373.6857 m

BS3:

C/I = 4.2011 dB

Eb/No = 37.5643 dB

Distance from BS1 to MS = 1699.2634 m

Using bsv(ms,bs), which is an output array from the System Simulator, the three base station coordinates and the original mobile station coordinates could be obtained. In this particular case they are as follows:

bsv(ms,1) = 19. This means first base station used in this calculation is equal to the 19th base station out of the statistics file. The ms indicates mobile station, which is equal to 1 due to the fact that only one mobile station is to be positioned. Therefore x and y coordinates of the 19th base station are obtained using the array xyb(ms, bs).

Now, xyb(1,19) = xyb(ms, 1st base station) = (0, 0).
In the same manner the other two base station coordinates are obtained, where:
xyb(ms, 56) = xyb(ms, 2nd base station) = (1500, -2.27*10^{-13}) and
xyb(ms, 3rd base station) = (750, -1299).
The mobile station coordinates are obtained using the array xym. The are 750 mobile positions to choose from, indicating a moving mobile. The first mobile position is used in this particular calculation, which is xym = (158.1, 293.81). All position measurements above are given in metres.

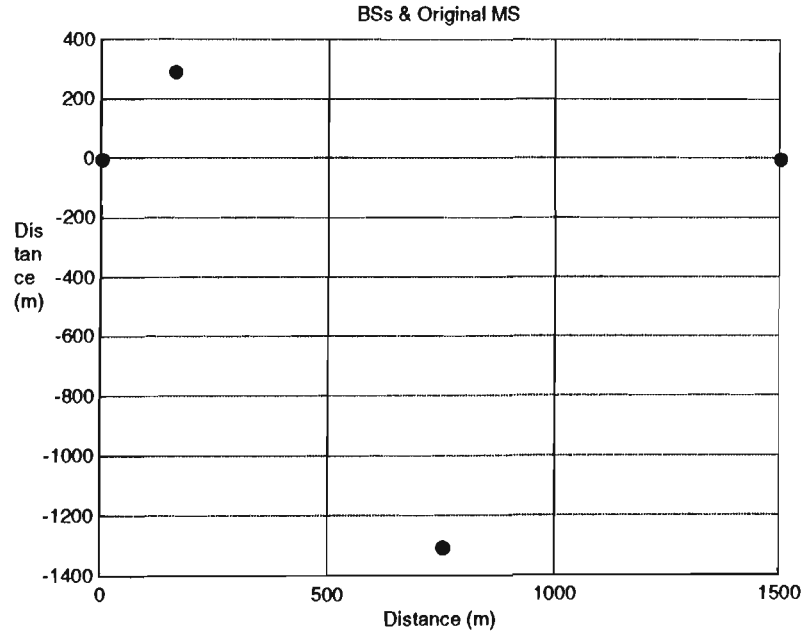

Figure 7.1: *Three Base Stations & Original Mobile Station.*

Figure 7.1 shows all base stations and the original mobile station according to their x and y coordinates. The blue circles indicate the 3 base stations and the green circle is the mobile station.

This method for position estimation uses only two base station at one given instant to find a mobile position. In fact two solutions are obtained from a pair of two base stations. For example, out of the 3 base station shown in figure 1, BS1 and BS2 will be involved in the calculation to obtain two solutions. Once the two solutions have been obtained, BS1 and BS3 are used, for 2 more solutions, and finally BS2 and BS3 for another 2 solutions. When all base station have been involved, a total of six solutions are obtained, providing there is a 3 base station system in the calculation.
Shown below is the calculation method for BS1 and BS3.

This original mobile station sends uplink signals to the operating base stations. For each sent signal, the estimated time of arrival (TOA) is calculated according to formulas given in chapter 6. For the signal to reach BS1 from the MS it takes approximately 1.0 μsec and 4.2 μsec from BS2 to MS. Therefore from this, the distance for each connection could be calculated using the relationship:

$$d = c * t \qquad (7.1)$$

where c is the speed of light equal to $3*10^8$ and t is the TOA estimate.

So, MS to BS1 = 1.0 μsec.

Therefore d = c * t

$d_1 = (3*10^8)*(1.0\ \mu sec)$

$d_1 = 300$ metres

For MS to BS2 = 4.2 μsec.

Therefore d = c * t

$d_2 = (3*10^8)*(4.2\ \mu sec)$

$d_2 = 1260$ metres

By substituting the above distances in the following two equations, 2 mobile estimated positions could be obtained.

Equation 1:

$$(X_m-X_{BS1})^2 + (Y_m-Y_{BS1})^2 = d_1 \qquad (7.2)$$

Equation 2:

$$(X_m-X_{BS2})^2 + (Y_m-Y_{BS2})^2 = d_2 \qquad (7.3)$$

By simultaneously solving the above two equations, two solutions are obtained. With BS1 and BS2 operating the two solutions are as follow:

Estimated mobile position 1:

$$X_{m1} = 250.8$$

$$Y_{m1} = 164.6188$$

Estimated mobile position 2:

$$X_{m2} = 250.8$$

$$Y_{m2} = -164.6188$$

Refer to Appendix D, location.m file for complete solution to the 2 equations.

These positions are shown in figure 7.2 below, indicated by the red circles.

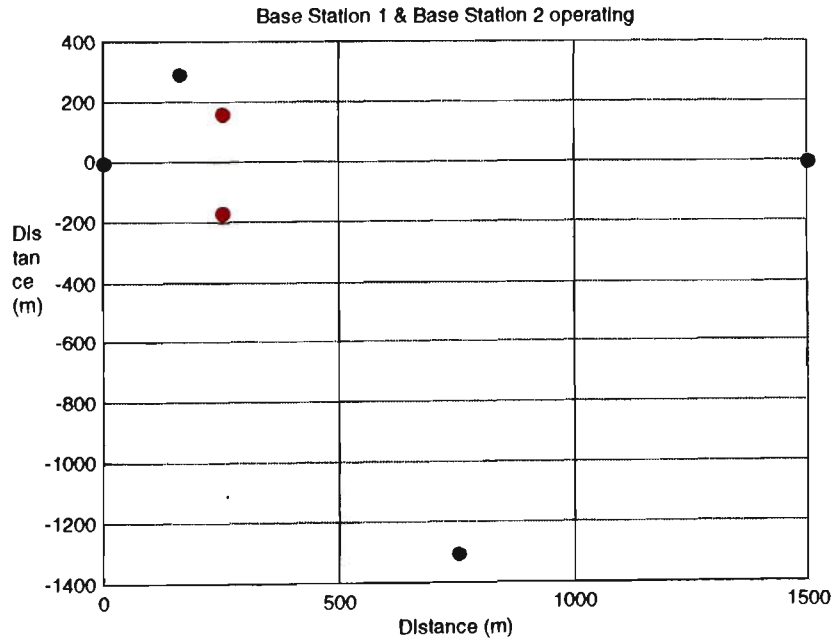

Figure 7.2: *Position estimates with BS1 & BS2 operating.*

Similarly, two other positions could be obtained when BS1 and BS3 are operating. For BS3, it takes approximately 5.2 μsec for the signal generated by the MS to reach BS3. Therefore using equation 7.1, distance from BS3 to MS is equal to 1560 meters. Other

data required to obtain the two estimated positions is BS3 x and y coordinates. As mentioned earlier, they are:

$$XY_{BS3} = (750, -1299)$$

With this data, the two estimated mobile positions, with BS1 and BS3 operating could be obtained using equations 7.2 and 7.3. The two solutions are listed below.

Estimated mobile position 1:

$$X_{m1} = 242.7766$$

$$Y_{m1} = 176.2371$$

Estimated mobile position 2:

$$X_{m2} = -274.0110$$

$$Y_{m2} = -122.1391$$

Figure 7.3 below shows these estimated mobile positions, together with the original mobile position and the three base stations.

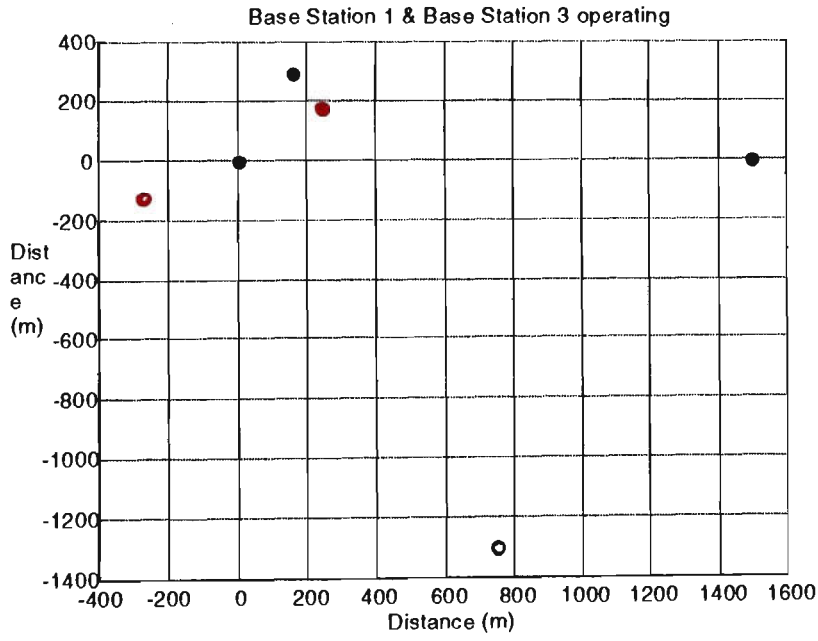

Figure 7.3: *Position estimates with BS1 & BS3 operating.*

Again the blue circles indicate the three base station, the green circle is the original mobile station and the two red circles indicate the estimated mobile positions. In the

same manner as above two estimated mobile positions are obtained for BS2 and BS3 operating.

The time of arrival from MS to BS1 is already known to be 1.0 μsec, giving a distance of 300 metres, and a time of 5.2 μsec from MS to BS3, giving a distance of 1560 meters. Therefore once again by simultaneously solving equations 7.2 and 7.3, the following estimated positions are obtained.

Estimated mobile position 1:

$$X_{m1} = 252.8760$$

$$Y_{m1} = 179.6709$$

Estimated mobile position 2:

$$X_{m2} = 2279.1$$

$$Y_{m2} = -990.2254$$

Figure 7.4 shows the graphical representation of the above positions.

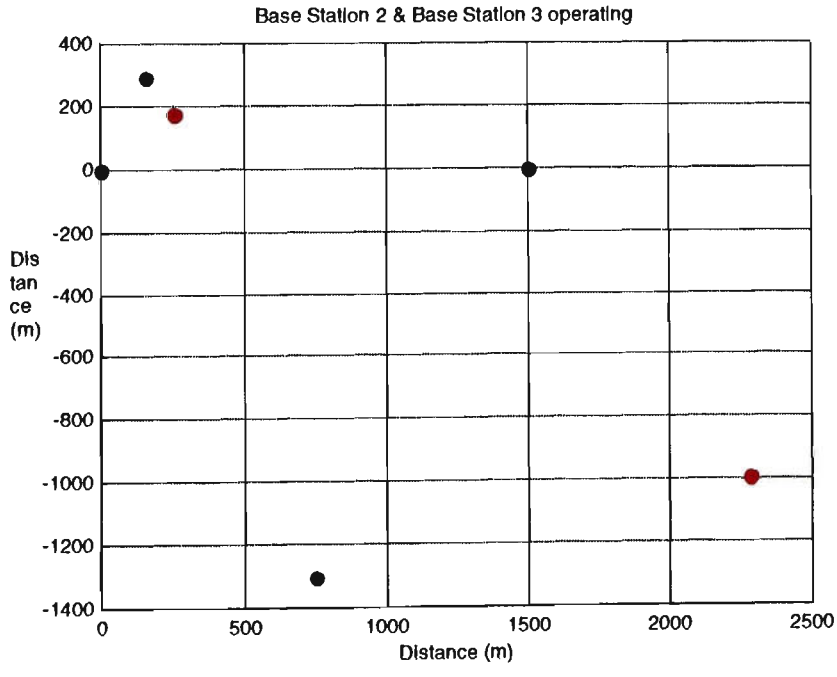

Figure 7.4: *Position estimates with BS2 and BS3 operating.*

From the six estimated mobile positions, the average is taken and is considered to be the final estimated mobile position.

Average position = (sum of all positions) / the number of positions.

For the above case average position is equal to the following:

Average mobile position: XY_{MS} = (500.3906, -126.1876).

This is shown in figure 7.5 below.

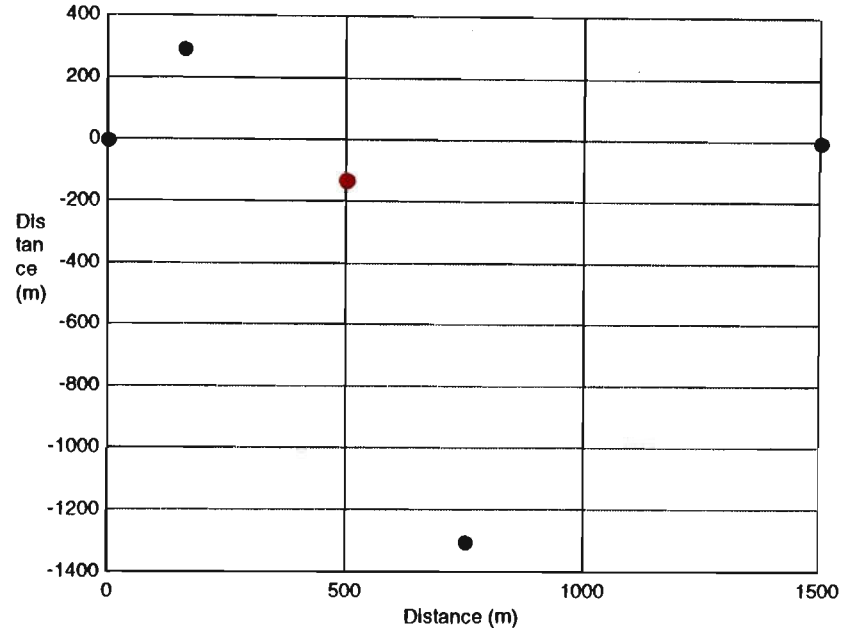

Figure 7.5: *Average estimated mobile position for a 3 BS system.*

The circular error for the above case could be obtained using the below formula:

$$rmse = \sqrt{\frac{1}{N}\sum_{i=1}^{N}\left((x_i - \hat{x}_i)^2 + (y_i - \hat{y}_i)^2\right)}$$

where N = number of mobile stations to be positioned, N = 1.

$(x_i, y_i) = (158.1, 293.81)$,

$(\hat{x}_i, \hat{y}_i) = (500.3906, -126.1876)$.

By substituting the above values in the equation a rms. error of 696.99 meters is obtained. An average mobile location error could not be accurately obtained by one set of simulation. Due to this fact a set of 30 different mobile locations has been simulated giving an average rms. error of 645 metres, for the three base station system.

In exactly the same fashion as for a three base station system, a five base station system was simulated, giving a more accurate mobile position. The root mean square error was obtained to be 281.8 metres. The graphical representation for a five base station system is shown in figure 7.6 below.

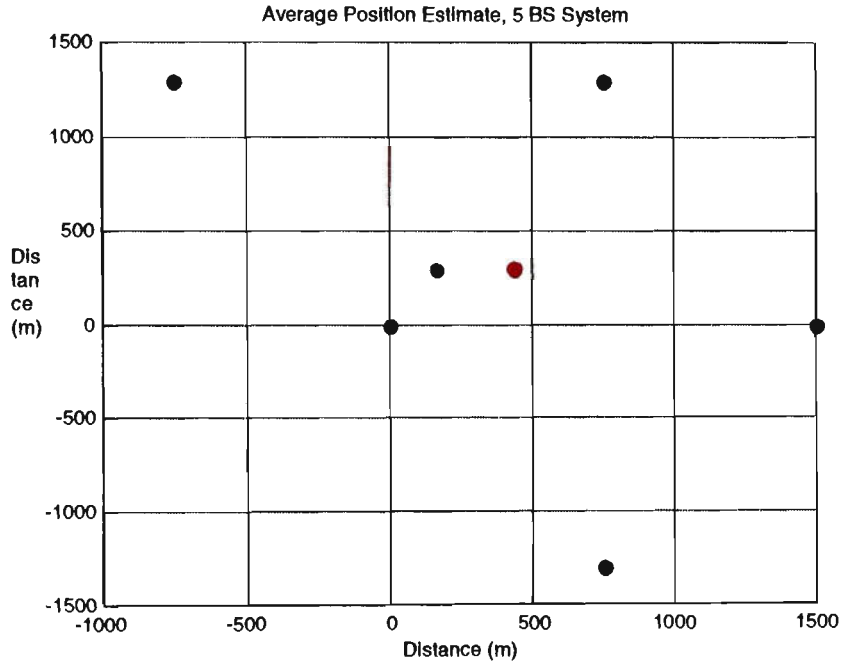

Figure 7.6: *Average estimated mobile position, for a 5 BS system.*

As it can be noticed, with an increase of base stations numbers, a more accurate estimation could be achieved.

With a 7 base station system the circular error was obtained, after 30 sets of simulations, at different mobile locations. The average estimated mobile position was worked out to be as shown below:

Average estimate: $XY_{MS} = (81.3563, 46.4616)$.
Using this estimate, the root mean square error obtained was:
rmse = 258.98 metres.

Figure 7.7 shows this graphically.

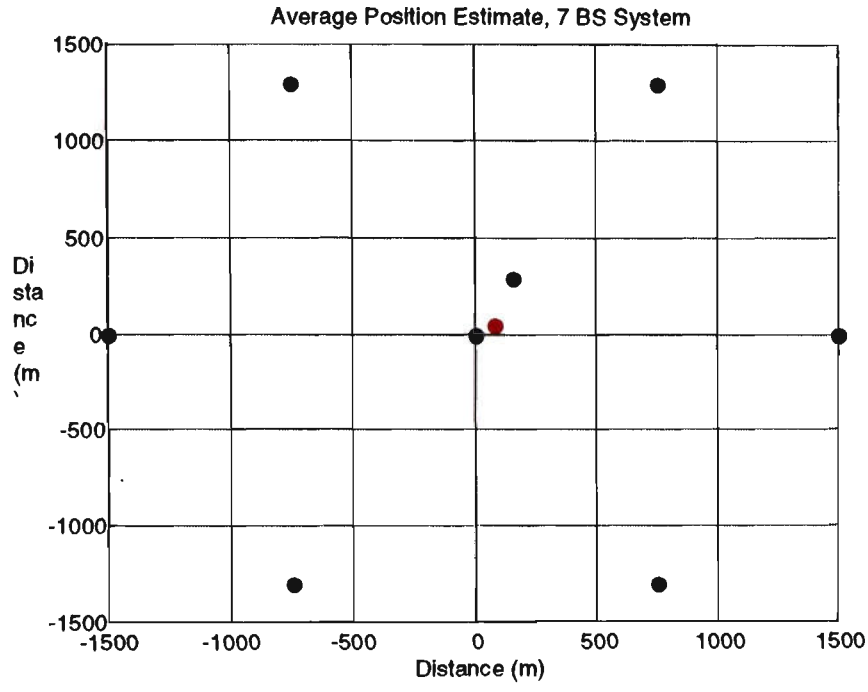

Figure 7.7: *Average estimated mobile position, for a 7 BS system.*

7.3 "More Preferable Solution" Positioning Method

I would now like to propose another method named "more preferable solution". The way the method operates is that, out of the two solution obtained as described in this chapter above using method 1, only one "more preferable" solution is taken, and the average is calculated as shown below:

$$\hat{x} = \frac{1}{n}\sum_{i=1}^{n} x_i \qquad \hat{y} = \frac{1}{n}\sum_{i=1}^{n} y_i$$

where n is the number of pairs considered.

The question may arise of how to choose a "more preferable" solution, out of the two possible solutions obtained by using method 1. The more preferable solution is chosen according to a distance from a third base station, which needs to be included in the calculation.

Consider Figure 7.8. Here, a three base station system is considered. When BS1 and BS2 are operating, BS3 is used to help decide which estimated position is closer to the

mobile station. When BS2 and BS3 are operating, which means that they are used to get two estimated positions, like in method 1, then BS1 is used for making a decision.

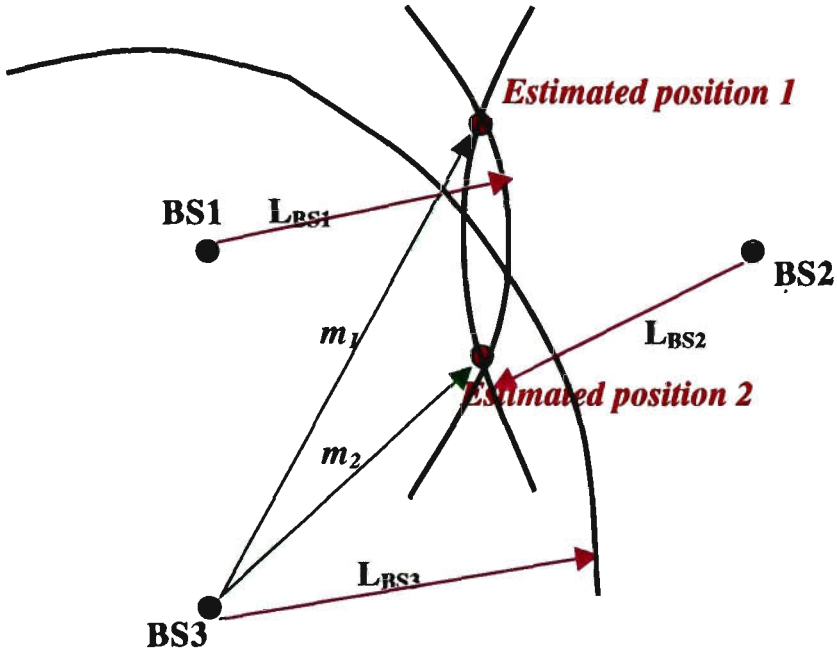

Figure 7.8: *Three base station system, Method 2, with BS3 deciding.*

The more preferable solution is chosen according to the following 2 rules:

if $|m_1-L_{BS3}| < |m_2-L_{BS3}|$ then choose *Estimated position 1*.

if $|m_1-L_{BS3}| > |m_2-L_{BS3}|$ then choose *Estimated position 2*.

In this method n = N/2, where N is a number of points in method 1. It should be noted that, if the number of base station is greater than 3, any one (only one) base station could be chosen for making the decision, while the two base stations are operating.

The MATLAB file that selects which is a more preferable pair is described below.

```
% Method 2 MATLAB file
% The file currently uses BS1 & BS2 as the two operating BS's, and BS3
% is used to make the decision.


Xe1 = 250.8;        % x coordinate of Estimated position 1.
Ye1 = 164.6188;     % y coordinate of Estimated position 1.

Xe2 = 250.8;        % x coordinate of Estimated position 2.
Ye2 = -164.6188;    % y coordinate of Estimated position 2.

Xbs3 = 750;         % x & y coordinates of base station used for making
Ybs3 = -1299;       % the decision.
```

```
L_bs3 = 1560;       % Distance of the decision making BS to MS.
                    % Obtained by using the TOA method.

m1 = sqrt( ((Xe1-Xbs)*(Xe1-Xbs)) + ((Ye1-Ybs)*(Ye1-Ybs)) );
m2 = sqrt( ((Xe2-Xbs)*(Xe2-Xbs)) + ((Ye2-Ybs)*(Ye2-Ybs)) );


if (abs(m1-L_bs) < abs(m2-L_bs))
sprintf('The position is Xe1=%d,Ye1=%d\n',Xe1,Ye1)
else
sprintf('The position is Xe2=%d,Ye2=%d\n',Xe2,Ye2)
end
```

As it can be seen in the file itself, the input values currently in it are: BS1 & BS2 operating, and BS3 is used for decision making. With a slight change to the input values, any pair could be input, to obtained a wanted solution.

After executing the above file, the estimated position selected is: Estimated position 1, which very clearly can be seen that this position is closer to the original MS than the estimated position 2. Figure 7.9 shows the graphical representation on this position.

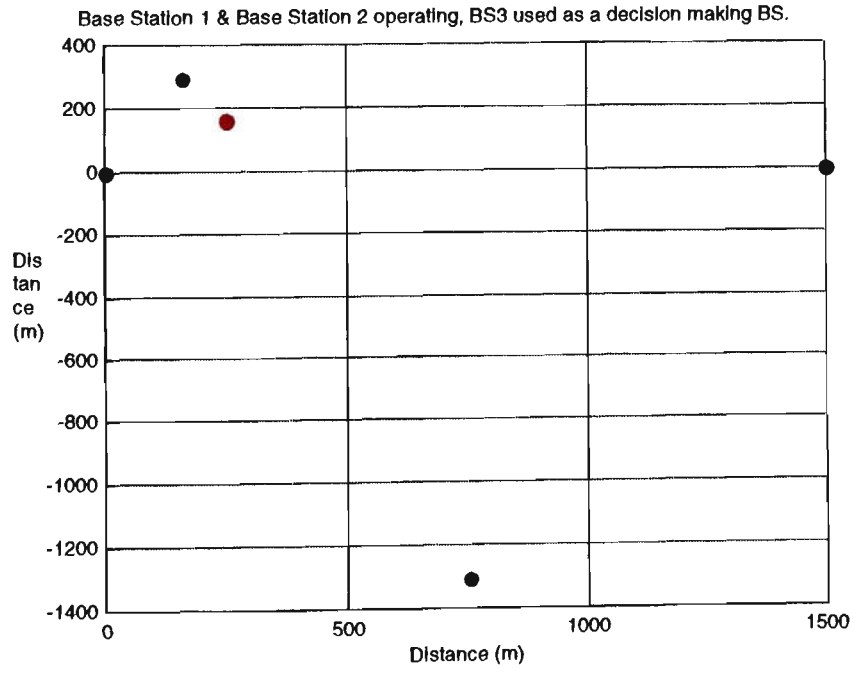

Figure 7.9: *BS1 & BS2 operating, while BS3 makes the decision, 3 BS system.*

If Figure 7.9 is compared with Figure 7.2, it can clearly be seen that the Estimated position 2, which is shown in Figure 7.2, is ignored in Figure 7.9 with the help of the

above MATLAB file. Once again in Figure 7.9, the blue circles are the three base stations, the green is the original MS and the red is the estimated MS.

For this particular case, when BS1 and BS2 are operating, and BS3 is used for decision making, the estimated position is: (250.8, 164.6188), as shown in Figure 7.9.

When BS1 and BS3 are operating, and BS2 is used for decision making, the estimated position is: (242.7766, 176.2371), as shown in Figure 7.10 below.

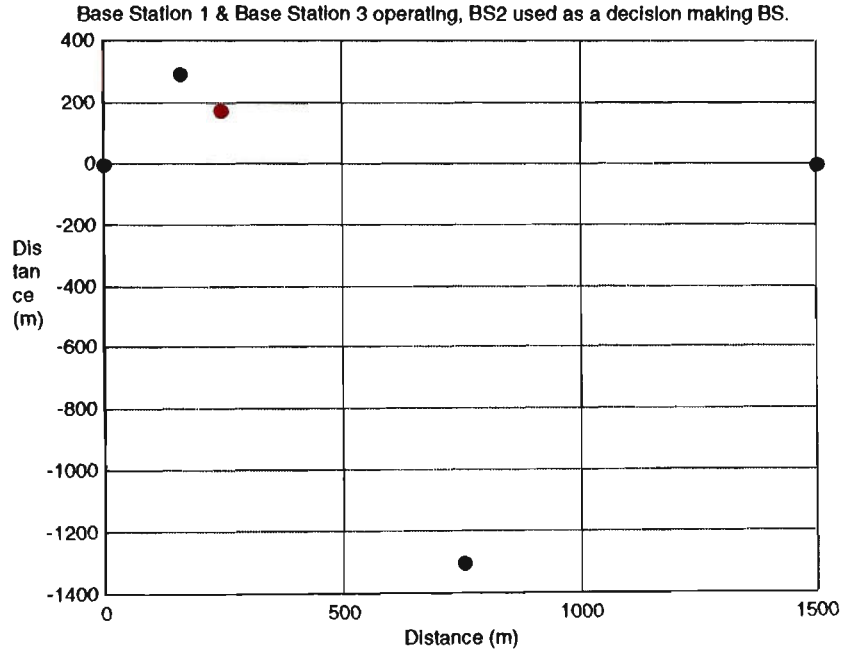

Figure 7.10: *BS1 & BS3 operating, while BS2 makes the decision, 3 BS system.*

When BS2 and BS3 are operating, the decision making base station is BS1. In this case the estimated mobile position is: (252.8760, 179.8709), as shown in Figure 7.11.

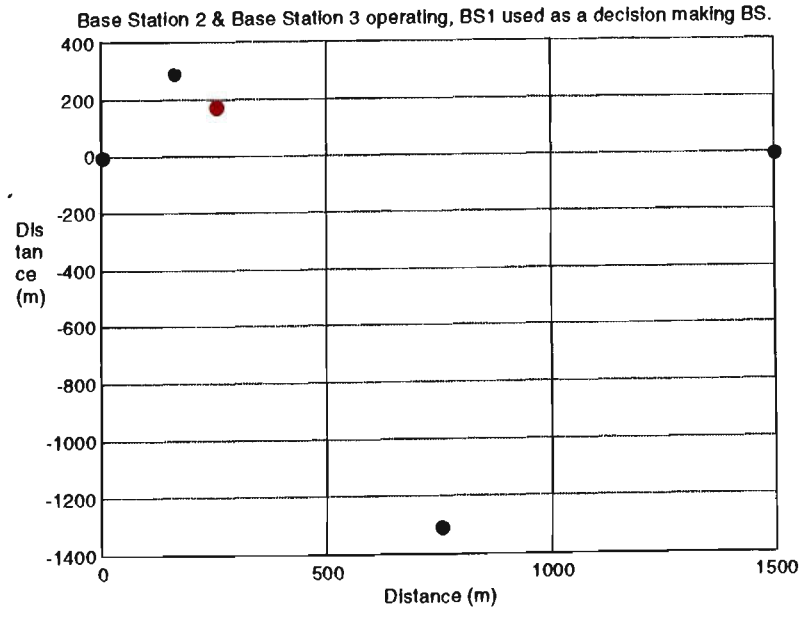

Figure 7.11: *BS2 & BS3 operating, while BS1 makes the decision, 3 BS system.*

Therefore, the average estimated mobile position in this particular case was calculated to be (248.8175, 173.5756), which is a much more accurate solution than the one found through method 1. In this situation the circular error was calculated to be 150.6186 meters. The accuracy is still not within the FCC requirements in which they are after a circular error of 125 metres, but it can be clearly said that method 2 is a much more accurate method than method 1. In fact with a three base station calculation, the accuracy has been improved by 546.3714 metres.

The system was simulated over 30 times for more reliable results. The overall root mean square error for a 3 base station system is displayed below:
rmse = 149.45.

For a 5 base station system using method 2, the average estimated position was calculated to be: (214.4060, 242.2321), giving a circular error of 76.3586 metres. It can be clearly seen that with 5 base stations being involved in the calculation, the FCC requirements are well satisfied, even in an urban environment. The average estimated position for a 5 base station system is shown in Figure 7.12.

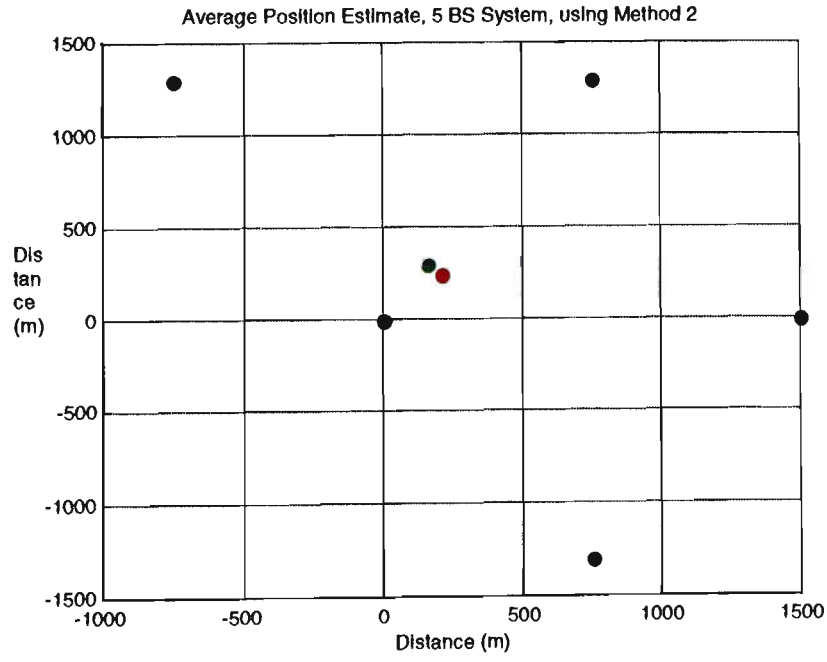

Figure 7.12: *Average position estimate, 5 BS system, using Method 2.*

For a 7 base station system, the average estimated mobile position using method 2 was calculated to be (187.046, 247.851), giving a circular error of only 54.31 metres. This results suggests that the FCC requirement of a circular error of 125 meters is well beaten. The average estimated position, using method 2 is displayed in Figure 7.13.

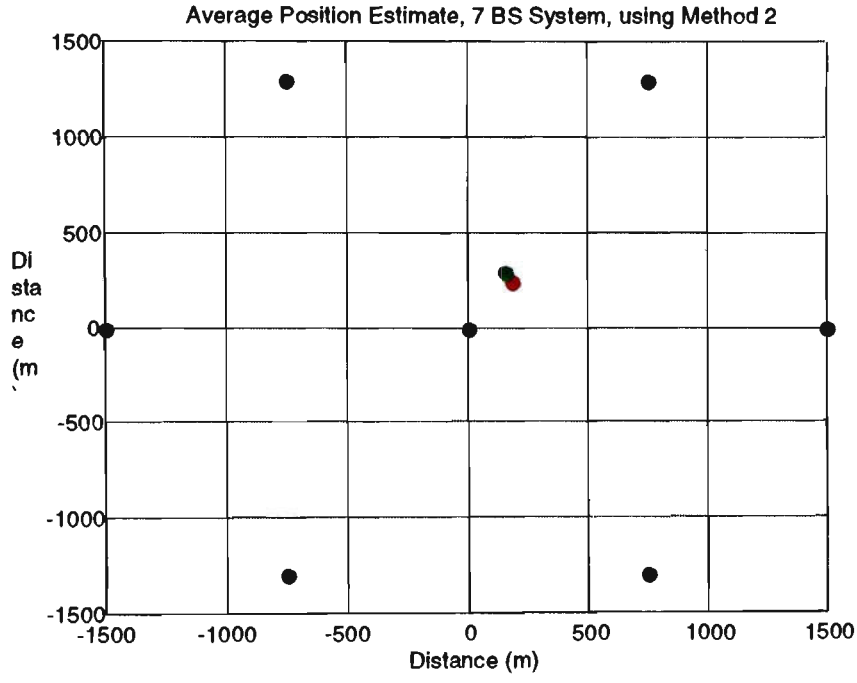

Figure 7.13: *Average position estimate, 7 BS system, using Method 2.*

As this chapter has shown, an increase in base station numbers gives a more accurate mobile position. But to satisfy the FCC requirements obviously a more accurate method needs to be defined, like method 2. Method 2 has satisfied the FCC requirements very well, giving a final circular error of only 54.31 meters, with a 7 base station calculation.

Chapter 8 introduces another method, method 3, named "Enhanced Fuzzy Method", which tries to improve the position accuracy to a greater degree.

CHAPTER 8

FUZZY LOGIC POSITIONING

8.1 Introduction to Fuzzy Logic

Fuzzy set theory, introduced by Zadeh [62] in 1965, has been shown to be an effective way to deal with qualitatively oriented terms and concepts. Fuzzy logic provides a simple way to draw definite conclusions from vague, imprecise information. In an intuitive sense, it resembles assertion concerning a mobile unit traveling on a local residential road:

" The speed of this mobile unit is high."

If the speed is 100 km/h, this statement is completely true. However, if 100 km/h is high, how about 99, 98, ... 90, ... 80, ... 70? At what degree does the statement suddenly become false? Since the speed can be changed gradually during a trip, it is hard to find a fixed value such that larger than that fixed value is "high" and less than that value is "not high". To resolve this fuzziness, a grade or a membership degree could be assigned to a certain speed. By correlating various speeds to grades, we turn the preceding statement into a fuzzy membership function. Therefore, it has often been said that fuzzy logic is a mathematical formalism intended to handle these kind of imprecise statements. It is different from traditional mathematical formalisms because fuzzy logic allows the user to model the vagueness in their mental decision-making process. Consequently, fuzzy logic is intuitive and easier to work with than traditional logic for many applications. Traditional logic would have a difficult time processing for the given statement. In the design of fuzzy inference system, there are three basic concepts: membership functions, fuzzy logic operations, fuzzy rules.

For membership functions, it can be denoted that the grade of a speed in high by assigning it a numerical "truth value". Truth-values may range anywhere between 0 and 1; and are typically considered to have meaning as suggested in Table 8.1, although it may not always have meaning. In this manner various grades could arbitrarily be assigned to "high" as a function of the speed, as shown in Table 8.2.

The membership functions given in the tables are illustrated in Figure 8.1. The curve in the Figure 8.1 illustrated how the membership function of a fuzzy concept is dependent on a measured value, for example, speed. When the relevant declarative assertions are combined into a single chart, more complicated curves are obtained. These curves are called fuzzy sets. The fuzzy concept "high" is called a label. For a speed such as 70 km/h, 0.7 is its grade in high. In other words, if the speed of this mobile is 70 km/h, the truth-value of the assertion "The speed of this mobile is high" is 0.7.

Truth Value	Meaning
0.0	Completely false
0.2	Mostly false
0.4	Somewhat false
0.6	Somewhat true
0.8	Mostly true
1.0	Completely true

Table 8.1: *Linguistic meanings of fuzzy logic values.*

Speed (km/h)	Grade in high
0	0.0
10	0.1
20	0.2
30	0.3
40	0.4
50	0.5
60	0.6
70	0.7
80	0.8
90	0.9
100	1.0

Table 8.2: *Membership function*

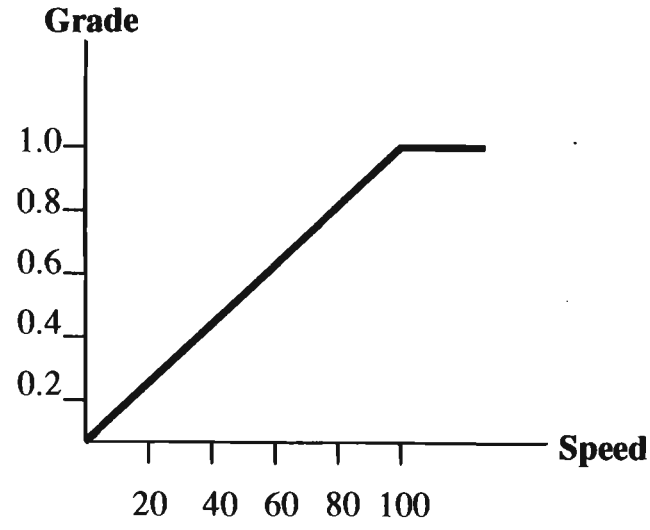

Figure 8.1: *Membership function chart.*

For fuzzy logic operations, consider the spoken language. In additional to the simple assertion statement presented earlier, logic operations are often used in spoken language to combine simple assertions into complex ones. Examples of such operators are "**AND**" and "**OR**". Assertions using these operators are called compound assertions. Similar operators could be used in fuzzy logic to help evaluate the truth-values of these assertions. These operations are called fuzzy logic operations. For example, another simple assertions could be defined:

" The distance to the next maneuver is short."

A compound assertion can now be created:

" The speed of this mobile is high **AND** the distance to the next maneuver is short."

Once a truth-value is assigned to each simple assertion, fuzzy logic operations can precisely evaluate the truth-values of compound assertions. Even though the compound assertion is vague, the evaluation results are ***crisp*** value. In other words, nothing is fuzzy in the actual fuzzy inference process.

As examples, how to evaluate truth values for statements containing the two simple operators, **AND** or **OR** could be examined. Mathematical functions are used by fuzzy logic to evaluate two arbitrary statements A and B. These statements can be either simple

or compound. The mathematical functions are listed in the right-hand column of Table 8.3. Each of them is associated with its corresponding operator in the left-hand column.

Compound operator on Statements A and B	Mathematical functions to evaluate truth
A AND B	minimum (min)
A OR B	maximum (max)

Table 8.3: *Fuzzy logic operations.*

From the definitions given in Table 8.3, the truth-value of any statement could easily be evaluated. If the truth value of A is 0.1 and the truth value of B is 0.8, the following could be obtained:

Assertion 1: A ***AND*** B = min(0.1, 0.8) = 0.1

Assertion 2: A ***OR*** B = max(0.1, 0.8) = 0.8

The crisp truth-value of assertion 1 is 0.1, whereas assertion 2 has a value of 0.8. It could be now known that a traditional logic such as Boolean logic is a special case of fuzzy logic. If there is any doubt about this statement, refer to Table 8.4, which lists various evaluation results for two compound assertions.

Logic Operator		Fuzzy Logic		Boolean Logic	
A	B	A AND B	A OR B	A AND B	A OR B
0	0	0	0	0	0
0	1	0	1	0	1
1	0	0	1	0	1
1	1	1	1	1	1
0	0.6	0	0.6	?	?
0.5	0.5	0.5	0.5	?	?
0.8	0.6	0.6	0.8	?	?
1	0.6	0.6	1	?	?

Table 8.4: *Comparison of Boolean Logic and Fuzzy Logic Operations.*

Both results obtained by applying fuzzy logic operators and Boolean logic operators are derived. It should be noted that both fuzzy logic and Boolean logic produce the same results when truth-values of the simple assertions are limited to 1 and 0. However, for values other than 1 or 0, fuzzy logic produces meaningful results while Boolean logic has no such operations defined.

For fuzzy rules, the following example could be considered. Suppose that the task is to determine when to announce a maneuvering instruction to a travelling mobile user during route guidance. One of the rules could be:

> **IF** the speed of the travelling mobile is high ***AND*** the distance to the next maneuver is short
>
> **THEN** announce the next maneuver instruction.

In other words, a rule has the following format:

> **IF** <condition> **THEN** <consequence>.

The condition part of a rule could be either a simple or compound statement and the consequence part is typically a simple statement. The input to a fuzzy-logic-based system is very similar to human language. The more complex a system is, the more rules it will generally have. Given the input grades in the condition part, each rule is evaluated to obtain an output grade in the consequence part.

The final result of this inference process depends on the combinational effect of many fuzzy rules in the process. Due to the fact that a single number is desired at the output, a defuzzifying operation is required. In other words, a defuzzification operator is used to compute one final crisp output value, which is to make a decision for the system to follow. The final step could be viewed as interpreting the evaluated grades as a measure of confidence in the corresponding conclusion. The most popular method used for this operation is to compute the centroid (weighted average) of the output from the fuzzy rules. By considering the grades as weights attached to the assertions, the final decision z is obtained by determining the weighted average of the support values associated with each output label.

The final decision z is defined by the following formula:

$$z = \frac{\sum_{i=1}^{n} x_i y_i}{\sum_{i=1}^{n} y_i}$$

where x is the position of the fuzzy output from the evaluation, y is the value (weight) of the corresponding fuzzy output, and n is the number of fuzzy outputs. In general, the outputs of fuzzy rule evaluation results are discrete values. For convenience, a curve is used in Figure 8.2 to explain the basic concept.

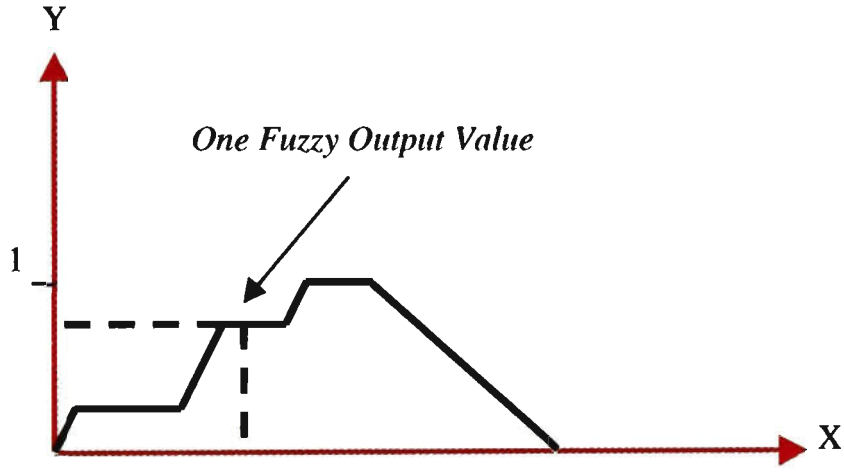

Figure 8.2: *Example of a fuzzy output curve.*

8.2 Enhanced Fuzzy Positioning Method

As method 2 in chapter 7 proved the FCC requirements of a circular error of 125 metres has well beaten. This section uses the fuzzy background, described in section 8.1 to produce a more accurate method 3, named "Enhanced Fuzzy Method". The method uses the above formulas, which has been derived according to the formula above, defined by z.

The method computes the weighted average of the output, where the output is the bit energy to noise power spectral density ratio, E_b/N_o, as described in chapter 4. The method uses similar assertions as described in section 8.1. Let's have a look at the following 3 base station system. The same values have been used in the calculations of method 1 and method 2, described in chapter 7. Consider the below figure, Figure 8.3.

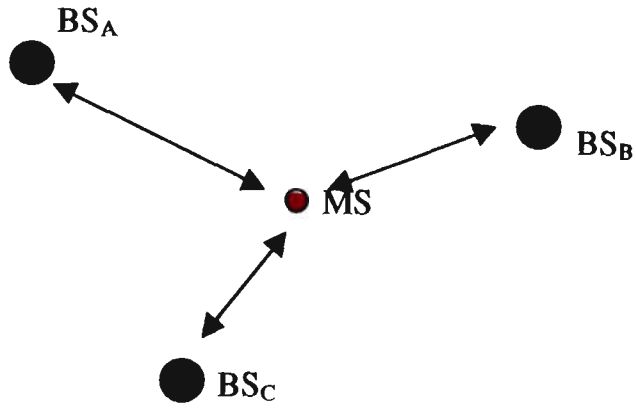

Figure 8.3: *Base station-Mobile station connections.*

Assertion 1 would be a solution of BS_A and BS_B operating. Assertion 2 is a solution of BS_A and BS_C operating, and assertion 3 is a solution of BS_B and BS_C operating. Consider the following assumptions:

Γ_A = bit energy / noise power spectral density ratio from BS_A

Γ_B = bit energy / noise power spectral density ratio from BS_B

Γ_C = bit energy / noise power spectral density ratio from BS_C

Now using the above assumptions and the fuzzy theory described in section 8.2, the weights for the three BS-MS connections could be worked out.

$\Gamma_1 = \max(\Gamma_A, \Gamma_B)$

$\Gamma_2 = \max(\Gamma_A, \Gamma_C)$

$\Gamma_3 = \max(\Gamma_B, \Gamma_C)$

From these values, the weighted values for each connection is worked out according to the following formula:

$$W_i = \frac{\Gamma_i}{50}$$

Because W_i is a belief degree to a certain solution, it is chosen to be displayed in a range between 0 and 1. ($0 < W_i < 1$). The highest bit energy to noise power spectral density ratio possible is 50 dB, therefore Γ_i is divided by 50 to get a belief degree between 0 and 1.

By executing the MATLAB file Example2.m, listed in Appendix C, the bit energy to noise power spectral density ratio values are obtained for all connections.

$\Gamma_A = 41.3556$ (dB)

$\Gamma_B = 14.0221$ (dB)

$\Gamma_C = 37.5643$ (dB)

Therefore,

$$\Gamma_1 = \max(41.3556, 14.0221) = 41.3556 \text{ (dB)}$$

$$\Gamma_2 = \max(41.3556, 37.5643) = 41.3556 \text{ (dB)}$$

$$\Gamma_3 = \max(14.0221, 37.5643) = 37.5643 \text{ (dB)}$$

From this, the weights could easily be worked out to be:

$$W_1 = 41.3356/50 = 0.8271$$

$$W_2 = 41.3556/50 = 0.8271$$

$$W_3 = 37.3653/50 = 0.7513$$

The final estimated location of the mobile is defined by the following two formulas:

$$\hat{x} = \frac{\sum_{i=1}^{n} W_i X_i}{\sum_{i=1}^{n} W_i} \qquad \hat{y} = \frac{\sum_{i=1}^{n} W_i Y_i}{\sum_{i=1}^{n} W_i}$$

Using the above formulas, the estimated x value of the mobile position is:

$$\hat{x} = \frac{(0.8271)(250.8) + (0.8271)(242.7766) + (0.7513)(252.8760)}{0.8271 + 0.8271 + 0.7513}$$

$$\hat{x} = 248.69(m)$$

The estimated y value of the mobile position for a 3 BS system is:

$$\hat{y} = \frac{(0.8271)(164.6188) + (0.8271)(176.23371) + (0.7513)(179.6709)}{0.8271 + 0.8271 + 0.7513}$$

$$\hat{y} = 173.3150(m)$$

Therefore, for a three base station system, the average estimated mobile position using the enhanced fuzzy method is (248.6900, 173.3150). The position is shown in Figure 8.4 below.

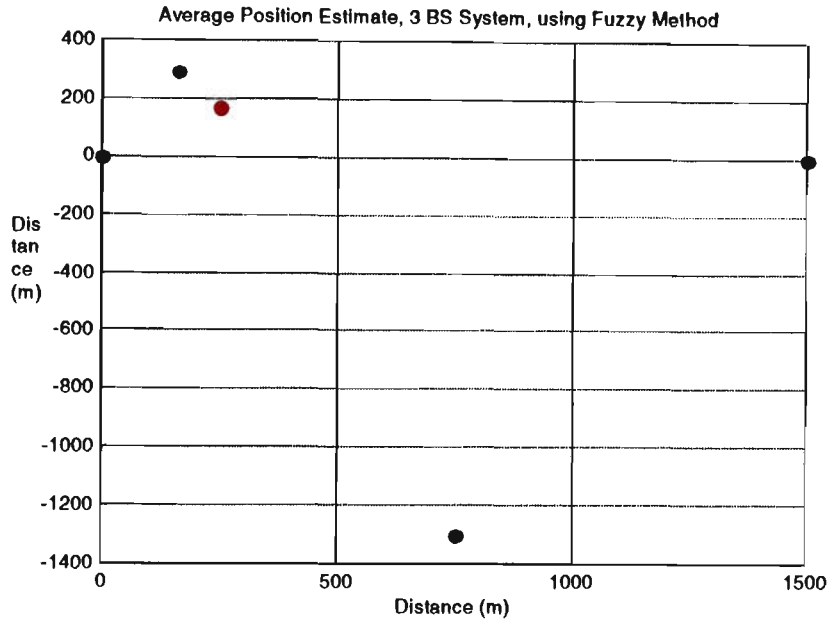

Figure 8.4: *Average position estimate, 3 BS system, using fuzzy method.*

The circular error for a 3 base station system is as follows:

$$rmse = \sqrt{(158.1 - 248.69)^2 + (293.81 - 173.31)^2}$$

$$rmse = 150.75 \text{ (m)}$$

where Original MS position, labeled green = (158.1, 293.81).

The system was simulated over 30 times for a more reliable result. The overall circular error of the enhanced fuzzy method for a 3 BS system was obtained to be 148.76 metres.

In the same manner, a 5 base station system was simulated according to a weighted average of the bit energy / noise power spectral density ratio. The final estimated average

position was worked out to be at x = 211.9476, and y = 237.57. This point is shown in Figure 8.5.

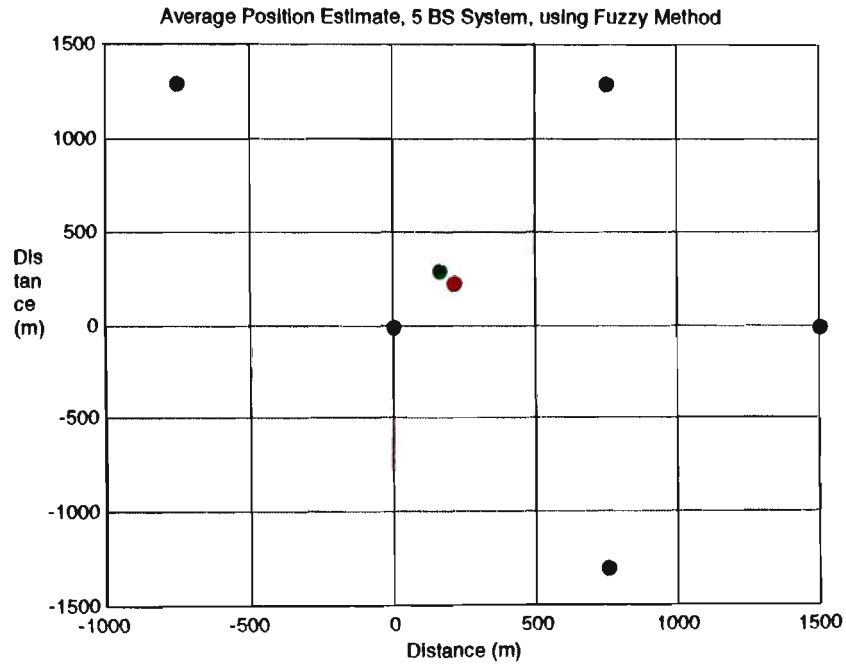

Figure 8.5: *Average position estimate, 5 BS system, using fuzzy method.*

The circular error of this system was calculated to be 78.0025 metres.

Once again, for a more accurate and average error the system was simulated approximately 30 times. The circular error of the overall system was calculated to be 75.9546 metres.

With 7 base stations involved in the calculation, the average estimated mobile position was calculated to be located at x = 186.340 and y = 249.851, giving an overall circular error of 52.25 metres, as shown below.

$$rmse = \sqrt{(x_i - \hat{x})^2 + (y_i - \hat{y})^2}$$

$$rmse = \sqrt{(158.1 - 187.046)^2 + (293081 - 249.851)^2}$$

$rmse$ = 52.25 metres.

After simulating the system over 30 times, a final estimated average position was obtained to be located at (185.45, 250.91). This point is shown in Figure 8.6. The circular error was obtained to be 50.8760 metres.

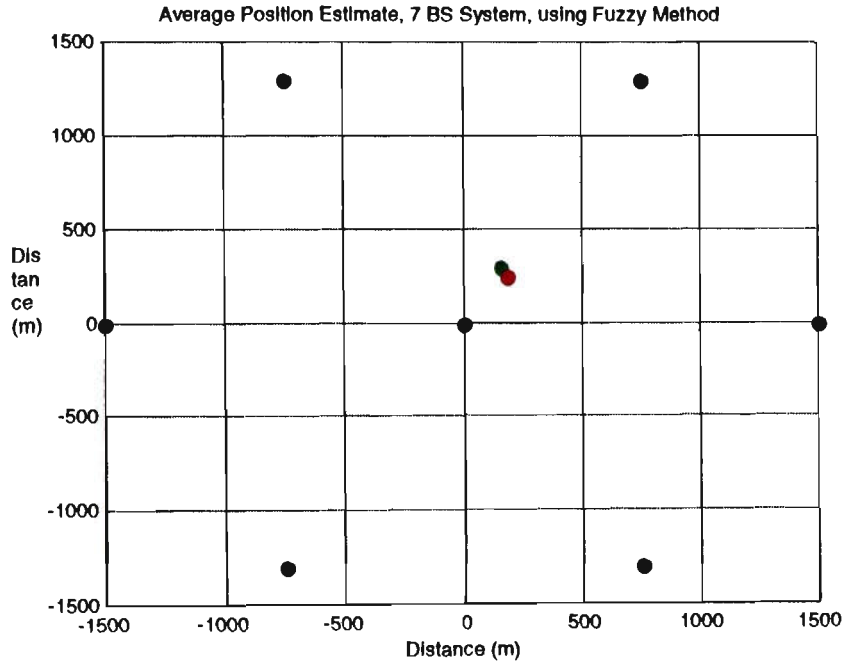

Figure 8.6: *Average position estimate, 7 BS system, using fuzzy method.*

As it has been seen in chapter 7 and in chapter 8 of this thesis, the Federal Communication Commission requirement of 125 metres circular error has been satisfied. In fact, out of the three introduced methods in this thesis, the "Enhanced Fuzzy Method" has provided the best possible results, in terms of mobile positioning. Conclusions and results of all three methods are summarised in chapter 9.

CHAPTER 9

COMPARISONS AND CONCLUSIONS

9.1 Introduction

As mentioned earlier in the thesis, the model is capable of extracting information on few environments. The environments are as follow:

- Urban environment
- Suburban environment
- Rural environment
- Bad Urban environment
- Hilly environment

As this is the most difficult and interesting case requiring a lot of research, the calculations in this thesis have concentrated only on Urban environment, which means that signals have traveled through densely populated areas, which includes multi-story buildings, offices and city centres. All methods have been simulated using the Urban environment, leaving the other environments for future work in this area.

9.2 Technique and Results Comparison

The results of all three methods have been summarised below.

Method 1

This method is the original method that has been used by Ericsson to locate a mobile station. It combines only two base stations at one time, and out of each pair there are two solutions. Finally the average is taken out of all positions and one final mobile location is obtained.

Number of BS's	Circular error (m)	Difference in meters from FCC's 125 (m) radius	Perc. at 125m [%]
3	> 500	+ > 500	24
5	281.80	+ 156.80	37
7	258.98	+ 133.98	48

Table 9.1: *Result summary for method 1.*

Method 2

This method for positioning chooses a more preferable solution out of the two solutions obtained from each pair in method 1. The more preferable solution is chosen according to a third base station, which helps chose the preferable solution. The results are summarised in Table 9.2 below.

Number of BS's	Circular error (m)	Difference in meters from FCC's 125 (m) radius	Perc. at 125m [%]
3	149.45	+ 24.45	72
5	76.35	- 48.65	95
7	54.31	- 70.69	95

Table 9.2: *Result summary for method 2.*

Method 3

This method computes the weighted average of the output, where the output is the signal to noise ratio, E_b/N_o, as described in chapter 4. The method uses assertions, which chose the higher signal to noise ratio for a certain BS-MS connection, and assign a weight to it. The weight is calculated according to the degree of greatness of the signal to noise ratio. The higher the signal to noise ratio, the higher the weight on that particular connection. The weight is in the range of 0 and 1. Results on this method are displayed below in Table 9.3.

Number of BS's	Circular error (m)	Difference in meters from FCC's 125 (m) radius	Perc. at 125m [%]
3	148.76	+ 23.76	73
5	75.95	- 49.05	97
7	52.25	- 72.75	97

Table 9.3: *Result summary for method 3.*

9.3 Conclusions

Most terrestrial-radio-based systems generally have a minimum error of at least 150 metres. The worst systems may have errors of up to 2,000 metres. As mentioned earlier, the performance of these systems often deteriorates when approaching urban canyon areas. The methods introduced in this thesis have shown that even in an urban environment, the results that have been achieved well satisfy the FCC requirement of a circular error of 125 metres. One particular technology, which has been used in method 3, enhanced fuzzy logic, has proven to be a successful method in reducing the positioning error. The difference in improvement is not great, in comparison with method 2, but nevertheless improvement has been noticed using fuzzy logic.

Fuzzy Logic Control (FLC) algorithms contribute a powerful tool for handling mobile communications problems. FLCs have provided noticeable performance improvements in terms of reducing the number of handovers, over the conventional handover and positioning techniques and they have demonstrated superb robustness under changing conditions. However, maturely to the novelty of this research area, the theory of FLC design is not yet well established in mobile communications. Researches around the world are trying to find answers to the following questions:

1. How to determine the optimal range for the FLC variables?
2. On which basis should the membership functions be determined in order to get the best possible mobile location?

9.4 Future Work

Most studies of hybrid methods are needed to further improve mobile positioning. For instance, one method to reduce the positioning error would be to implement filtering techniques in the mobile device, which uses the relationship between carrier Doppler phases measurements and range estimates changes. Interested readers can find information on various other radio location technologies and systems in [63] and [64].

Many of these technologies have very promising potential for use in mobile location applications.

Another method to reduce the circular error in positioning of a mobile unit base the weighted average on the signal strength between the mobile that needs to be positioned and operating base stations. Once the weights have been correctly split up, the use of fuzzy logic could chose, which base station, has a higher signal strength, and decide to use that base station.

Another method to reduce positioning error would be to use both, the signal to noise ratio and the signal strength of a signal. In this case the weighted average could be chosen using both of these measurements. Take the following as a guide.

$$W_i = W_{Si} * W_{\Gamma i}$$

W_i = Weighted average of a signal or total belief degree

W_{Si} = Belief degree based on signal strength

$W_{\Gamma i}$ = Belief degree based on signal to noise ratio.

The belief degree could possible be chosen in the following fashion:

$W_i = \min (W_{Si}, W_{\Gamma i})$.

REFERENCES

[1] M.D. Yacob, "Foundations of Mobile Radio Engineering", Boca Raton, FL: CRC Press, 1993.

[2] Federal Communications Commission, "Reports and Order and Further Notice of Proposed Rulemaking, CC Docket No.94.102, Revision of the Commission's Rules to Ensure Compatibility with Enhanced Emergency Calling Systems", Released July 26, 1996.

[3] J. Cisneros, D. Delly and L.A. Greenbaum, "An Urban Positioning Approach Applying Differential Methods to commercial FM Radio Emissions for Ground Mobile Use", Proceedings of ION 50th Annual Meeting, pp. 83-94, June 1994.

[4] D.C. Kelley, D.T. Rackley and V.P. Berglund, "Navigation and Positioning Systems and Methods Using Uncoordinated Beacon Signals", United States Patent, No.5173710, Dec. 1992.

[5] O. Grimland and B. Gudmundson, "Handover Strategies in Microcellular Systems", in IEEE Vehicular Technology Conference, pp.505-510, 1991.

[6] A. Murase, I.C. Symington and E. Green, "Handover Criterion for Macro Cellular Systems", in IEEE Vehicular Technology Conference, pp.524-530, 1991.

[7] R. Vijayan and J.M. Holtzman, "A Method for Analyzing Handover Algorithms", in IEEE Trans. on Vehicular Technology, pp.251-356, Aug. 1993.

[8] W.R.Mende, "Evaluation of a Proposed Handover Algorithm for the GSM Cellular Systems", 40th IEEE Trans. on Vehicular Technology, pp.264-269, 1990.

[9] S.T.S. Chia, R.J. Warburton, "Handover Criteria for City Micro Cellular Radio System", 40th IEEE Trans. on Vehicular Technology, pp.276-281, 1990.

[10] S.T.S. Chia, "Handover Initiation and Control for Highway Microcells", Fourth Nordic Seminar Mobile Radio Communications", DMR IV, June 1990.

[11] G. Falciasecca, M. Frullone, G. Riva, A.M Serra, "Comparison of Different Handover Strategies for High Capacity Cellular Mobile Radio Systems", 39th IEEE Trans. on Vehicular Conference, pp.122-127, 1989.

[12] B. Gudmundson and O. Grimlund, "Handover in Microcellular Based Personal Telephony Systems", In S. Nanda and D.J Goodman, eds., Third Generation Wireless Information Networks, pp.187-203, Kluwer Boston, 1992.

[13] O.E. Kelly and V.V. Veeravalli, "A Locally Optimal Handover Algorithm", in 6th IEEE International Symposium on Personal, Indoor and Mobile Radio Communications (PIMRC'95), pp.809-813, Toronto, Sep. 1995.

[14] M. Gudmundson, "Analysis of Handover Algorithms", IEEE 41st Trans. Vehicular Conference. pp. 537-542, 1991.

[15] M.D. Austin and G.L. Stuber, "Direction Based Handover Algorithm for Urban Macrocells", in IEEE Vehicular Technology Conference, pp.101-105, Atlanta 1994.

[16] E. Hepsaydir and W. Yates, "Performance Analysis of Mobile Positioning Using Existing CDMA Network", in IEEE Vehicular Technology Conference, pp.190-192, 1994.

[17] A. Salmasi, "On the System Design Aspect of CDMA Applied to Digital Cellular and PCN", Proceedings of 41st IEEE Trans. Vehicular Conference, pp.303-312, May 1991.

[18] R. Steele, "Mobile Radio Communications", Pentech Press, 1992.

[19] H.L. Song, "Automatic Vehicle Location in Cellular Communications Systems", in IEEE Vehicular Technology Conference, Vol. 43, No. 4, pp.902-908, 1994.

[20] L.A. Zadeh, "Fuzzy Sets", Information and Control, Vol. 8, pp.338-353, 1965.

[21] D. Driankov, H. Hellendoorm, M. Reinfrank, "An Introduction to Fuzzy Control", Springer-Verlag Berlin Heidelberg, USA, 1993.

[22] C.J. Harris, C.G. Moore, "Intelligent Identification and Control for Autonomous Guided Vehicles Using Adaptive Fuzzy-Based Algorithms", Engineering Applications of Artificial Intelligence, Vol. 2, pp.267-285, Dec. 1989.

[23] C.C. Lee, "Fuzzy Logic in Control Systems, Fuzzy Logic Controller-Part II", IEEE Trans. on Fuzzy Systems, Man and Cybernetics, Vol. 20, No. 2, pp.419-435, 1990.

[24] S. Assilian, "Artificial Intelligence Techniques in Control of Real Dynamic Systems", PhD-thesis, Queen Mary College, University of London, 1974.

[25] E.H. Mamdani, "Applications of Fuzzy Algorithms for Control of Simple Dynamic Plant", Proceedings IEEE, No. 121, pp.1585-1588, 1974.

[26] T. Takagi, M. Sugeno, "Derivation of Fuzzy Control Rules from Human Operator's Control Action", Proceedings of IFAC Symposium on Fuzzy Information, Knowledge Representation and Decision Analysis, pp.55-60, Marseillaise France, July 1983.

[27] C.J. Harris, C.G. Moore, "Phase Plane Analysis Tools for a Class of Fuzzy Control Systems", IEEE Trans. of Fuzzy Systems, Vol. 2, No. 1, pp.511-518, 1992.

[28] S. Shu-Fai Lau, K.F. Cheung, J.C.I. Chuang, "Fuzzy Logic Adaptive Handoff Algorithm", IEEE Conference, pp.509-512, Clear Water Bay, Hong Kong, 1995.

[29] P.S.K. Leung, "Application of Fuzzy Logic to Handover Control in Cellular Mobile Communications Networks", Fuzzy Systems Design, Social and Engineering Applications, Physica-Verlag, Heidelberg New York, pp.323-334, 1998.

[30] P. Lundqvist, "Final Positioning Channel Model", Ericsson Document, Sweden, 1998.

[31] P. Lundqvist, H. Asplund, S. Fisher, "Evaluation of Positioning Measurements System", T1P1.5/98-110, 1998.

[32] J. Brice, "The use of a weighted RMS function to reliably represent the distribution to location measurements" Cambridge Positioning Systems, T1P1.5/99-389, 1999.

[33] J. Brice, "Results from Medium scale trail of an E-OTD system in an urban environment, CPS, T1P1.5/99-390, 1999.

[34] P.A. Cross, "Advanced Least square applied to position-fixing, ISSN 0260-9142, 1990.

[35] M. Hata, "Empirical Formula for Propagation Loss in Land Mobile Radio Service", IEEE Trans. on Vehicular Technology, Vol. VT-29, No. 3, pp.317-325, 1980.

[36] E. Larsson, "Proposal for Common System Simulator", Ericsson, T1P1.5/98-107, March 1998.

[37] P. Lundvist, "Final Positioning channel model", Ericsson Document, Doc. No. T/U 98:301, 1998.

[38] W.R. Braun and U. Dersch, "A physical radio channel model", IEEE Trans. on Vehicular Technology, Vol. 40, No. 2, May 1991.

[39] J. Jimenez, et. al., "Final propagation model", R2020/TDE/PS/DS/P/040/b1, June 1994.

[40] M.A. Birchler and D.A. Jones, "Multipath Channel Behaviour Characterization Data", T1P1.5/98-100, 1998.

[41] M.A. Birchler and D.A. Jones, "Supplemental Multipath Channel Behaviour Characterization Data", T1P1.5/98-098.

[42] M.A. Birchler and D.A. Jones, "Additional Multipath Channel Behaviour Characterization Data", T1P1.5/98-122.

[43] P. Lundqvist, H. Asplund and S. Fisher, "Evaluation of Positioning Measurement System", T1P1.5/97-477R2, 1997.

[44] H. Asplund, "Wideband channel measurements in central Stockholm", T1P1.5/98-242, 1998.

[45] L.J. Greenstein, V. Erceg, Y.S. Yeh and M.V. Clark, "A new path-gain/delay-spread propagation model for digital celular channels", IEEE Trans. on Vehicular Technology, Vol. 46, No. 2, May 1997.

[46] J.A. Wepman, J.R. Hoffman, L.H. Loew, W.J. Tanis II and M.E. Hughes, "Impulse response measurements in the 902-928 and 1850-1990 MHz bands in macrocellular environments", ICUPC'93, pp.590-594, Ottawa Canada, 1993.

[47] E.S. Sousa, V.M. Jovancevic and C. Daigneault, "Delay spread measurements for digital cellular channel in Toronto", IEEE Trans. on Vehicular Technology, Vol. 43, No. 4, Nov. 1994.

[48] G. Lovnes, S.E. Paulsen, R. Raekken, "Wideband propagation measurements in large cells", RMTP/CC/NT01, Teledirektoratats forsknigsavdeling, Kjeller, Norway.

[50] A.G. Burr, "Power-delay profile of spartial channel model", COST 259 TD(97) 666, Lisbon, Sept. 1997.

[51] W.C.Y. Lee, "Effects on correlation between two mobile radio base station antennas", IEEE Trans. Communications, Vol. COM-21, No. 11, pp.1214-1224, Nov. 1973.

[52] K.I. Pedersen, P.E. Mogensen and B.H. Fleury, "Power azimuth spectrum in outdoor environments", IEEE Electronics Letters, 28th, Vol. 33, No. 18, Aug. 1997.

[53] A. Klein, W. Mohr, R. Thomas, P. Weber and B. Wirth, "Direction-of-arrival of partial waves in wideband mobile radio channels for intelligent antenna concepts", Proceedings of VCT'96, Atlanta 1996.

[54] A. Akeyma, "UHF band spatial correlation characteristics of mobile base station antennas", Electronics and Communications in Japan, Part I, Vol. 74, No. 7, 1991.

[55] F. Adachi, M.T. Freeney, A.G. Williamson and J.D. Parsons, "Crosscorrelation between the envelope of 900 MHz signals received at a mobile radio base station site", IEE Proceedings, Vol. 133, Pt. F, No. 6, Oct. 1986.

[56] A. Stojcevski, L. Reznik, M. Faulkner, "Trends in Cellular Position Location Techniques-An Overview", Proceedings of SCIRF'99, pp.69-73, Melbourne Australia, 1999.

[57] S. Fisher, H. Grubeck, A. Kangas, H. Koorapathy, E. Larsson, P. Lundqvist, "Time of arrival estimation of narrow-band TDMA signals for mobile positioning", Proceedings of PIMRC'98, pp.451-455, Boston USA, Sept. 1998.

[58] S. Fisher, H. Koorapathy, E. Larsson, A. Kangas, "System performance evaluation of mobile positioning methods", Proceedings of VCT'99, Houston Texas, May 1999.

APPENDIX A

Example1.m file

```
% Aleksandar Stojcevski
% Usage example of the system simulator sanpshots files %
% with graphs %

% Initialization %

clear all
close all

load urb_outdoor_39

Noise_level = 1.58e-15;  % in [Watts]

% Evaluate C/(I+N) for positioning on UL %

% Caluculate C/(I+N)

CIN_ul = 10 * log10 ( cumb ./ (iumb + Noise_level) );

% Sort C/I in descending order, but place C/I for serving BS first %
% Serving BS is given by the vector b for each MS %

CIN_ul_sorted = zeros(size(CIN_ul));
CIN_ul_sorted(:,1) = CIN_ul( index( 1:nm, s', nm)).';
CIN_ul( index( 1:nm, s',nm)) = -inf;
CIN_temp = fliplr(sort(CIN_ul,2));
CIN_ul_sorted(:,2:size(CIN_ul_sorted,2)) =
CIN_temp(:,1:size(CIN_ul_sorted,2)-1);

% Plot figure %

figure(1)
plot(CIN_ul_sorted(:,1));
hold on
plot(CIN_ul_sorted(:,2),'-.');
plot(CIN_ul_sorted(:,3),'--.');
plot(CIN_ul_sorted(:,3),':');
%legend('serving BS','2nd BS','3rd BS','4th BS',4);
title('UL C/I, ALL BS');
xlabel('dB');
ylabel('%');
axis([-15 20 0 1]);

% print -deps -f1 Example1.esp

% *** <eof> *** %
```

RadioLink_Simulator.m file

```
function TOA = Example2_radiolink(CI,CN,dist)

% Eb/No = C/N * Noise_bandwidth / Bit_rate

EbNo = CN * 200/270.833;

disp(['Estimating TOA for C/I = ' num2str(10*log10(CI)) 'dB, Eb/No = '
num2str(10*log10(EbNo)) 'dB, Distance = ' num2str(dist) 'm']);


% eof %
```

NewExample.m file

```
%
%       Example script for channel model functions
%
% Aleksandar Stojcevski


SampRate = 16;                  % internal sampling rate (no. of
samples/bit)
Fs = SampRate*(13e6/48);        % SampRate times bit rate


MonteCarloRuns = 300;

%=============== propagation model parameters

ChannelType = 'BadUrban';       % 'Urban'
                                % 'BadUrban'
                                % 'Suburban'
                                % 'Rural'
                                % 'Mountains'
                                % 'OnePeak'
DiffuseDelay= 15e-6;            % Only for 'Mountains':
                                % The excess delay at which the diffuse
                                % reflection arrives
lambda      = 0.32;             % Wavelength in meters
Distance    = 1;                % MS-BTS distance in km
x = [0:0.04:8.64];          % Distances at which the channel shall
                % be calculated (in meters)
BTSAntennaCoord = [-1.5 0       % Cartesian coordinates (x,y) of each
                    1.5 0];     % base station antenna (in meters)
AOA = 45;                       % Angle from the BTS to the MS in degrees
                                % as obtained in the same coordinate

system as
                                % BTSAntennaCoord
```

```
HoppingFreqs = [200,          % Hopping frequencies [Hz]
                800,
                1400,
                2000]'*1e3;

HoppingMode = 'cyclic';       % 'cyclic' or 'random'

NAntennas = size(BTSAntennaCoord,1);

rand('seed',41)
randn('seed',11)

%%%%%%%%%%%%%%%%%%%%%%%%%%%%%%%%%%%%%%%%%%%%%%%%%%%%%%%%%%%%%%%%%%%%%%%%%%%%
%%%%%


% ==== Calculate basic channel
[sc,atrms] = chanmod(Distance,ChannelType,DiffuseDelay,MonteCarloRuns)


% ==== Pick one realisation, e.g. no 6. and calculate the channel
impulse
%      responses
t = 6;
Imp =
getchan(sc,lambda,x,t,BTSAntennaCoord,AOA,Fs,HoppingFreqs,HoppingMode);


%%%%%%%%%%%%%%%%%%%%%%%%%%%%%%%%%%%%%%%%%%%%%%%%%%%%%%%%%%%%%%%%%%%%%%%%%%%%
%%%%%


% ==== Plot the channel impulse responses
%      The circles correspond to the fading of each peak at different x
values
figure
stem(abs(Imp(:,:,1)).^2')
set(gca,'XLim',[0 30])
xlabel('Delay Time [samples] (16 samples=1bit)')
ylabel('Amplitude')
title('Antenna 1')

figure
stem(abs(Imp(:,:,2)).^2')
set(gca,'XLim',[0 30])
xlabel('Delay Time [samples] (16 samples=1bit)')
ylabel('Amplitude')
title('Antenna 2')
```

APPENDIX B

This Appendix displays the channel model MATLAB files.

Chanmod.m file

```
% 22/6/99
% Alex Stojcevski
% m file for chanmod, genetation of scaterers

function [scatters, atrms] = chanmod(d,environment,NRe,trms);


environment = 'UrbanA';
NRe = 1; % number of channel realizations
d = 1; % distance from base station in km

c = 3e8; % speed of light

if nargin < 4 % check if the delay spread value is already given

   switch environment
   case {'UrbanA'}
      T1 = 0.4e-6;
      deps = 0.5;
      sigmay = 4; %(dB)
   case {'UrbanB'}
      T1 = 0.4e-6;
      deps = 0.3;
      sigmay = 4; %(dB)
   case {'BadUrban'}
      T1 = 1.0e-6;
      deps = 0.3;
      sigmay = 4; %(dB)
   case {'Suburban'}
      T1 = 0.3e-6;
      deps = 0.3;
      sigmay = 4; %(dB)
   case {'Rural'}
      T1 = 0.1e-6;
      deps = 0.3;
      sigmay = 4; %(dB)
   case {'OnePeak'}
      T1 = 0;
      deps = 1;
      sigmay = 4;
   otherwise
      disp('Bad environment specifications');
      return;
   end;


   Y = sigmay*randn(1,NRe);
```

```
   y = 10.^(Y/10);

   % Get delay spread values
   trms = T1*d^deps*y;

else
   % Delay spread given as a function argument
   trms = trms*ones(1,NRe);
end;

% Generate scatterers %

switch environment
   %UrbanA or Bad Urban
case {'UrbanA','BadUrban'}
   NScatt = 20;

   % Mean power of each scatt.

   for ind = 1:NRe
      Omega(ind,1:NScatt) = 0.5+rand(1,NScatt);
      Omega(ind,:) = Omega(ind,:)/sum(Omega(ind,:));
   end;

   m = ones(NRe,NScatt);

   alfa = 2*pi*rand(NRe,NScatt);

   Tb_Max = trms*3.58;

   % Delay of each scatterer
   for ind  = 1:NRe
      Tbi(ind,:) = Tb_Max(ind)*rand(1,NScatt);
      Omega(ind,:) = Omega(ind,:).*exp(-6*Tbi(ind,:)/Tb_Max(ind));
      Omega(ind,:) = Omega(ind,:)/sum(Omega(ind,:));

      % Calculation of the actual delay spread
      MeanDelay(ind) = sum(Tbi(ind,:).*Omega(ind,:))/sum(Omega(ind,:));
      RMSDelaySpread(ind) = sqrt(sum((Tbi(ind,:) -
MeanDelay(ind)).^2.*Omega(ind,:))/sum(Omega(ind,:)));
   end;



   % Test channel %

case 'OnePreak'
   NScatt = 1;
   Omega = 1;
   Tbi = 0;
   alfa = 0;
   m = 10000;

   RMSDelaySpread = 0;

otherwise
   disp('Bad environment specification');
```

```
      return;
end;


% Generate angles of arrival at the base station %

sigmatheta = (c*Tbi/(d*1000));
theta = sigmatheta.*rand(NRe,NScatt);

% Create output matrix %

scatterers = zeros(NRe,NScatt,5);

scatterers(:,:,1) = Omega;
scatterers(:,:,2) = Tbi;
scatterers(:,:,3) = alfa;
scatterers(:,:,4) = m;
scatterers(:,:,5) = theta;

atrms = RMSDelaySpread;
```

subscatt.m file

```
% START %
% subsct m file %

function subsct = subscatt(sct);

NRe = 1;
NScatt = 20;

sct = zeros(NRe,NScatt);

Nw = 100;
Salfa = 0.15;

% Parameters for input matrix %

Omega = sct(:,1);
tau = sct(:,2);
alfa = sct(:,3);
m = sct(:,4);
theta = sct(:,5);
NScatt = size(sct,1);

Somega = sqrt(Omega/Nw.*(1-sqrt(1-1./m)));

for ind = 1:NScatt
   A(ind,:) = abs(Somega(ind)*randn(1,Nw));

   if m(ind)>1
      A(ind,1) = sqrt(Omega(ind)*sqrt(1-1/m(ind)));
   end;
```

```
   NormFact = sum(A(ind,:).^2);
   A(ind,:) = A(ind,:)*sqrt(Omega(ind)/NormFact);

   phi(ind,:) = -pi+2*pi*rand(1,Nw);

   palfa(ind,:) = alfa(ind)+Salfa*randn(1,Nw);
end;

subsct = zeros(NScatt*Nw,4);

A = A';
phi = phi';
tt = kron(tau,ones(1,Nw));
tt = tt';
th = kron(theta,ones(1,Nw));
th = th';

subsct(:,1) = A(:);
subsct(:,2) = phi(:);
palfa = palfa';
subsct(:,3) = tt(:);
subsct(:,4) = palfa(:);
subsct(:,5) = th(:);
```

channel.m file

```
% channel m file %

function Ac = channel(subsct,x,lambda,b,aoa);

x = [0:0.04:8.64];
lambda = 0.32;

if nargin < 4
   b = [0 0]
   aoa = 0;
elseif nargin < 5
   aoa = 0;
end;

Nb = size(b,1);

% Base antenna into polar form %
[tb,rb] = cart2pol(b(:,1),b(:,2));

dt = subsct(:,3);
dt2 = sort(dt);
delaytimes = dt2(find(diff(sort([-1; dt]))));

% Create output matrix %

Ac = zeros(length(delaytimes),2,length(x),Nb);

for indb = 1:Nb
   for ind = 1:length(x)
```

```
      argz = 2*pi*x(ind)/lambda*cos(subsct(:,4));

      dargz = 2*pi/lambda*rb(indb)*cos(tb(indb)-(subsct(:,5)+aoa));
      argz = argz+dargz;

      for ind2 = 1:length(delaytimes)

         occ = find(dt == delaytimes(ind2));

         Ac(ind2,1,ind,indb) =
sum(subsct(occ,1).*exp(i*(subsct(occ,2)+argz(occ))));

         % Store the delay value %

         Ac(ind2,2,ind,indb) = delaytimes(ind2);
      end;
   end;
end;
```

getchan.m file

```
% getchan.m %

function [h] =
getchan(sc,lambda,x,t,b,aoa,Fs,hopp_frqs,HoppingMode,HoppSeed)

%inputs%

sc = 20;
lambda = 0.32;
x = [0:0.04:8.64];
t = 6;
b = [-3 0 3 0];
aoa = 45;
SampRate = 16;
Fs = SampRate*(13e6/48);
hopp_freqs = [200,800,1400,2000]'*1e3;
HoppingMode = 'cyclic';

%main program starts here%

sct = squeeze(sc(t,:,:));

if size(sc,2)==1 %"OnePeak" case%
   subsct = subscatt(sct.');
else
   subsct = subscatt(sct);
end

Ac = channel(subsct,x,lambda,b,aoa);

if HoppingMode == 'random'
   if nargin ~10
      HoppSeed = 15;
```

```
   end
   SeedTemp = rand('seed');
   rand('seed',HoppSeed);

   Nfreq = length(hopp_freqs);
   index = round(rand(1,length(x))*Nfreqs+0.5);
   df = hopp_freq(index);

   rand('seed',SeedTemp);
elseif HoppingMode == 'cyclic'
   df =[];
   for i=1:floor(length(x)/length(hopp_freqs))
      df=[df hopp_freqs];
   end
   if (length(x)-length(df)) > 0
      df=[df hopp_freqs(1:length(x)-length(df))];
   end
else
   error(sprintf('ERROR (getchan): Unknown Hopping Mode
"%"!',HoppingMode));
end


% take the wideband channel and filter out the GSM channel %

NumberOfBaseAntennas = size(Ac,4);
NumberOfScatters = size(Ac,1);

tau = (0:1/Fs:30e-6);

for tt=1:NumberOfBaseAntennas

   if size(Ac,1)==1
      Acit = squeeze(Ac(:,:,:,tt));
      Aci(1,:,:) = Acit;
   else
      Aci = squeeze(Ac(:,:,:,tt));
   end

   if size(sc,2)~=1
      for xi=1:length(x)
         Aci(:,1,xi) = exp(sqrt(-1)*2*pi*pf(xi)*Aci(:,2,xi))
.*(Aci(:,1,xi));
      end
   end

   % LP filter the wideband channel %

   htemp = zeros(size(Ac,3),length(tau));
   for ttt=1:NumberOfScatters
      Atemp = squeeze(Aci(ttt,:,:)).';
      if length(x) > 1
         tau1 = Atemp(1,2);
      elseif length(x) == 1
         tau1 = Atemp(2);
      end
      while ~isempty(find(tau1-tau ==0))
```

```
         tau1=tau1+esp;
      end
      if length(x) > 1
         %low pass filter%
         htemp = htemp + Atemp(:,1)*(sin(pi*Fs*(tau1-tau))./(pi*(tau1-
tau)));
      elseif length(x) == 1
         htemp = htemp + Atemp(1)*(sin(pi*Fs*(tau1-tau))./(pi*(tau1-
tau)));
      end
   end

   %scaling sampled impulse response%
   h(:,:,tt) = htemp/Fs;
end
```

APPENDIX C

This MATLAB file extracts information on the connections between base stations and mobile stations. Information output is: Carrier to Interference ratio and Bit Energy to Noise Power Spectral ratio.

Example2.m file

```
% Usage example of the system simulator snapshot files %
% Example code to run system simulation based on statistics file %

clear all
close all

load urb_outdoor_39

%%%%%%%%%%%%%%%
% Select BS's %
%%%%%%%%%%%%%%%

nbs = 3;
epsilon = 1e-6;

CellCentre=xyb + meshgrid(fib,1:nm);
  for ROW=1:nm,
   ServingCC(ROW,1)=CellCentre(ROW,s(ROW));
   CCDist(ROW,:)=abs(CellCentre(ROW,:)-ServingCC(ROW,1));
  end
[Cs,Bs]=sort(CCDist');
bsv=reshape(Bs(find(Bs-meshgrid(s,1:nb))),nb-1,nm)';
bsv=[s,bsv];


%%%%%%%%%%%%%%%%%%%%%%%%%%%%
% Run radio link simulator %
%%%%%%%%%%%%%%%%%%%%%%%%%%%%

Montecarlo_runs = 1;

Noise_level = 1.5800e-15;  % -118 dB

TOA = zeros(Montecarlo_runs, nbs);

for ms = 1 : Montecarlo_runs

   for bs = 1 : nbs
     TOA(ms,bs) = Example2_radiolink( ...
        cumb(ms,bsv(ms,bs))/iumb(ms,bsv(ms,bs)) ,...    % C/I ratio
        cumb(ms,bsv(ms,bs))/Noise_level         ,...  % C/N ratio
        abs( xym(ms) - xyb(ms,bsv(ms,bs)) ))   ; % Actual Distance
   end
```

```
 end
% *** <eof> *** %
```

APPENDIX D

This MATLAB file outputs the location of the estimated mobile station.

location.m file

```
% Matlab file that sovles position location of mobile.
% Inputs are base station coordinates.


%Enter here BS coordinates

Xbs1 = 0;
Ybs1 = 0;

Xbs2 = 1500;
Ybs2 = -2.27e-13;


% Enter distances from BS's to MS

d1 = 300;       % MS to BS1
d2 = 1260;     % MS to BS2


% Solve equation 1, which BS1.

%((Xm-Xbs1)*(Xm-Xbs1)) + ((Ym-Ybs1)*(Ym-Ybs1)) = (d1*d1);

%(Xm*Xm)-(Xbs1*Xm)-(Xbs1*Xm)+(Xbs1*Xbs1) + (Ym*Ym)-(Ybs1*Ym)-
(Ybs1*Ym)+(Ybs1*Ybs1) = (d1*d1);

a=Xbs1*Xbs1;
b=Ybs1*Ybs1;
c=d1*d1;

% Now equation 1 is:
%(Xm*Xm)-(Xbs1*Xm)-(Xbs1*Xm)+a + (Ym*Ym)-(Ybs1*Ym)-(Ybs1*Ym)+b = c;

%(Xm*Xm)-((Xbs1-Xbs1)*Xm))+a + (Ym*Ym)-((Ybs1-Ybs1)*Ym))+b = c;

%(Xm*Xm)-((Xbs1-Xbs1)*Xm))+(Ym*Ym)-((Ybs1-Ybs1)*Ym))+a+b-c = 0;

d=a+b-c;

% Now equation 1 is:

%(Xm*Xm)-((Xbs1-Xbs1)*Xm))+(Ym*Ym)-((Ybs1-Ybs1)*Ym))+d = 0;

z=Xbs1-Xbs1;
y=Ybs1-Ybs1;

% Therefore equation 1 is:
```

```
%(Xm*Xm)-(z*Xm))+(Ym*Ym)-(y*Ym))+d = 0;



% Solve equation 2, which is BS2.

%((Xm-Xbs2)*(Xm-Xbs2)) + ((Ym-Ybs2)*(Ym-Ybs2)) = (d2*d2);

%(Xm*Xm)-(Xbs2*Xm)-(Xbs2*Xm)+(Xbs2*Xbs2) + (Ym*Ym)-(Ybs2*Ym)-
(Ybs2*Ym)+(Ybs2*Ybs2) = (d2*d2);

e=Xbs2*Xbs2;
f=Ybs2*Ybs2;
g=d2*d2;

% Now equation 2 is:
%(Xm*Xm)-(Xbs2*Xm)-(Xbs2*Xm)+e + (Ym*Ym)-(Ybs2*Ym)-(Ybs2*Ym)+f = g;

%(Xm*Xm)-((Xbs2-Xbs2)*Xm))+e + (Ym*Ym)-((Ybs2-Ybs2)*Ym))+f = g;

%(Xm*Xm)-((Xbs2-Xbs2)*Xm))+(Ym*Ym)-((Ybs2-Ybs2)*Ym))+e+f-g = 0;

h=e+f-g;

% Now equation 2 is:

%(Xm*Xm)-((Xbs2-Xbs2)*Xm))+(Ym*Ym)-((Ybs2-Ybs2)*Ym))+h = 0;

k=Xbs2-Xbs2;
j=Ybs2-Ybs2;

% Therefore equation 2 is:

%(Xm*Xm)-(k*Xm))+(Ym*Ym)-(j*Ym))+h = 0;


% Now use simultanious equations. Eq1-Eq2.

%((Xm*Xm)-(z*Xm))+(Ym*Ym)-(y*Ym))+d)  -  ((Xm*Xm)-(k*Xm))+(Ym*Ym)-
(j*Ym))+h) = 0;

%((-z+k)*Xm) + ((-y+j)*Ym) + (d-h) = 0;

n=-z+k;
m=-y+j;
p=d-h;

% Therefore

%(n*Xm) + (m*Ym) + p = 0;

%(n*Xm) = -(m*Ym)-p;

% So Xm is:
```

```
%Xm = -((m/n)*Ym) + (p/n);

a1=m/n;
a2=p/n;

%Xm = -(a1*Ym) + a2;

% Now sub this equation of Xm in equation 2.

%(Xm*Xm)-(k*Xm))+(Ym*Ym)-(j*Ym))+h = 0; % this is equation 2.

%((-a1*Ym + a2)*(-a1*Ym + a2)) - (k*(-a1*Ym + a2)) + (Ym*Ym) - (j*Ym) +
h = 0;

%(((a1*a1)*Ym*Ym)-(a1*a2*Ym)-(a2*a1*Ym)+(a1*a2)) - (-k*a1*Ym + k*a2) +
(Ym*Ym) - (j*Ym) + h = 0;

s1=a1*a1;
s2=a1*a2;
s3=k*a1;
s4=k*a2;

%(s1*Ym*Ym - s2*Ym -s2*Ym + s2) - (-s3*Ym + s4) + (1*Ym*Ym) - (j*Ym) +
h = 0;

%s1*Ym*Ym - (s2+s2)*Ym + s2 + s3*Ym - s4 + 1*Ym*Ym - j*Ym + h = 0;

q1=s2+s2;

%s1*Ym*Ym - q1*Ym + s2 + s3*Ym - s4 + 1*Ym*Ym - j*Ym + h = 0;

%(s1+1)*Ym*Ym - (q1+s3-j)*Ym + (s2-s4+h) = 0;

t1=s1+1;
t2=q1+s3-j;
t3=s2-s4+h;

% t1*Ym*Ym - t2*Ym + t3 = 0;

% Quadratic formula:

Ym1 = (-t2 + (sqrt(t2*t2 - 4*t1*t3)) / (2*t1));

Ym2 = (-t2 - (sqrt(t2*t2 - 4*t1*t3)) / (2*t1));

% end of file %
```